PLASMA PROTEOME ANALYSES OF EXPERIMENTAL HUMAN AND MURINE THYROID DISEASE MODELS

INAUGURALDISSERTATION

zur Erlangung des akademischen Grades eines
Doktors der Naturwissenschaften (Dr. rer. nat.)
der
Mathematisch-Naturwissenschaftlichen Fakultät
der
Ernst-Moritz-Arndt-Universität Greifswald

vorgelegt von
Beatrice Engelmann
geboren am 11.09.1989

Greifswald, 31.07.2017

Dekan: Prof. Dr. Werner Weitschies

1. Gutachter: Prof. Dr. Uwe Völker

2. Gutachter: Prof. Dr. Klaudia Brix

Tag der Promotion: 12.02.2018

TABLE OF CONTENT

ABBREVIATIONS

(m/m) / (m/v) / (v/v)	(mass to mass) / (mass to volume) / (volume to volume)
ABC	ammonium bicarbonate
ACN	acetonitrile
A.dest	destilled water
ANOVA	analysis of variance
BMI	body mass index
BSA	bovine serum albumine
CID	collision induced dissociation
DNA	desoxyribonucleic acid
DMSO	dimethylsulfoxide
DTT	dithiothreitol
EDTA	ethylene diaminetetraacetic acid
(F)T3	(free) 3,3’,5-triiodo-L-thyronine
(F)T4	(free) thyroxine
FTMS	Fourier transform mass spectrometer
HCD	higher energy collision
HDL	high density lipoprotein
HPLC	high performance liquid chromatography
i.d.	internal diameter
IAA	iodoacetamide
IPA	Ingenuity Pathway Analysis
$KClO_4$	potassium perchlorate
LC	liquid chromatography
LDL	low density lipoprotein
L-T_4	levothyroxine
LTQ	linear trap quadrupole
m/z	mass to charge
MMI	methimazole
MS	mass spectrometry

PBS	phosphate buffered saline
PCA	principal component analysis
PCR	polymerase chain reaction
RCT	reverse cholesterol transport
rpm	revolutions per minute
RNA	ribonucleic acid
RP	reverse phase
RXR/LXR	retinoid/liver X receptor
rT3	3,3’,5’-triiodo-L-thyronine (reverse T3)
SD	standard deviation
TCA	trichloroacetic acid
TH	thyroid hormones
Tris	tris(hydroxymethyl)aminomethane
TR	thyroid hormone receptor
TRE	thyroid hormone response element
TRH	TSH releasing hormone
TSH	thyrotropin (thyroid-stimulating hormone)
UPLC	ultra performance liquid chromatography
UT	urea/thiourea
VLDL	very low density lipoprotein

SUMMARY

The thyroid as the largest endocrine gland mainly produces and secretes the thyroid hormones (TH): 3,3',5-triiodo-L-thyronine (T3) and its pro-hormone L-thyroxine (T4). Thyrotropin (TSH) produced in and secreted from the pituitary gland stimulates thyroidal TH production and secretion. In turn, TH repress TSH production exerting a sensitive negative feedback control. Besides the impact on growth, normal development, bone marrow structure, the cardiovascular system, body weight and thermogenesis, TH play a vivid role in many metabolic regulatory mechanisms in almost all tissues. Thyroid diseases are relatively prevalent and cause, due to the resulting TH imbalances, a broad spectrum of effects. Many of them manifest in pathologically increased or decreased TH levels defined as hyperthyroidism or hypothyroidism, respectively. Metabolic complexes regulated by TH include carbohydrate as well as cholesterol homeostasis. TH also influence primary and secondary hemostasis. Routinely, determination of the thyroid state is based on the assessment of the classical markers TSH and free T4. However, this practice has several drawbacks: For instance, subclinical cases of hyper- and hypothyroidism might not be detected, resulting in detrimental health consequences. Moreover, elucidation of the pleiotropic effects of TH on multiple molecular pathways is mostly based on cell culture, tissue and rodent models. Analysis of animal biofluids like serum and urine using metabolomics approaches demonstrated the extensive impact of TH on other body compartments. In contrast, proteome profiling has not been exploited for the comprehensive characterization of the general metabolic effects of TH. In humans, analysis of biofluids was performed only in a targeted approach by analyzing specific proteins. Plasma as a large and diverse compartment of the human proteome provides a great opportunity to identify novel protein markers of thyroid function as well as to characterize metabolic effects of TH in humans.

Therefore, a study of experimental thyrotoxicosis was performed with 16 male volunteers treated with 0.25 mg/d levothyroxine (L-T_4) for 8 weeks to induce a hyperthyroid state. Plasma samples were collected before the L-T_4 application started, two times during the treatment and additionally two times after withdrawal. Proteome analysis revealed remarkable alterations including increased levels of two known proteins known to

correlate with TH levels, namely sex hormone-binding globulin (SHBG) and cystatin C (CYTC). The correlation with free T4 levels revealed 76 out of 437 detected proteins with a Pearson correlation coefficient of $r \geq |0.9|$. One prominent signature included 10 coagulation cascade proteins exhibiting significantly increased plasma levels during thyrotoxicosis, thereby revealing a trend towards a hypercoagulative state in hyperthyroidism. Among these were the pro-coagulation factor XIII subunit B (F13B), II (F2), XI (F11) and IX (F9). Exemplarily, routine ELISAs were performed for F9 and F13 yielding the same pattern as the proteomics derived data, thus confirming the proteomics results. To overcome the statistical drawbacks of the Pearson correlation analysis, additionally a mixed-effect linear regression model using serum free T4 concentrations as exposure and protein abundances as outcome while controlling for age, BMI, and batch was implemented. Application of this model resulted in the detection of 63 proteins with significant associations to free T4 levels. Besides the already mentioned augmented coagulation, a significant drop in the amounts of three apolipoproteins (ApoD, ApoB-100 and ApoC3) was observed. Furthermore, an increased abundance of proteins assigned to the complement system was detected, namely of several complement factors and complement components as well as mannose-binding protein C (MBL) and mannan-binding lectin serine protease 2 (MASP-2).

Inspired by the data of the experimentally induced thyrotoxicosis model, a similar study was designed for studying mid-term hypothyroidism, including 15 patients - mostly women. However, due to the different age, BMI and medical history the group displayed a much more pronounced variability. Thus, the established markers SHBG and CYTC revealed no clear trend in level. Additionally, only minor alterations were detected in the metabolome analysis. Thus, the chances of detecting promising alterations in the proteome compaosition were very low and the full scale proteome profiling was not performed. Since coagulation proteins comprised one distinct signature in the study of induced thyrotoxicosis, F9 was measured by ELISA. The results revealed decreased F9 levels during the hypothyroid state.

Experimental studies in humans were complemented by corresponding analyses in murine models. Mice represent a well-established model for disease research allowing the study of underlying pathomechanisms and the efficacy of administered drugs as well as development of new therapies. In the special context of TH-induced changes in

metabolism, several murine studies have assessed alterations in hepatic gene expression patterns. In the current work, plasma samples of two murine studies including male C57BL/6 wild type mice were analyzed to elucidate the impact of thyroid dysfunction on the plasma proteome. The first study was similarly designed as the human model of experimentally induced thyrotoxicosis and assigned the animals to three groups: a control group, a T4 treatment group, and a T4 recovery group, whereupon the latter first received T4 followed by a subsequent TH normalization period. A high proportion of plasma proteins exhibited significantly different protein levels during T4 application (n = 120), where 90 of these also showed a corresponding reverse trend after T4 withdrawal (T4 recovery vs. T4), thereby displaying transient alterations. The molecular pattern of hyperthyroidism in the murine model indicated, as in the human study, a pronounced decrease in apolipoproteins. However, in clear contrast to the human data, the levels of proteins related to the coagulation cascade and complement system were also transiently decreased in mice, while being increased in humans.

The second murine analysis focused on the impact of hyper- and hypothyroidism caused by T3 or T4 treatment and MMI/$KClO_4$ application, respectively. In general, compared to the first murine study less clear alterations of protein levels were detected. Proteins related to the complement system revealed fewer changes in the T3 group and only marginal changes after T4 induction. Unexpectedly, the MMI/$KClO_4$-induced hypothyroidism caused a reduction of the levels of several proteins assigned to the complement system, although different components and factors were affected. Only four proteins exhibited a significant inverse trend in hyper- and hypothyroidism, namely the apolipoproteins A2 and C1, major urinary protein 6 and buturylcholine esterase.

Generally, rodent studies partially provided a divergent picture of TH action as compared to human studies. However, in spite of inconsistent results in studies regarding the effects of TH that are possibly due to species-specific differences, an important role of TH on several metabolic and other pathways, e.g. in the process of blood coagulation and apolipoprotein regulation, is evident. The results from both murine and human studies presented here provide novel insights into changes in the plasma proteome in the context of thyroid diseases which might contribute to a better understanding of TH action on metabolism and other pathways.

1 INTRODUCTION

Thyroid hormone action

The thyroid is the largest endocrine gland and plays a fundamental role in regulating numerous metabolic processes throughout the whole body and in virtually all tissues. Coordination of normal development and growth rate as well as metabolic activities and the cardiovascular system are strongly affected by the thyroid. The thyroid hormones (TH) L-thyroxine (T4) and 3,3',5-triiodo-L-thyronine (T3) as the main secretion products of the thyroid mediate all these functions (Figure 1). Production, release and transport of TH constitute a finely tuned system which needs tight regulation to maintain physiological reference ranges.

A **B**

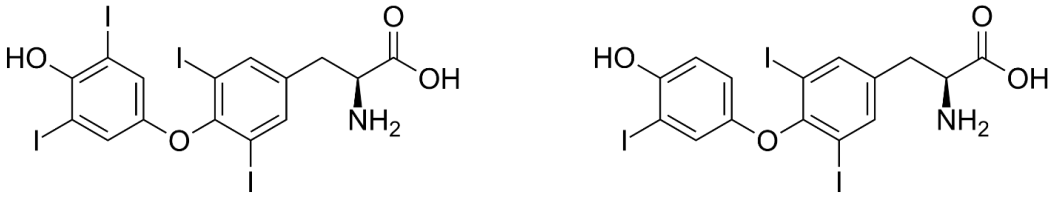

Figure 1 Chemical structure of TH; **A)** T4: L-thyroxine; **B)** T3: 3,3',5-triiodo-L-thyronine

Several dysfunctions are caused and manifested by hormonal imbalances. Resulting disorders can affect both the structure and function of the gland. Due to the broad spectrum of thyroid hormone effects thyroid diseases are amongst the most prevalent medical conditions. Worldwide, the most common cause of thyroid disorders is iodine deficiency which manifests as goiter and clinical hypothyroidism. In iodine-replete areas autoimmune diseases affecting the thyroid are also more common. The prevalence of

spontaneous hypothyroidism is 1-2 %, more common in older women and overall ten times more likely in women than in men. The prevalence for hyperthyroidism is 0.5-2 % in women [1]. Thyroid cancer is rare but at the same time the most common malignant endocrine tumor [2].

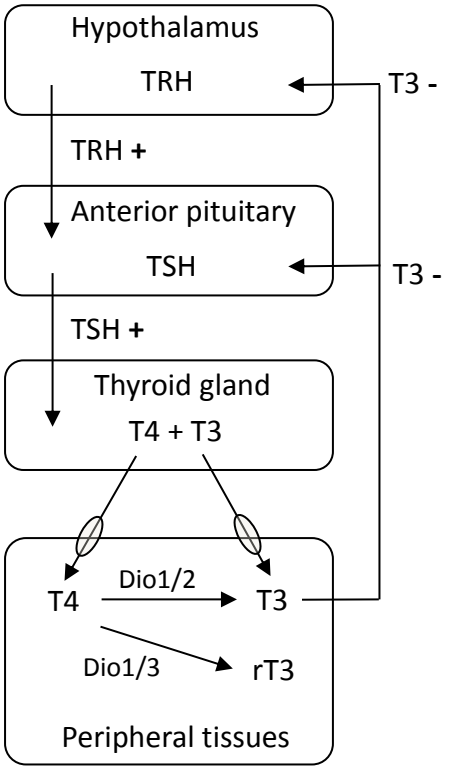

Figure 2 Overview of the hypothalamus-pituitary-thyroid (HPT) - axis and the systematic regulation of thyroid hormones (TH). After uptake of T4/T3 by target cells, T4 undergo deiodination by one of the deiodinases Dio1-3 resulting in active hormone T3 or inactive reverse T3 (rT3).

The gland itself is located at the front of the neck and is structurally butterfly shaped. The thyroid is made up of two main specific cell types, follicular and para-follicular cells. The former are responsible for producing TH. The thyroid gland is controlled through a feedback system involving the hypothalamus and the pituitary. The resulting regulatory circuit is called hypothalamus-pituitary-thyroid (HPT) – axis and refers to the close interaction between the three tissues/organs (Figure 2) [3]. The hypothalamus produces thyrotropin releasing hormone (TRH), a tripeptide binding to receptors in thyrotroph cells in the pituitary. Subsequently, TRH causes production and secretion of thyrotropin also called thyroid stimulating hormone (TSH). By binding to its receptor on follicular thyrocytes, TSH represents primary regulator of thyroid hormone production and secretion. The blood concentrations of the TH L-thyroxine (T4) and 3,3',5-triiodo-L-thyronine (T3) are predominantly controlled by a negative feedback system, where increased levels of circulating TH suppress the release of both TSH and TRH. Most of the circulating T4 in blood is bound to transport proteins, mainly serum albumin, transthyretin and thyroid hormone-binding globulin [4]. Only a very small fraction (0.03 % of T4) is unbound [4] and hence biological active [5]. Production of TH is based on the tyrosine-rich precursor protein thyroglobulin which is produced by the follicular thyrocytes and released into the so-called colloid by exocytosis. Iodine is transported into the cell *via* a Na^+/I^-symporter and shuttled across the apical membrane

into the colloid. Here, iodine is oxidized by thyroid peroxidase, and catalyzed by the same enzyme, covalently bound to the phenol rings of tyrosyl groups of the thyroglobulin. Adjacent tyrosine residues are enzymatically linked resulting in monoiodinated (MIT) and diiodinated (DIT) residues. Thyroglobulin re-enters the follicular cell by endocytosis initiated by binding of TSH to the TSH receptor on the basolateral membrane of the cells. The internalized thyroglobulin undergoes proteolytic digestion [6]. Generated T3 (MIT + DIT) and T4 (DIT + DIT) cross the follicular cell membrane and are released into the blood stream [5]. Thyroid hormones enter target cells *via* specific TH transporters [7]. Most of T3 which represents the active form of the hormone is produced by deiodination in the outer ring of T4. This reaction is catalyzed by both type I and type II deiodinases (DIO1 and DIO2). Deiodination occurring in the inner ring of T4 results in reverse T3 (rT3) which lacks known thyroid hormone receptor-mediated biological activity and therefore leads to inactivation of the hormone [8].

Currently, it is assumed that TH action is primarily exerted *via* nuclear thyroid hormone receptors (TR) [9]. The genes *THRA* and *THRB* encode different isoforms of the receptor. TRα1, TRβ1 and TRβ2 can bind T3[10]. Although *THRA* and *THRB* are generally widely expressed [11], they are differentially expressed in tissues and organs. The major isoform in brain, bone and heart is TRα1 whereas the beta-form is more abundant in liver, kidney and thyroid. Most actions of TH are initiated by binding of T3 to the nuclear T3 receptor which are bound to thyroid hormone response elements (TREs) in the promotor regions of TH target genes. TR can bind to TREs as homodimers, but more frequently as heterodimers with the retinoid X receptor (RXR) [12]. Besides, heterodimers with PPARα or liver X receptors (LXR) are also possible [12].

Binding of T3 results in modified interaction of TR with associated proteins, namely co-repressors and co-activators, and subsequently in altered target gene expression. By cell- and organ-specific TH uptake and activation as well as TH receptor synthesis, TH can induce tissue and cell specific responses. In doing so, T3 as the major ligand of nuclear TH receptors is metabolically most relevant.

T3 directly and indirectly influences the regulation of cholesterol synthesis and efflux. It induces 3-hydroxy-3-methyl-glutaryl coenzyme A reductase, thereby promoting cholesterol synthesis. Additionally, expression of the genes encoding low density lipoprotein (LDL) receptor and ApoA1 are strongly induced by T3, leading to increased

LDL-levels and consequently cholesterol uptake in periphery tissues and the liver [13]. The LDL receptor gene is also positively regulated by the transcription factor SREBP-2 which itself is a direct target of TH [14]. Degradation of cholesterol is achieved *via* transcriptional induction of the gene *CYP7A1* encoding cholesterol 7α-hydroxylase. This enzyme catalyzes the first and rate-determining step in the production of bile acid from cholesterol [15]. The gene encoding the key regulator for reverse cholesterol transport namely cholesteryl ester transfer protein also respond to changes in TH levels [16].

Besides lipid metabolism also carbohydrate metabolism is affected through TH. Effects of thyroid hormones on liver, white adipose tissue and skeletal muscle influence the plasma glucose level [17]. T3 stimulates gluconeogenesis by increasing the expression of phosphoenolpyruvate carboxykinase PCK1 [18] and glucose-6-phosphatase G6PC [19], two enzymes mediating rate-limiting steps in this pathway. Furthermore, TH can upregulate hepatic glucose production [20].

Additionally to the primary effect of T3 *via* transcriptional regulation, non-genomic effects of TH also play a role [21]. Thyroid hormones can interact with membrane integrin receptors and cytosolic TH receptors, resulting in the initiation of phosphorylation cascades [7].

A fine-tuned hormonal balance of T4 and T3 supports the maintenance of metabolic and physiological functions. In a broad range of diseases, TH levels are pathologically increased or decreased which results in a dysfunctional state. Thyroid diseases show diverse manifestations leading to functional impairments in hormonal balances. Depending on the systemic impact, hyper-and hypothyroidism are distinguished. Almost one-third of the world's population live in areas where the daily iodine intake is < 50 µg resulting in goiter, and in more extreme cases congenital hypothyroidism [1]. In contrast, thyroidal autoimmune diseases represent the predominant form in iodine-replete areas [1].

The physiological state associated with a normal functioning of the thyroid is referred to euthyroidism while hyperthyroidism is defined as a condition characterized by excessive production of TH by the thyroid. Patients suffering from hyperthyroidism present with increased endogenous levels of free T3 and T4 levels and a highly suppressed TSH level. In turn, thyrotoxicosis is defined by excessive thyroid hormone levels, regardless of the origin of the TH. The term thyrotoxicosis therefore includes hyperthyroidism.

The most frequent cause for hyperthyroidism in iodine-replete regions is Graves' disease. This condition is characterized by the presence of circulating autoantibodies directed against the TSH receptor, resulting in a constitutive stimulation by TSH, leading to increased synthesis of T4 and T3. Patients also demonstrate hypertrophy and hyperplasia of thyroid follicular cells causing an enlarged thyroid referred as goiter [22]. Hyperthyroid patients exhibit an increased basal metabolic rate, often accompanied by weight loss [22]. Already in 1930, reduced total cholesterol levels in serum were described for hyperthyroidism. In addition, hyperthyroid women were reported to exhibit lower HDL-cholesterol and ApoAI levels as compared to healthy controls [23]. Hyperthyroidism is also known to induce hepatic gluconeogenesis and glycogenolysis. The alanine transport into hepatocytes is increased during treatment with T4, resulting in an increased conversion of the amino acid to glucose [24]. For the *PCK1* mRNA an increase of 3.5fold was demonstrated in thyrotoxic compared to normal rats, indicating that hyperthyroidism is associated with increased glucose production due to increased gluconeogenesis [9].

Thyroid dysfunctions also affect the heart and cardiovascular system. T3 regulates several genes of cardiac myocytes including those encoding sarcoplasmic reticulum Ca^{2+} ATPase (SERCA2), phospholamban and the myosin heavy chains α and β, thereby influencing cardiac contractile function [25–27]. Additionally, T3 is involved in the regulation of multiple plasma-membrane located transporters like Na^{+}/K^{+} ATPase, thus modulating electrochemical characteristics of the myocardium [26]. In hyperthyroidism, cardiac contractility is enhanced which coincides with an increase in the blood volume, finally resulting in an augmented cardiac output [25,28]. Furthermore, tachycardia is frequently manifested clinically in patients with hyperthyroidism.

Besides the strong influences on the lipid and carbohydrate metabolism as well as heart and cardiovascular system, the impact of thyroid hormones on primary and secondary hemostasis leading to several coagulative dysfunctions is also of importance. An influence of hyperthyroidism on the levels of proteins involved in coagulation has already been described in the literature. One of the first reports was published 1987 by Orwoll *et al.* [29] describing connections between thyroid dysfunctions and abnormalities in hemostasis and coagulation. In hyperthyroid patients, increased activities of coagulation factor FVIII and levels of von Willebrand factor (VWF) were measured which normalized after treatment [30]. Furthermore, Erem *et al.* detected increased levels of fibrinogen,

VWF, coagulation factor IX and plasminogen activator inhibitor (PAI-1) in hyperthyroid patients indicating an pro-coagulative state [31]. Van Zaane *et al.* analyzed healthy volunteers treated with levothyroxine to induce hyperthyroidism [32]. Determination of multiple coagulation variables revealed increased levels of fibrinogen, VWF, coagulation factors VIII, IX, and X, as well as a pronounced increase of PAI-1 upon levothyroxine administration. All these findings suggested a shift in the hemostatic balance towards a hypercoagulable and hypofibrinolytic state. Additionally, altered clot structure is discussed to refer to an increased thrombotic risk in hyperthyroidism [33].

Hypothyroidism is a common disorder characterized by an underactive thyroid with insufficient production of TH. Primary hypothyroidism is caused by an inadequate function of the thyroid itself, mostly due to iodine deficiency. This causes elevated TSH levels combined with diminished T3 and T4. Thyroid autoimmune diseases represent the dominating cause for hypothyroidism. Importantly, Hashimoto's thyroiditis is characterized by migration of T lymphocytes in the thyroid contributing to the autoimmune process and destruction of the gland [34]. Besides, autoantibodies against specific thyroid antigens contribute to the disease progress. Autoantibodies against thyroid peroxidase and thyroglobulin are found in almost all patients with Hashimoto's disease [35]. The role of antibodies against the thyroid hormone receptor have been already mentioned in the context of Grave's disease, but the possibility of blocking the receptor activation instead of stimulating the receptor function should not be underestimated. Even with no or mild clinical symptoms, the condition should not be left untreated. Hypothyroid patients often gain weight owing to the reduced metabolic rate.

The disorder is also accompanied with hypercholesterolemia due to decreased LDL receptor expression in the liver resulting in impaired cholesterol uptake [25]. Lipid levels found in plasma are dependent on the metabolism of very-low density lipoprotein (VLDL) apolipoprotein B as a precursor of LDL [36]. Since cholesterol turnover and excretion is disturbed, increased ApoB levels can be observed.

As already described for hyperthyroidism, carbohydrate metabolism is also effected when inadequate TH release und distribution occur. In hypothyroidism the decreased availability of T3 leads to decreased glucose utilization by peripheral tissues [9]. Clinical manifestations according to the cardiovascular system are opposite to the signs in hyperthyroidism displayed as bradycardia, mild hypertension, cold intolerance and

fatigue. Due to decreased levels of thyroid hormones reduced SERCA2 activity can be observed leading to impaired calcium cycling and left ventricular diastolic dysfunction [26,37].

Like hyperthyroidism, condition of abnormally low TH levels has influence on the hemostasis in patients. Acquired von Willebrand syndrome is frequently observed in hypothyroidism characterized by reduced activity of coagulation factor VIII and von Willebrand antigen levels leading to a tendency of bleeding [38,39]. Egeberg as well as Simone *et al.* reported significant protein activity reductions in coagulation factors VIII, IX and XI [40,41]. In contrast, mild hypothyroidism is reported to be associated with hypercoagulative tendencies [42]. Subclinical and overt hypothyroidism can be also distinguished according the pattern of fibrinolytic activity. Low levels of plasminogen activator inhibitor (PAI-1) and high D-Dimer levels indicate elevated fibrinolytic activity in an overt disease state while high and low concentrations of PAI-1 and D-Dimers respectively suggest reduced fibrinolytic activity in subclinical conditions [43].

Animal models in research

Mice share many organ systems with humans, among these the endocrine system including the thyroid. Considering all research topics annually 115 million animals are used worldwide for experiments or to supply biomedical industry [44]. Therefore, it is important to emphasize the advantages when using animals in research. One point is the biological similarity of mice and men mirrored by 99 % of shared genome sequences between both species [45]. It is thus not surprising that many diseases affect both animals and humans. Further advantages address experimental procedures. By controlling diet, temperature and lighting, unwanted disturbance variables were kept at a minimum. Additionally, small animals like rodents have a shorter life cycle allowing studies over the whole lifespan and even across generations. When looking back in history, major progress in clinical research was achieved by using animals as study objects. One prominent example is the insulin treatment for patients suffering from Type I diabetes, first tested and validated in dogs and rabbits.

Animal models used in basic research are excellent objects to decipher molecular pathomechanisms. One big advantage is the opportunity to create specific knock-out strains to study the role of specific genes and their products.

As blood and brain physiology, nervous system, endocrine and exocrine secretion and, immunological responses are all systemically connected, various situations cannot be appropriately studied in *in vitro* settings due to the complexity of living organism. Therefore, research on whole organs and organ systems and consequently animal models remains unavoidable, even if the demand for alternatives such as tissue and cell culture models is rising. Besides the obvious harm and ethical concern questioning research on animals, other issues arose in the scientific community. The big central question concerns the transferability of specific animal research findings to humans. Seok *et al.* reported limited translational potential of mouse models of inflammation based on the low correlation in gene expression changes in patients compared to the corresponding mouse model [46]. Takao and Miyakawa who used the same data set for their analysis argued against this conclusion [47]. Thus, the evidence that animal models can be used to predict human disease outcome has to be carefully evaluated in each specific research question under investigation.

In thyroid research, there are several mouse models available for the investigation of systemic and organ specific TH effects. Availability of techniques for genetic manipulation of the mouse genome allowed for the construction of *Thra* and/or *Thrb* knockout mice with non-functional TH receptors, enabling the analysis of tissue specific actions of TH [10,48]. Many studies in the context of TH-induced changes in metabolism investigated gene expression patterns in terms of mRNA levels. Proteomic studies of TH action in metabolic active tissues or even in biofluids are not yet very prominent neither in animal models nor in humans. Earlier investigation of thyroidal dysfunctions focused on thyroid specific phenotypes e.g. the pathology of Graves' orbitopathy or thyroid cancer and related issues. Former studies of induced thyrotoxicosis analyzed side effects resulting from amiodarone intake [49]. Amiodarone is an antiarrhythmic drug used for the treatment of atrial fibrillation which is structurally similar to thyroxine and also contains iodine, resulting in thyroid-specific side effects.

The impact of T3 or T4 exposure on healthy volunteers was so far only investigated with respect to hemostasis. In a targeted approach, specific coagulation effectors and fibrinolytic proteins and genes were analyzed [32] addressing specific questions. However, an overall, unbiased view of TH action on the metabolism is still missing.

Brief insight in proteomics

The entirety of all proteins in a cell, tissue, organ or other physiological compartment at a specific time under defined conditions is referred to as the corresponding proteome [50]. While the idea of studying proteins in a holistic manner rose even earlier the term was introduced by Wilkins in 1994 [51]. The analysis of the proteome was called proteomics [52]. Since then, the terms proteome and proteomics have been widely adopted. Initially, the idea was to visualize all proteins of a proteome on a 2D gel [53,54]. Back then, the favored quantitative method in proteomics was the comparative 2D gel approach where differences in protein abundances were determined by comparing stained gel spots combined with protein identification *via* mass spectrometry [55]. Drawbacks associated with this technique include limited ability of detection of hydrophobic membrane proteins, extreme acidic and basic proteins, as well as proteins with very high and very low molecular mass [56]. Also, low abundant proteins were not covered due to limitations in loading capacity and staining sensitivity. Trying to overcome these restrictions in protein detection, non-gel based approaches were implemented and replaced 2D gel analysis for the analysis of complex proteome samples [57]. The gel free techniques involve two major strategies. First one is the top-down approach where intact proteins including post-translational modifications and alternative splice variants are preserved and analyzed [58]. Problems of this approach are the need of high sample amounts [59] and the limitations in obtaining data in a broad dynamic range [60].

Due to these limitations in top down proteomics, the bottom up technique, also called shotgun proteomics, has been the commonly used approach for proteome analyses for a long time. In this context quantitation can be accomplished by two different approaches either the use of stable isotope labelling or label-free techniques. Several labelling approaches can be incorporated into shotgun experiments. Common labelling techniques involve modified peptides with isobaric tags for relative and absolute quantification (iTRAQ) [61], labeling of proteins with isotope-coded affinity tags (ICAT) [62], stable isotope labeling by amino acids in cell culture (SILAC) [63], chemically synthesized peptide standards [64] or tandem mass tags (TMT) [65]. Often labeling is regarded as more accurate in quantitating protein abundances [66]. However, it cannot be applied easily to all types of samples. Additionally, labeling requires expensive chemicals, involves

extensive sample preparation and struggles with incompleteness [67]. In contrast, label-free approaches provide a higher dynamic range, offer higher proteome coverage and the number of experimental conditions to be compared is not restricted. Due to simple biochemical workflows and less time-consuming processing steps, this approach also allows the analyses of larger sample sets. For smaller amounts of sample material, it is also the method of choice.

Currently, two widely used strategies for quantification can be distinguished in the field of label free proteomics: (i) the spectral counting approach relying on the number of the fragment spectra identifying peptides of a certain protein [68]. (ii) the ion-intensity based approach whereby mass spectrometric signal intensities of peptide precursor ions belonging to a particular protein are measured and compared [69].

Mass spectrometric technologies continuously improved dramatically since 1994. During the past decade, proteomics evolved significantly. Proteomic tools are now also capable of addressing biomarker questions very effectively.

Plasma proteomics

In the context of thyroid dysfunction research, proteomic studies were not frequently used until now. Few exceptions addressed T3 effects on liver and skeletal muscle in hypothyroid rats [70,71]. Besides the analysis of the main target tissues of TH, the search for peripheral markers of thyroid dysfunction in plasma represents an excellent opportunity. Of all human tissues and bodyfluids plasma likely displays the most dynamic and most complex proteome [72] and was described to have great potential for detecting novel biomarkers [73]. Biofluids like plasma represent one focus of proteomics to investigate disease-specific alteration in protein pattern [74].

Plasma is defined as the cell-free liquid component of blood which in contrast to serum comprises all clotting factors. Water constitutes the majority of the plasma (up to 95 %) with proteins, glucose, electrolytes, hormones and breathing gas in solution. Plasma serves as protein stock and as systemic transport medium. It also plays a vital role by maintaining the colloid-osmotic pressure and protecting the body against infections. In 1984, Putman *et al.* described true plasma proteins as those fulfilling their function in the circulation [75]. Classification of plasma proteins has been refined by Anderson *et al.* in 2002 [76]: (1) Tissue-secreted proteins acting in plasma are defined as *classical plasma*

proteins and originate primarily from the liver. One defining feature of those proteins is a molecular mass of larger than 45 Da exceeding the kidney filtration cutoff which ensures a relatively long half-life in the circulation. (2) *Immunoglobulins* acting functionally in plasma but representing a specific unique protein class because of their high complexity and are produced in and secreted from B-lymphocytes. (3) *Long distance receptor ligands* encompassing all classical peptide and protein hormones. (4) *'Local' receptor ligands* which include cytokines and other short distance mediators of cellular responses. (5) *'Temporary' passengers* which covers non-hormone proteins using the circulation as transport compartment, e.g. secretory lysosomal proteins that are taken up *via* other receptors. Another important plasma protein class is defined as *tissue leakage products* (6). These originally cellular proteins are released into plasma after cell damage or cell lysis. Particularly this group might contain many putatively valuable diagnostic biomarkers. (7) Yet another class is named *aberrant secretions*. It contains proteins with no obvious function in plasma, which are released from tumor or other diseased tissue into the circulation.

As the withdrawing of blood samples is minimally invasive and can easily be performed in the clinical routine, plasma represents a well established source for diagnostic purposes and a promising source for biomarker research. In contrast, the collection of material from tissue biopsies is generally associated with higher risk for the donors. Already in 2002, Anderson proclaimed that the human plasma proteome holds the promise of a revolution in disease diagnostics and therapeutic monitoring [76]. On the other hand, it has to be emphasized that plasma proteome analyses are challenging. Plasma represents the most difficult-to-handle protein-containing sample type due to the large portion of serum albumin (up to 55 %) and a wide dynamic range with up to 10 orders of magnitude in protein concentrations.

Some criteria for an optimal biomarker were described in the literature. First, it should be cost-effective and easily measurable. Furthermore, the alterations in level of a protein biomarker should ideally provide diagnostic information facilitating medical decision. As mentioned above proteomic studies in search for suitable biomarkers are well established in the field of cardiovascular research. For cardiovascular diseases, several circulating biomarkers were evaluated, e.g. cardiac troponin T and I which are used for the diagnosis of myocardial infarction [77]. Technical developments and software tools allow

quantitative assessment of the proteome. Today, proteomics has become a powerful tool to unravel and evaluate molecular changes presented in different disease conditions. This provides the possibility of screening for biomarkers which can be of advantage (i) for diagnosis of the disease, (ii) for the assessment of the disease progression, (iii) for monitoring therapy effects and (iv) for understanding molecular mechanisms underlying the disease development.

Aims of the study

TH play a crucial role in the coordination of normal development and growth, affect the cardiovascular system, and are involved in many metabolic regulatory mechanisms in almost all tissues. Hence, TH imbalance causes a broad spectrum of effects, mostly manifested in pathologically increased (hyperthyroidism) or decreased (hypothyroidism) TH levels. Determination of the thyroid state is routinely based on the assessment of the classical serum markers TSH and free T4 which, however, entails several drawbacks. Furthermore, elucidation of the pleiotropic effects of TH on multiple molecular pathways is mostly based on cell culture, tissue and rodent models. In humans, several studies investigated the TH impact on plasma proteins in a targeted approach, but a comprehensive characterization of human biofluids has not been performed until now. Therefore, the focus of the present work was to elucidate the plasma proteome in the context of thyroid diseases. To gain more insight into this issue, a proteome analysis of an experimentally induced mid-term human thyrotoxicosis model was performed. The detection of proteins exhibiting free T4-associated plasma levels allowed the identification of specific TH-related molecular signatures. Additionally, protein alterations in the plasma of patients with reduced TH levels were analyzed, where this approach represented a study design of a human mid-term hypothyroidism model, opposite to the thyrotoxicosis study.

The second objective regarding the influence of TH-related diseases focused on murine studies. Mice as animal models are well-established for disease research and allow the study of underlying pathomechanisms. So far, several murine studies analyzed exclusively the hepatic gene expression profile in the context of TH-induced changes in metabolism. However, comparable proteome studies have not been performed yet. Therefore, to address the impact of thyroid dysfunctions on the murine plasma proteome, two studies

were performed in the framework of this thesis. The results of both murine and human studies might contribute to a deeper understanding of TH action on metabolism and specific molecular pathways.

2 MATERIAL & METHODS

2.1 Human and murine studies

2.1.1 Biological samples from human clinical studies

There are established laboratory tests for the evaluation of thyroid function and differentiation of causes for thyroid dysfunctions. Currently diagnosis regarding dysfunction and treatment options largely relies on the determination of TSH and free T4. However, under certain specific conditions such as subclinical disease states their diagnostic value is limited. Therefore, for the screening for novel peripheral biomarkers of thyroid function and characterization of TH-associated signatures an untargeted proteome approach was used. The respective experimental studies were performed at the University of Lübeck, Germany. Blood sampling was done using EDTA-vacutainers. Subsequently, plasma was send on dry ice and stored at -80 °C until use.

The first study included 16 healthy male volunteers. The Body mass index of the participants ranged from 21 to 30 kg/m^2, the age from 22 to 34 years. All volunteers filled out thyrotoxicosis questionnaires. Furthermore, 24 h blood pressure and pulse rate activity were measured. All clinical data and data from standard laboratory measurements were summarized in Table 1.

The second study included 15 patients suffering from manifested hypothyroidism. Hashimoto's thyroiditis also known as chronic lymphocytic thyroiditis caused the condition in 13 cases. The remaining two patients suffered from Graves' disease also known as toxic diffuse goiter. The majority of patients (13/15) are women and one patient has undergone thyroidectomy. The age ranged from 19 to 54 years. All clinical collected data are summarized in Table 2.

Both studies have been approved by the ethics committee of the University of Lübeck and written informed consent was received from all participants prior to the study. All medical and basic examinations were performed according to the WMA Declaration of Helsinki.

Table 1 Clinical characteristics of all participants during the study of experimental human thyrotoxicosis. Mean and standard deviation (SD) of measured data at the different time points (t1-t5). t1: baseline; t2 and t3: 4 and 8 weeks after levothyroxine treatment; t4 and t5: 4 and 8 weeks after stopping the treatment.

Characteristics	**t1**	**t2**	**t3**	**t4**	**t5**
Age [years]			27.8 (3.8)		
BMI [kg/m^2]			24.1 (2.4)		
FT4 [pmol/l]	13.2 (1.4)	28.6 (6.5)	25.9 (5.7)	11.5 (1.5)	12.8 (1.5)
FT3 [pmol/l]	5.27 (0.51)	9.19 (2.01)	8.92 (2.25)	4.61 (0.33)	4.86 (0.55)
TSH [mU/l]	2.10 (1.02)	0.02 (0.03)	0.01 (0.01)	2.30 (1.31)	2.18 (0.90)
SHBG [nmol/l]	30.2 (10.2)	50.6 (16.2)	55.9 (16.3)	36.3 (11.8)	29.3 (9.3)
CYTC [mg/l]	0.68 (0.06)	0.79 (0.08)	0.86 (0.12)	0.71 (0.07)	0.68 (0.06)
Serum glucose [mmol/l]	5.18 (0.35)	5.22 (0.42)	5.26 (0.39)	5.09 (0.31)	5.18 (057)
Insulin [µU/l]	8.35 (3.63)	7.94 (4.32)	7.78 (3.62)	8.33 (4.06)	8.07 (3.38)
HDL-Chol. [mmol/l]	1.43 (0.27)	1.21 (0.20)	1.23 (0.25)	1.46 (0.29)	1.43 (0.37)
LDL-Chol. [mmol/l]	2.70 (0.72)	2.15 (0.57)	2.27 (0.53)	2.91 (0.75)	2.76 (0.79)
Cholesterol [mmol/l]	4.53 (0.75)	3.81 (0.61)	4.06 (0.61)	5.04 (0.70)	4.61 (0.68)
Triglycerides [mmol/l]	1.26 (0.76)	1.14 (0.58)	1.29 (0.56)	1.31 (0.63)	1.35 (0.82)
ALT [µkatal/l]	0.51 (0.21)	0.38 (0.10)	0.65 (0.42)	0.61 (0.29)	0.50 (0.14)
AST [µkatal/l]	0.49 (0.41)	0.34 (0.14)	0.43 (0.17)	0.43 (0.14)	0.43 (0.23)
GGT [µkatal/l]	0.41 (0.09)	0.45 (0.11)	0.49 (0.11)	0.45 (0.15)	0.43 (0.11)
Total Bilirubin [µmol/l]	12.5 (8.4)	12.6 (8.7)	13.5 (7.3)	11.9 (6.4)	11.9 (7.3)
Direct Bilirubin [µmol/l]	2.86 (1.35)	3.04 (1.35)	3.28 (1.24)	2.84 (1.03)	3.03 (1.39)
Complement C3 [g/l]	1.15 (0.27)	1.21 (0.16)	1.17 (0.11)	1.10 (0.14)	1.11 (0.14)
Complement C4 [g/l]	0.24 (0.06)	0.25 (0.05)	0.24 (0.05)	0.23 (0.05)	0.24 (0.05)

FT4 free thyroxine, *FT3* free triiodothyronine, *TSH* thyrotropin, *SHBG* sex hormone-binding globulin, *CYTC* cystatin C, *HDL* high density lipoprotein, *LDL* low density lipoprotein, *Chol.* Cholesterol, *ALT* alanine aminotransferase, *AST* aspartate aminotransferase, *GGT* γ-glutamyl transpeptidase

Table 2 Clinical characteristics of all patients suffering from hypothyroidism. Mean and standard deviation (SD) of measured data is displayed at the different time points (t1-t5). t1: baseline under L-T_4 medication; t2 and t3: 4 and 8 weeks under reduced medication; t4 and t5: 4 and 8 weeks after returning to previous medication.

Characteristics	t1	t2	t3	t4	t5
Age [years]			36.2 (12.3)		
FT4 [pmol/l]	16.29 (2.23)	13.96 (2.23)	14.12 (2.33)	16.37 (2.19)	16.75 (3.06)
FT3 [pmol/l]	3.89 (0.52)	3.52 (0.47)	3.57 (0.62)	4.00 (0.53)	4.02 (0.37)
TSH [mU/l]	2.14 (2.24)	11.08 (20.24)	14.87 (23.25)	2.55 (1.98)	5.46 (13.56)
SHBG [nmol/l]	48.8 (29.6)	39.6 (27.9)	41.5 (27.4)	41.8 (30.3)	29.4 (29.7)
CYTC [mg/l]	0.73 (0.11)	0.72 (0.09)	0.71 (0.11)	0.74 (0.10)	0.74 (0.10)
Serum glucose [mmol/l]	4.88 (0.48)	5.00 (0.53)	4.87 (0.44)	4.91 (0.40)	4.95 (0.53)
HDL-Chol. [mmol/l]	1.65 (0.50)	1.70 (0.50)	1.47 (0.44)	1.67 (0.43)	1.65 (0.41)
LDL-Chol. [mmol/l]	2.68 (0.62)	2.82 (0.66)	2.79 (0.67)	2.69 (0.57	2.68 (0.71)
Cholesterol [mmol/l]	5.03 (0.76)	5.25 (0.72)	5.30 (0.82)	5.03 (0.72)	4.07 (0.72)
Triglycerides [mmol/l]	1.18 (0.38)	1.25 (0.36)	1.24 (0.49)	1.17 (0.46)	1.20 (0.32)
ALT [µkatal/l]	0.44 (0.24)	0.47 (0.30)	0.38 (0.14)	0.43 (0.21)	0.48 (0.30)
AST [µkatal/l]	0.32 (0.07)	0.34 (0.11)	0.30 (0.07)	0.29 (0.07)	0.34 (0.11)
GGT [µkatal/l]	0.46 (0.18)	0.49 (0.27)	0.41 (0.11)	0.47 (0.21)	0.51 (0.30)
Complement C3 [g/l]	1.18 (0.17)	1.18 (0.18)	1.12 (0.15)	1.16 (0.18)	1.15 (0.18)
Complement C4 [g/l]	0.25 (0.08)	0.24 (0.07)	0.23 (0.07)	0.23 (0.06)	0.24 (0.07)

FT4 free thyroxine, *FT3* free triiodothyronine, *TSH* thyrotropin, *SHBG* sex hormone-binding globulin, *CYTC* cystatin C, *HDL* high density lipoprotein, *LDL* low density lipoprotein, *Chol.* Cholesterol, *ALT* alanine aminotransferase, *AST* aspartate aminotransferase, *GGT* γ-glutamyl transpeptidase

2.1.2 Biological samples from murine studies

For the animal studies 3-4 months old male C57BL/6 wild type mice were used. All mice were individually housed on a 12/12 h light/dark cycle at 21-22 °C and had *ad libitum* access to standard diet and water. Animal care procedures were in accordance with the guidelines set by the European Community Council Directives (86/609/EEC) and approved by Stockholm's Norra Djurförsöksetiska Nämnd.

Both studies were carried out within corporation projects with the University of Lübeck, Germany.

Mice of the transient thyrotoxicosis study were assigned to a control, T4 and T4 recovery group of 8 animals each. While the control group stayed untreated during the study

period, both T4 and T4 recovery group received oral dosages of T4 by T4-containing drinking water (1 mg/l in 0.1 % in BSA containing tap water) for 14 days. At this time point plasma samples were obtained from the T4 group and the control group while mice of the T4 recovery group were maintained in cages for another period of 14 days with no T4 in their drinking water. Blood samples were obtained from these animals 28 days after the start of the experiment. Mean TH levels of the animals and other characteristics are summarized in Table 3.

Table 3 Characteristics of mice included in the study of transient thyrotoxicosis. Mean and standard deviation (SD) of measured data is displayed for the three different groups.

Characteristics	Controls	T4 group	T4 recovery group
TT4 [µg/dl]	4.94 (0.38)	17.63 (2.14)	5.37 (0.36)
TT3 [ng/ml]	1.11 (0.10)	2.55 (0.20)	0.98 (0.10)
Weight before death [g]	30.15 (1.23)	32.74 (1.05)	29.54 (1.13)
Food intake last week [g]	47.03 (9.16)	44.95 (7.74)	29.73 (1.65)
Mean food intake per day [g]	6.72 (1.31)	6.42 (1.10)	4.25 (0.25)
Water intake last week [g]	38.99 (4.55)	52.56 (4.65)	29.46 (2.51)
Mean water intake per day [g]	5.57 (0.65)	7.51 (0.66)	4.21 (0.36)

TT4 total thyroxine, *TT3* total triiodothyronine

In the second murine study the effects of T4/T3-induced hyperthyroidism and MMI/$KClO_4$-induced (methimazole/potassium perchlorate) hypothyroidism were investigated. All supplements were supplied in the drinking water - 1 mg/l T4, 0.5 mg/l T3 and 0.1 % MMI/0.2 % $KClO_4$. All mice were sacrificed after 14 days (control/T4/T3 group) and 21 days (MMI/ $KClO_4$ group), respectively. Mean TH levels of included mice can be found in Table 4.

Table 4 Mean TH levels of mice included in the study of hyper- and hypothyroidism. Mean and standard deviation (SD) of measured data is displayed for the four different mice groups.

Group	TT4 [µg/dl]	TT3 [ng/ml]
Controls	1.38 (0.75)	1.66 (0.38)
T3 group	0.12 (0.04)	8.36 (0.44)
T4 group	10.42 (0.99)	3.42 (0.49)
MMI/$KClO_4$ group	0.10 (0.00)	0.92 (0.25)

TT4 total thyroxine, *TT3* total triiodothyronine

2.1.3 Human primary hepatocytes

Cryopreserved human primary hepatocytes were purchased from KaLy cell (Plobsheim, France). Three different donors were chosen according to their phenotypical data (race [Caucasian], gender [male] and age [45-48 years]) and grown following the manufacturer's protocol (see 2.3.2).

2.2 Materials

2.2.1 Chemicals, enzymes & kits

Table 5 Chemicals, enzymes and kits

Chemical	Company
2-Propanol	Carl Roth, Karlsruhe, Germany
Acetic acid	Carl Roth, Karlsruhe, Germany
Acetone	Merck Millipore, Darmstadt, Germany
Acetonitrile	J.T. Baker, Inc., Deventer, Netherlands
Ammonium bicarbonate	Sigma-Aldrich, St. Louis, Mo, USA
Bovine serum albumin	Sigma-Aldrich, St. Louis, Mo, USA
Bradford reagent	Bio-Rad Laboratories, Hercules, CA, USA
Buffer A/Buffer B for MARS application	Agilent Technologies Inc, Santa Clara, CA, USA
Chloroform	Carl Roth, Karlsruhe, Germany
Dimethylsulfoxide	Sigma-Aldrich, St. Louis, Mo, USA
Dithiothreitol	Thermo Fisher Scientific Inc., Waltham, MA, USA
ELISA kit, AssayMax™ human factor IX (Cat. # EF009-1)	Assaypro, St. Charles, MO, USA
ELISA kit, AssayMax™ human factor XIII (Cat. # EF013-1)	Assaypro, St. Charles, MO, USA
Ethanol	Carl Roth, Karlsruhe, Germany
Guanidine hydrochloride	Sigma-Aldrich, St. Louis, Mo, USA
Human hepatocyte thawing medium	KaLy Cell, Plobsheim, France
Human hepatocyte seeding medium	KaLy Cell, Plobsheim, France
Human hepatocyte maintenance medium	Primacyt, Schwerin, Germany
Iodoacetamide	Sigma-Aldrich, St. Louis, Mo, USA
L-thyroxine	Sigma-Aldrich, St. Louis, Mo, USA
Phosphate buffered saline 10x	PAA Laboratories, Pasching, Austria
Sodium hydroxide	Carl Roth, Karlsruhe, Germany
Sodium chloride	Carl Roth, Karlsruhe, Germany
Thiourea	Sigma-Adrich, St. Louis, Mo, USA
Trichloroacetic acid	Carl Roth, Karlsruhe, Germany
TRIzol®	Thermo Fisher Scientific Inc., Waltham, MA, USA
Trypan blue staining, 0.4 %	Thermo Fisher Scientific Inc., Waltham, MA, USA
Trypsin	Promega, Madison, WI, USA
Urea	Sigma-Aldrich, St. Louis, Mo, USA
Water, HPLC-grade	J.T. Baker Inc., Deventer, Netherlands

2.2.2 Specific accessories

Table 6 Specific accessories

Accessory	Company
µC18-columns, ZipTip®	Merck Millipore, Darmstadt, Germany
Centrifugal filter units, Ultrafree® 0.22 µm	Merck Millipore, Darmstadt, Germany
Culture dish (6-well plate, collagen-coated)	Primacyt, Schwerin, Germany
Glass vial 1.5 ml + micro insert 0.1 ml with septum or screw cap 8 mm	VWR International, Darmstadt, Germany
Multi affinity removal column human 6	Agilent Technologies Inc, Santa Clara, CA, USA
Multi affinity removal column mouse 3	Agilent Technologies Inc, Santa Clara, CA, USA
Neubauer improved counting chamber	Marienfeld, Lauda-Königshofen, Germany
Pipette tips, low protein binding (epT.I.P.S. 10 µl/1000 µl)	Eppendorf, Hamburg, Germany
Pipette tips, low protein binding (stack pack 100 µl)	Sarstedt, Nürnbrecht, Germany
Reaction tube, low protein binding (0.65 ml, 1.7 ml)	Sörensen™ BioScience Inc., Salt Lake City, UT, USA

2.2.3 Instruments & accessories for mass spectrometry

Table 7 Instruments and accessories used for mass spectrometry

Instrument/Accessory	Company
Acclaim™ PepMap 100-C18 (2 cm x 75 µm, 3 µm, 100 Å), pre-column	Thermo Fisher Scientific Inc., Waltham, MA, USA
Accucore 150-C18 (25 cm x 75 µm, 2.6 µm, 150 Å), analytical column	Thermo Fisher Scientific Inc., Waltham, MA, USA
Dionex UltiMate® 3000, HPLC	Thermo Fisher Scientific Inc., Waltham, MA, USA
LTQ-Orbitrap Velos™, mass spectrometer	Thermo Fisher Scientific Inc., Waltham, MA, USA
NanoAcquity BEH130 C18 (10 cm x 100 µm, 1.7 µm), analytical column	Waters Corporation, Milford, MA, USA
NanoAcquity, UPLC	Waters Corporation, Milford, MA, USA
NanoAcquity UPLC 2G-V/Mtrap Symmetry C18 (2 cm x 180 µm, 5 µm), pre-column	Waters Corporation, Milford, MA, USA
Nanospray Flex™ Ion source	Thermo Fisher Scientific Inc., Waltham, MA, USA
PicoTip® Emitter	New Objective Inc., Woburn, MA, USA
TriVersa NanoMate	Advion Inc., Ithaca, NY, USA
Q Exactive™ Orbitrap, mass spectrometer	Thermo Fisher Scientific Inc. Waltham, MA, USA

2.2.4 Software

Table 8 Software

Software	Company
32 Karat software Version 7.0	Beckman Coulter, Brea, CA, USA
Chromaster software 1.1	VWR International, Darmstadt, Germany
Genedata Refiner MS Version 7.6.6 – 10.0.3	Genedata AG, Basel, Switzerland
Genedata Analyst Version 7.6.6 – 10.0.3	Genedata AG, Basel, Switzerland
GraphPad Prism 5	GraphPad Software Inc., La Jolla, CA, USA
Ingenuity Pathway Analysis Version 31813283	QIAGEN, Hilden, Germany
MaxQuant 1.5.3.8	Cox group, Max Planck Institute of Biochemistry, Martinsried, Germany
Microsoft Office 2013	Microsoft, Redmond, WA, USA
RStudio	RStudio Inc., Boston, MA, USA
SkanIt RE for Varioskan Flash 2.4.3	Thermo Fisher Scientific Inc., Waltham, MA, USA
Swift II	GE Healthcare, Issaquah, WA, USA
Xcalibur 2.1	Thermo Fisher Scientific Inc.

2.2.5 Composition of solutions

Table 9 Composition of solutions

Buffer	Quantity	Composition
Dithiothreitol (10 ml, 25 mM)	0.375 g 10 ml	dithiothreitol ammonium bicarbonate (20 mM) solution in HPLC grade water
Guanidine hydrochloride (500 ml, 0.3 M)	14.3 g 475 ml 25 ml	guanidine hydrochloride 100 % ethanol HPLC grade water
Iodoacetamide (1 ml, 100 mM)	0.018 g 1 ml	iodoacetamide ammonium bicarbonate (20 mM) solution in HPLC grade water
Thyroxine stock solution (500 µl, 12.9 mM)	5 mg 50 µl 450 µl	Thyroxine Sodium hydroxide (1 M) solution in HPLC grade water Sodium hydroxide (0.4 M) solution in HPLC grade water
Thyroxine (32.5 ml, 100 µM)	250 µl 32.25 ml	Thyroxine stock solution HPLC grade water
1x UT solution (4 ml)	1.92 g 0.61 g 2 ml	urea thiourea HPLC grade water

Table 10 LC solvent compositions for mass spectrometric applications

LC buffer	Composition
Solvent A_1	5 % ACN 0.1 % acetic acid in HPLC grade water
Solvent B_1	0.1 % acetic acid in ACN
Solvent A_2	2 % DMSO 2 % ACN 0.1 % acetic acid in HPLC grade water
Solvent A_3	0.5 % DMSO 2 % ACN 0.1 % acetic acid in HPLC grade water
Solvent B_2	5 % DMSO 0.1 % acetic acid in ACN

2.3 Methods

2.3.1 Immunoassays

All immunoassays were performed at the Institute for Clinical Chemistry and Laboratory Medicine, University Medicine Greifswald, Germany. An exception was the measurement of human factor IX plasma levels using an enzyme linked immunosorbent assay.

Thyroid hormones and thyrotropin

Serum levels of free triiodothyronine (free T3) and free thyroxine (free T4) as well as thyrotropin (TSH) were measured using immunoassays on a Dimension VISTA system (Siemens). The functional sensitivity was 0.005 mU/l for TSH, 0.77 pmol/l for FT3 and 1.3 pmol/l for FT4.

Proteins (SHBG, cystatin C, complement factors C3 and C4, factor IX and XIII)

Serum levels of sex hormone-binding globulin (SHBG) were determined *via* a chemiluminescent enzyme linked immunosorbent assay. Measurement was carried out on an Immulite 2000XPi analyzer. The functional sensitivity was 0.02 nmol/l. Serum cystatin C (CYTC) was measured using a nephelometric assay on a Dimension Vista® system (Siemens) with a functional sensitivity of 0.05 mg/l. The determination of the levels of human complement factors C3 and C4 was performed using a Flex® reagent cartridge on the same system. Using specific antibodies both proteins can form immune complexes that are able to scatter transmitted light. Measurement is based on the dependency of scattered light intensity and protein concentration. Plasma levels of both factor XIII (F13) and factor IX (F9) were determined using an ELISA kit (AssayMax™ human factor IX and XIII, Assaypro) with a sensitivity of 2.5 ng/ml and 1.56 ng/ml, respectively.

Enzyme linked immunosorbent assay (ELISA) of human factor IX

Plasma levels of human factor IX were measured using an ELISA kit (AssayMax™ human factor IX, Assaypro). This assay employs a quantitative sandwich enzyme immunoassay technique that measures whole length FIX. The provided 96-well plate was pre-coated with a polyclonal antibody specific for FIX. The assay was performed as described in the manufacturer's protocol. Briefly, a human factor IX standard solution (100 ng/ml) was

used to prepare a serial dilution series in the range of 1.563 ng/ml to 100 ng/ml. The provided dilution buffer served as a blank (0 ng/ml).

Undepleted plasma samples of patients suffering from hypothyroidism were diluted 1:500 in 1x dilution buffer. Fifty µl of each diluted sample and standard was added in duplicates onto the pre-coated 96-well plate. After incubation for 2 h at room temperature wells were washed five times with 1x washing buffer. To each well 50 µl of biotinylated human factor IX antibody was added and incubated for 1 h. Wells were washed again before loading 50 µl of streptavidin-peroxidase conjugate. The washing step was repeated after 30 min and subsequently 50 µl of chromogen substrate was added. The development of color density was interrupted after 10 min by adding 50 µl of stop solution to each well. The absorbance was measured immediately at a wavelength of 450 nm using a Varioskan™ Flash plate reader. The plasma levels of FIX were calculated *via* the standard curve which was determined by regression analysis using a four-parameter logistic curve-fit.

2.3.2 Methods used for analysis of human primary hepatocytes

For cultivation of the human hepatocytes the manufacturer's instructions (KaLy-Cell) were followed. Initially, the supplied thawing medium and seeding medium were pre-warmed to 37 °C before starting the cultivation. For revitalization, cells in cryo-vials were thawed quickly at 37 °C in a water bath. Whole content of the vial was poured into 40 ml of thawing medium, the vial rinsed with medium and volume filled up to 50 ml afterwards. The cell suspension was gently inverted prior to centrifugation for 25 min at 22 °C and 170 x g. The supernatant was removed by decanting without disturbing the cell pellet. Cells were loosed by carefully flicking the bottom of the tube. For resuspension of the cells 2-5 ml seeding medium were used.

After counting the viable cells, cell suspension was adjusted to a concentration of 0.76 Mio cells/ml. Two ml were plated on collagen coated 6-well plates resulting in a total cell number of 1.5 Mio cells/well. Cells were allowed to adhere for 6 h at 37 °C and 5 % CO_2 in a humidified incubator. Subsequently, the medium was removed and 2 ml fresh seeding medium were applied without a previous washing step. After cultivation overnight seeding medium was exchanged with human hepatocyte maintenance medium and grown for another 8 h at 37 °C and 5 % CO_2 in a humidified incubator.

Determination of cell count

The determination of the cell count of human primary hepatocytes was performed by a Neubauer improved chamber. Such a chamber consists of nine great squares, each with an area of 1 mm^2 and a depth of 0.1 mm. For determination of cell count the central square was used. For counting of viable cells only, the Trypan blue exclusion method was applied. Cell suspension and Trypan blue were mixed in a ratio of 1:1. The solution was then transferred to the counting chamber and the viable cells (not stained blue) were counted. To calculate the cell count per µl the number was multiplied by the dilution factor and divided by the area and depth of the chamber (Equation 1).

$$cells\ per\ \mu l = \frac{cell\ count}{1\ mm^2\ (area)\ x\ 0.1\ mm\ (depth)}\ x\ 2\ (dilution\ of\ Trypan\ blue)$$

Equation 1 Calculation of cells per volume using the Neubauer improved counting chamber.

Induction experiment

After the cells reached confluence they were induced with T4. Prior to stimulation, maintenance medium was removed and cells were washed with 1 ml PBS. For induction, 1 ml of human hepatocyte maintenance medium supplied with 10 nM T4 was added. Cells cultivated with the same medium without supplementary thyroxine served as controls. Media were exchanged every 24 h.

Sampling

Cells as well as culture supernatants should be collected for subsequent analyses. At desired time points the supernatant was transferred into reaction tubes. Prior to harvesting, cells were washed twice with 1 ml PBS. Next, 700 µl of TRIzol® reagent was added to each well of the 6-well plate. To remove the cell layer properly a cell scraper was used. Cell lyses was supported by extensive pipetting before collecting the lysate in reaction tubes. Both, supernatants and cell lysates were immediately frozen in liquid nitrogen and stored at -80 °C until further use. To conduct all further preparations without splitting of the sample, 2 ml reaction tubes were used.

After defrosting samples were incubated 5 min at room temperature before 140 µl chloroform was added. Samples were shaken and incubated for 3 min at room

temperature. For appropriate phase separation, samples were centrifuged for 15 min at 4 °C and 12000 x *g*. The aqueous phase was transferred into a new reaction tube and stored for RNA isolation. For DNA precipitation 210 µl of 100 % ethanol was added and the sample mixed properly. After incubation (3 min, room temperature) samples were centrifuged for 5 min at 4 °C and 2000 x *g* to pellet DNA. The obtained protein containing supernatant was transferred to a new tube and mixed with 1.05 ml 100 % 2-propanol. For precipitation samples were incubated for 10 min at room temperature and proteins subsequently pelleted by centrifugation for 10 min at 4 °C and 12000 x *g*. The protein pellets were mixed with 0.3 M guanidine hydrochloride in 95 % (v/v) ethanol and incubated 20 min at room temperature with gentle movement on a tumbling shaker (70 rpm). After centrifugation for 5 min at 4 °C and 7500 x *g* the washing step was repeated two more times. Subsequently, 1.4 ml 100 % ethanol was added, the sample was vortexed, incubated again for 20 min at 70 rpm on the tumbling shaker and centrifuged for 5 min at 4 °C and 7500 x *g*. Once the supernatant was removed, the resulting proteins were air dried and dissolved in 100-200 µl 1x urea/thiourea (UT) solution according to the size of the pellet. After incubation for 30 min at 20 °C and 1400 rpm in a thermomixer, non-soluble particles were pelleted by centrifugation for 10 min at 4 °C and 10000 x *g*. The protein containing fraction was transferred to a new reaction tube and stored at -80°C.

Precipitation of secreted proteins in the supernatant using ethanol

For precipitation purposes, the protocol of Colantonio et al. was used [78]. Originally intended for the albumin depletion in serum, it was adopted to enrich proteins secreted by human primary hepatocytes into the culture supernatant and simultaneously deplete bovine serum albumin from the sample.

First, 50 µl of 1.1 M NaCl were added to 500 µl supernatant to a final concentration of 0.1 M NaCl. After incubation on a rotation shaker for 1 h at 4 °C, 420 µl 96 % (v/v) ethanol were added slowly together with 30 µl A.dest. and incubated again under the same conditions. Afterwards, samples were centrifuged at 13.000 rpm at 4 °C for 45 min. Now, the supernatant contained the main fraction of albumin. Thus, after removing the supernatant, pellet was dissolved in 30 µl 1x urea/thiourea (UT) solution and further processed for analysis.

2.3.3 Plasma specific sample preparation

Depletion of plasma proteins

Depletion of six highly abundant proteins (serum albumin, serotransferrin, immunoglobulin G, immunoglobulin M, haptoglobin and α1-antitrypsin) was performed using a multi affinity removal column (human MARS 6) according to a modified manufacture's protocol (Agilent). The column was operated on a VWR Hitachi Chromaster HPLC or on the 2nd dimension of a PF2D system. Mouse plasma samples were processed in a similar manner, using a MARS 3 column to remove 3 highly abundant proteins (serum albumin, serotransferrin, immunoglobulin G).

Plasma samples were thawed on ice. Thirty µl of plasma were diluted in 90 µl of buffer A (Dilution 1:4), passed through a 0.22 µm spin filter and centrifuged for 2 min at 4 °C and 13000 rpm to remove particles. Eighty µl of the remained volume were loaded on a column with buffer A at a flow rate of 0.25 ml/min for 9 min. The unbound fraction which is referred to as the *flow through fraction* was collected between 2.0 – 4.0 min. Bound highly abundant proteins were eluted from the column with buffer B at a flow rate of 1 ml/min for 3.5 min. The *elution fraction* was also collected and both fractions were stored at -80 °C until further processing.

Protein precipitation

Precipitation of proteins present in the *flow through fraction* (depleted plasma) was achieved using trichloroacetic acid (TCA-final concentration 15 %) which was found to be the most efficient method to precipitate proteins from diluted solutions (personal communication with Leif Steil). To break tertiary protein structure and reduce proteins, initially dithiothreitol (DTT) was added to a final concentration of 8 mM to the sample. The solution was vortexed properly and incubated for 30 min at 37 °C followed by the addition of 100 % (w/v) TCA to a final concentration of 15 % (v/v). After incubation on ice for 1 h the sample was centrifuged for 45 min at 4 °C and 13000 rpm. The supernatant was discarded and the protein pellets were washed twice with 500 µl ice-cold acetone followed by a centrifugation step (15 min, 4 °C and 13000 rpm). Afterwards, the pellets were dried in a vacuum centrifuge (*Speedvac*) before they were dissolved in 1x UT

solution. For better solubilization the samples were incubated for 20 min at 20 °C and 1400 rpm in a thermomixer.

2.3.4 Sample preparation for mass spectrometry

Determination of protein concentration

Protein concentrations were determined with a colorimetric assay according to Bradford [79]. The dye Coomassie Brilliant Blue G-250 in the reagent shifts its maximum absorbance from 465 nm to 595 nm when it binds to basic side chains of proteins. Due to van der Waals forces and ionic interactions the dye is stabilized in its anionic sulfonate form which appears blue. The increasing absorbance at 595 nm is proportional to the amount of bound proteins in the sample and can be determined with a photometer.
For the analysis, samples were diluted in a ratio 1:10 in 1x UT solution. Ten µl of the dilution were mixed with 790 µl HPLC grade water and 200 µl of Bradford reagent were added. Ten µl of UT solution served as blank sample. Samples were measured in three replicates at 595 nm at a photometer within 15 min. Protein concentrations were calculated using the mean absorbance based on a calibration curve of bovine serum albumin with a linear concentration range of 1 µg/µl to 12 µg/µl.

Proteolytic digestion with trypsin

Prior to proteolytic digestion, 4 µg of each sample in 1x UT were diluted with 20 mM ammonium bicarbonate to a volume of 10 µl. Disulfide bonds of proteins were reduced with 2.5 mM dithiothreitol and incubation of samples for 1 h at 60 °C and 550 rpm in a thermomixer. To quench the reaction the volume was filled up to 18 µl with 20 mM ammonium bicarbonate. Resulting thiol groups were alkylated with 10 mM iodoacetamide for 30 min at 37 °C in the dark preventing re-oxidation of SH-groups. For tryptic proteolysis overnight at 37 °C, trypsin was added in a protease to protein (m/m) ratio of 1:25. Digestion was stopped by addition of 5 % (v/v) acetic acid to a final concentration of 1 %.

Peptide purification

Obtained peptides were desalted and purified using pipette tips containing C18 material with a capacity of 2 µg (ZipTip®). For equilibration, the tips first were washed three times with 100 % acetonitrile (ACN) and then stepwise five times with 80 % (v/v) ACN in 1 % (v/v) acetic acid, 50 % (v/v) ACN in 1 % (v/v) acetic acid, 30 % (v/v) ACN in 1 % (v/v) acetic acid and twice in 1 % (v/v) acetic acid (Table 11).

Table 11 Solution used for equilibration of the C18 material packed tip (ZipTip®).

	80 % ACN in 1 % acetic acid	**50 % ACN in 1 % acetid acid**	**30 % ACN in 1 % acetic acid**	**1 % acetic acid**
100 % ACN	1200 µl	750 µl	450 µl	-
HPLC grade water	-	450 µl	750 µl	1200 µl
5 % acetic acid	300 µl	300 µl	300 µl	300 µl

The sample was then loaded onto the material by pipetting up and down 20 times or pipetting the whole volume twice for sample volumes bigger than 100 µl, respectively. After washing the ZipTip® five times with 1 % (v/v) acetic acid, the peptides were eluted by pipetting up and down first with 50 % (v/v) ACN in 1 % (v/v) acetic acid and then with 80 % (v/v) ACN in 1 % (v/v) acetic acid. Both eluates were combined in a micro vial and dried in a vacuum centrifuge or in a lyophilizer, respectively. The dried peptides were dissolved in 20 µl buffer A to reach a peptide concentration of 100 ng/µl.

2.3.5 Mass spectrometric analysis

The mass spectral data for the secretome and the intracellular proteome of human primary hepatocytes was acquired with a Q Exactive™ Orbitrap mass spectrometer. The same instrument was used for the mass spectrometric data acquisition in the murine study of hyper- and hypothyroidism. Plasma protein samples of the human thyrotoxicosis study and plasma protein samples of the murine transient thyrotoxicosis study were measured with a LTQ-Orbitrap Velos™ mass spectrometer.

Analysis of tryptic peptides using a Q Exactive™ Orbitrap mass spectrometer

Mass spectrometric data acquisition was performed on a Q Exactive™ Orbitrap mass spectrometer coupled on-line with an UltiMate® 3000 Nano HPLC system. For nanospray ionization a TriVersa NanoMate nano source or a Nanospray Flex™ Ion Source was used.

Initially, peptides were trapped onto a n Acclaim PepMap 100-C18 pre-column (3 µm particle size, 150 Å pore size, 2 cm x 75 µm) before separation on a 25 cm Accucore 150-C18 analytical column (i.d. 75 µm, 2.6 µm, 150 Å). The binary buffer system was formed of solvent A_1 and solvent B_1 (Table 10). Peptides were eluted at a flow rate of 300 nl/min with a linear gradient of solvent B_1 from 2 % up to 25 % in 120 min with a total run time of 145 min per sample (Table 12).

Table 12 LC gradient used for peptide separation prior to Q Exactive™ Orbitrap MS measurements.

Time [min]	0.0	10.0	130.0	135.0	137.0	142.0	145.0
Solvent B_1 [%]	2	2	25	40	90	90	2

Full scan data was generated in profile mode with a scan range of 300 - 1650 m/z, a scan resolution for MS scans of R = 70000 and for MS/MS scans of R = 17500, respectively. Out of the survey scan in data dependent mode the 10 most intense precursor signals with charge state ≥ +2 were selected for MS/MS fragmentation in centroid mode using high energy collisional dissociation (HCD). Other parameters set for the analysis were: intensity thresholding (AGC): $2x10^5$, isolation window: 3 m/z, fixed first mass: 100 m/z, normalized collision energy: 27.5 %, dynamic exclusion time: 30 s. Charge states of +1 and > +6 were excluded of the analysis.

Analysis of tryptic peptides using a LTQ-Orbitrap Velos™ mass spectrometer

The analysis was performed on a nanoAcquity UPLC connected to a LTQ-Orbitrap Velos™ mass spectrometer which is equipped with a nano-ESI source.

Prior to data acquisition, peptides were concentrated on a 2 cm trap column (nanoAcquity UPLC 2G-V/Mtrap Symmetry, C18, i.d. 180 µm, 5 µm, 100 Å) and separated on a 10 cm nanoAcquity UPLC RP column (BEH130 C18, i.d.100 µm, 1.7 µm). The separation was achieved using a 92 min non-linear gradient formed of a binary buffer system of solvent A_2 and solvent B_2 (Table 13).

Table 13 LC gradient used prior all LTQ-Orbitrap Velos™ MS measurements.

Time [min]	0.0	2.0	65.0	90.0	91.0	92.0
Solvent B_2 [%]	2	5	25	60	99	2

Since different LC solvents have been used across measured sample sets, the binary buffer systems are specified in Table 14, buffer compositions can be found in Table 10.

Peptides were eluted at a constant flow rate of 400 nl/min. Subsequently, eluted peptides were measured by automatically switching the mass spectrometer between Orbitrap-MS and LTQ-MS/MS data acquisition for MS and MS/MS events. Survey full scan MS spectra in an m/z-range from 300 – 1700 were generated in profile mode in the Orbitrap with a resolution of R = 30000. For fragmentation, MS/MS scans were acquired with a data-dependent strategy in centroid mode using collision induced dissociation (CID). The method enabled isolation of up to 20 most abundant ions depending on their signal intensity. Fragmentation was carried out with an isolation window of 2 Da and a target value of 1×10^4 or with a maximum ionization time of 100 ms. Already selected target ions were dynamically excluded for 60 s. Ion selection threshold was 2000 counts for MS/MS, activation time was 10 ms and the normalized activation energy was 35 %. Only +2 and +3 charged ions were triggered for fragmentation.

Table 14 LC binary buffer system for two different sample sets measured on the LTQ Orbitrap Velos™ MS.

Sample set	Binary buffer system
Human plasma	Solvent A_2
	Solvent B_2
Murine plasma	Solvent A_3
	Solvent B_2

2.3.6 Processing steps for mass spectrometric raw data

Quality control using XCalibur™ software

After measurement, obtained chromatograms were checked visually using the XCalibur™ software. Samples displaying huge differences regarding intensities and chromatographic pattern were considered as outliers and not included in subsequent data analyses.

Processing steps using Genedata software

MS raw data were imported into Genedata Refiner MS software. First, the individual chromatograms of all files were cleaned by removing small structures in retention time and m/z direction and by subtracting background noise followed by a smoothing

procedure applied to all peaks. Next, an alignment search across all chromatograms based on the concept of a pairwise alignment based tree was performed in a search distance of 2 min. After (i) chromatogram peak detection, (ii) isotope clustering, (iii) MS/MS consolidation and (iv) chromatogram single filter activity, an automated database search was performed using the MASCOT algorithm (version 2.5). Uniprot/Swissprot databases were selected according to the processed sample set. Settings applied for the search engine and the peptide validation depended on the mass spectrometer and software version (Table 15).

Table 15 Description of settings for database search and peptide validation.

Parameter	**Set 1[(a)]**	**Set 2[(a)]**	**Set 3[(a)]**	**Set 4a[(a)]**
Mass spectrometer	LTQ-Orbitrap Velos™	LTQ-Orbitrap Velos™	Q Exactive™ Orbitrap	Q Exactive™ Orbitrap
Release version of Genedata software	vs. 7.6.6	vs. 9.0.0	vs. 10.0.3	vs. 10.0.3
Species	Homo sapiens	Mus musculus	Mus musculus	Homo sapiens
Mass tolerance for precursor ions	10 ppm	10 ppm	10 ppm	10 ppm
Mass tolerance for fragment ions	0.6 Da	0.6 Da	0.02 Da	0.02 Da
# missed cleavages permitted	0	0	0	0
Fixed modification	Carbamidomethylation at cysteine			
Variable modification	Oxidation on methionine			
Database/release	Human Uniprot/ Swissprot 2012/08	Murine Uniprot/ Swissprot 2014/04	Murine Uniprot/ Swissprot 2014/04	Human Uniprot/ Swissprot 2015/06
Peptide validation	Ion score ≥ 20 Rank = 1	Ion score ≥ 20 Rank = 1	FDR ≤ 1 %	FDR ≤ 1 %
Quantification	Summed intensity over all peptides per protein	Summed intensity over all peptides per protein	Hi3 quantification	Summed intensity over all peptides per protein
Min. peptide count	1	1	1	1

(a) Set 1 human plasma study of experimental induced thyrotoxicosis, *Set 2* murine plasma study of transient thyrotoxicosis and recovery, *Set 3* murine plasma study of hyper- and hypothyroidism; *Set 4a* intracellular proteome of human primary hepatocytes

As general parameters for LTQ-Orbitrap™ Velos mass spectrometer searches a peptide tolerance of 10 ppm and a fragment mass tolerance of 0.6 Da were used. For data

generated with a Q Exactive™ Orbitrap mass spectrometer these settings were fixed to 10 ppm peptide tolerance and 0.02 Da fragment mass tolerance. Only ion charges of +2 and +3 were considered for database search with no missed cleavages. Carbamidomethylation at cysteine (+57.02 Da) was set as fixed modification and oxidation on methionine (+15.98 Da) was set as variable modification.

Processing steps using MaxQuant software

The MaxQuant software version 1.5.3.8 was used to analyze the MS raw data of the human primary hepatocytes' supernatant (**set 4 b**) generated with a Q Exactive™ Orbitrap mass spectrometer. Derived peak lists were submitted to the Andromeda search engine using a Swissprot/Uniprot database limited to human entries (2016/09). Additionally, a contaminant database comprising all proteins included in FCS-containing media was used. The precursor mass tolerance was set to 10 ppm and the fragment mass tolerance was set to 0.02 Da. One missed cleavage was allowed. As before, carbamidomethylation at cysteine was defined as fixed and oxidation on methionine as variable modification. The minimum peptide length had to be six amino acids and the minimum of unique peptides was set to 1. The 'match between run' time window for the transfer of identifications was set to 0.7 min.

Intensities and LFQ were calculated by the software. The LFQ values were generated from the raw intensities using a special normalization procedure and a particular aggregation method [80].

2.3.7 Proteome data analysis

For data analysis of the human plasma proteome (**set 1**, n = 80), peptide search results were validated based on the defined search scores (ion score ≥ 20, peptide rank = 1). After peak annotation, all cluster information was imported into the Genedata Analyst software. Annotated clusters were merged to peptides. After filtering, solely unique peptides were summed up to proteins.

Only proteins with less than 40 % missing values were considered for quantification. Next, protein intensities were $\log_{10}$ transformed and normalized to the median of all protein intensities without missing values across all samples in the data set. All samples were adjusted for age, BMI, and experimental batch and time point t2 to t5 per subject were

standardized on baseline (t1) before calculating the mean value of every protein at one time point. Subsequently, the free thyroxine levels and the protein abundances were correlated according to Pearson.

Another evaluation strategy included a mixed-effect linear regression model with serum FT4 concentrations as exposure and protein levels as outcome. Serum FT4 was determined as a fixed effect due to the repeated measurement character of the study whereas the participants were considered as a random factor in the model. All analyses were adjusted for age, BMI, and experimental batch. Proteins with a false discovery rate ≤ 0.05 were seen as significant. Further details are described elsewhere [81]. Regression model and further analysis were performed by Maik Pietzner (Institute for Clinical Chemistry and Laboratory Medicine, University Medicine Greifswald).

The proteome analysis of the mouse plasma samples of the transient thyrotoxicosis study (**set 2**, n = 24) was done in a similar manner. After summation of unique peptides to proteins, only those with 50 % valid values were considered for quantification. Differences plasma samples were identified using two-way ANOVA. Proteins with a *p*-value ≤ 0.05 were used for further analysis. The identification of differently abundant proteins between the groups (T4 *vs.* control, T4 *vs.* T4R, T4R *vs.* control) was performed *via* a Welch's t-test and a significance threshold of *p*-value *(FDR)* ≤ 0.05 was set.

For the data analysis of the second murine study (**set 3**, n = 16) and the set of human primary hepatocytes (**set 4 a**) Genedata Refiner software version 10.0.3 was used. In this release, peptide false discovery rate could be estimated as a function of the search score by using decoy information of peptides generated during Mascot search. Thereby, database search was not restricted and peptides were validated afterwards applying a maximum false discovery rate of 1 %.

For **set 3**, the next step included the protein inference activity which derived protein intensities based on the peptide search results. Redundant proteins were filtered out according to the Occam's razor principle. Also, peptides which are shared across different protein groups were ignored. Peptides which are shared by the same protein group were kept though. For relative protein quantification, protein intensities were calculated based on the top3 protein quantification method proposed by Silva *et al.* [82]. Only the average top three peptides per protein across all samples were considered and kept for analysis.

Subsequently, provided protein intensities were imported into the Genedata Analyst software, $\log_{10}$ transformed and normalized to the median of all protein intensities without missing values across all samples in the data set.

After peptide validation, summation to proteins was done as described for **set 1**.

Differentially abundant proteins in the second murine study were identified by comparing the induction groups (T4, T3, MMI/$KClO_4$) with the control group using a Welch's t-test. Proteins were regarded as significant with a *p*-value ≤ 0.05.

For the data analysis of the intracellular proteome of human primary hepatocytes (**set 4 a**), median normalized intensities were used to build a ratio between the T4 treated cells and the control cells of the same donor.

For quantification purposes of the secretome deriving from the same hepatocytes (**set 4 b**), LFQ values calculated by MaxQuant were extracted. All proteins with more than two missing values were excluded from the analysis. The remaining protein LFQ were used to build a ratio in the same way as it was done for the intracellular proteome.

Functional classification of proteins

The functional classification of significantly altered proteins was performed using the Ingenuity Pathway Analysis (IPA) software (2014-2017). Based on the whole human or murine genome database ("Ingenuity knowledge base"), genes were grouped into functional categories. Significance of the enrichment of proteins among functional categories was assessed *via Fisher's exact test*.

3 RESULTS

3.1 Studies on human plasma

3.1.1 Human model of experimentally induced thyrotoxicosis

The results of the study have been published in Engelmann *et al.*, 2015 and Pietzner *et al.*, 2017 [81,83].

Study design and phenotypical data

The aim of the human plasma study was to screen for novel peripheral biomarkers of thyroid function and to characterize physiological signatures associated with free thyroxine. Therefore, the influence of levothyroxine treatment (the pharmaceutical equivalent to circulating T4) on the human plasma proteome was investigated.

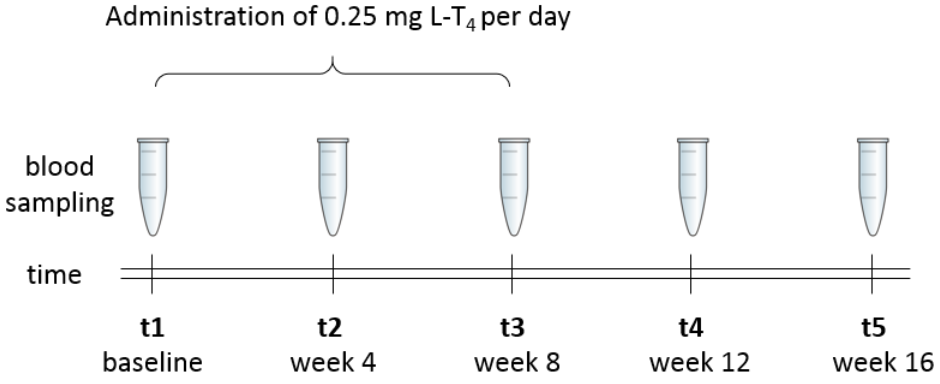

Figure 3 Study design of experimental human thyrotoxicosis including sampling time points (t1-t5) and duration of levothyroxine administration.

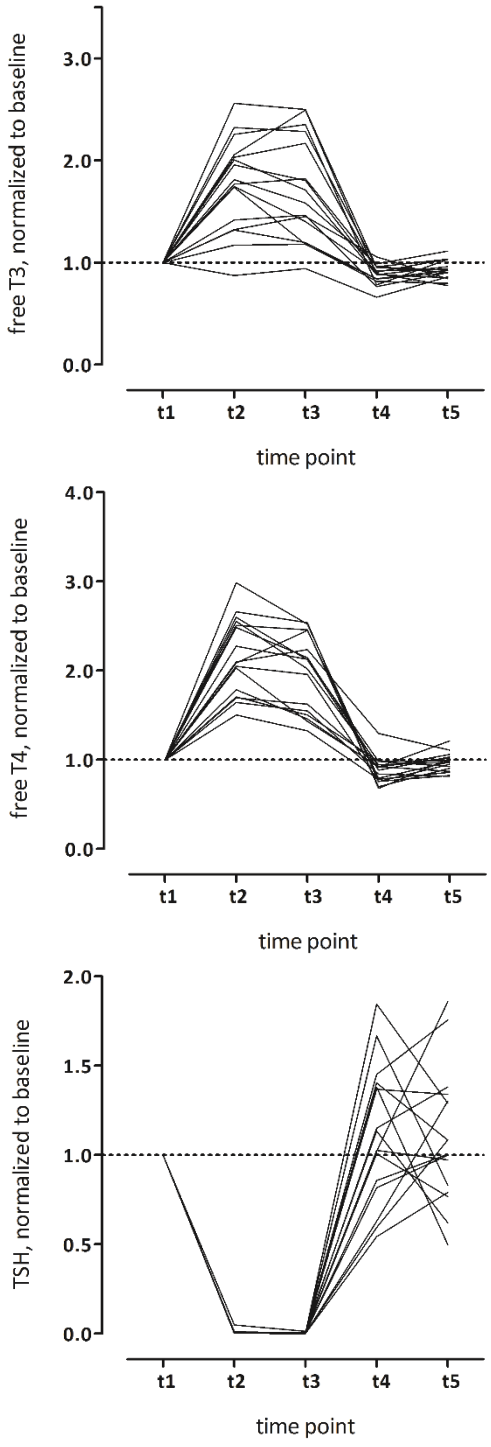

Figure 4 Individual serum levels normalized to baseline of thyroid hormones (TH) and TSH for each time point during the human study of experimental thyrotoxicosis (t1-baseline, t2 and t3-4 and 8 weeks of levothyroxine treatment, t4 and t5- 4 and 8 weeks after stopping the application).

The study included a plasma sample set of 16 healthy male volunteers. They were treated with a daily dose of 0.25 mg levothyroxine (L-T_4, Henning-Berlin, Berlin, Germany) for 8 weeks. Blood sampling was done before the administration started (t1, baseline), after 4 and 8 weeks under treatment (t2 and t3) as well as 4 and 8 weeks (t4 and t5) after stopping the application (Figure 3, N = 80 samples).

All subjects developed biochemical thyrotoxicosis, and this effect was reversed within the first 4 weeks of follow-up. After 4 weeks of treatment with levothyroxine (t2), the mean free T4 levels rose from 13.24 ± 1.4 pmol/l (SD) at baseline (t1) to 28.6 ± 6.5 pmol/l, associated with an increase of free T3 levels from 5.26 ± 0.51 to 9.19 ± 2.01 pmol/l. TSH was 2.1 ± 1.02 mU/l at baseline, dropping to 0.017 ± 0.03 mU/l after 4 weeks and staying at this low level (0.007 ± 0.01 mU/l) after 8 weeks (t3) as well. After stopping the levothyroxine administration levels of TH and TSH returned to pretreatment levels (t4) and stabilized over the study period (t5) (Figure 4, further information in table S1). Importantly, none of the volunteers reported any subjective symptoms of thyrotoxicosis assessed by comprehensive questionnaires. Though plasma levels of thyroid hormones, especially T3, show variances, the observed decrease in TSH level is very consistent across all subjects.

Furthermore, effects of thyroxine treatment on well-known TH responsive clinical measures i.e. sex hormone-binding protein (SHBG) and cystatin C (CYTC) and blood lipids were assessed. L-T_4 treatment resulted in a transient decline of cholesterol as well as HDL/LDL-cholesterol (Figure 5) while total triglyceride content was unaffected (data not shown).

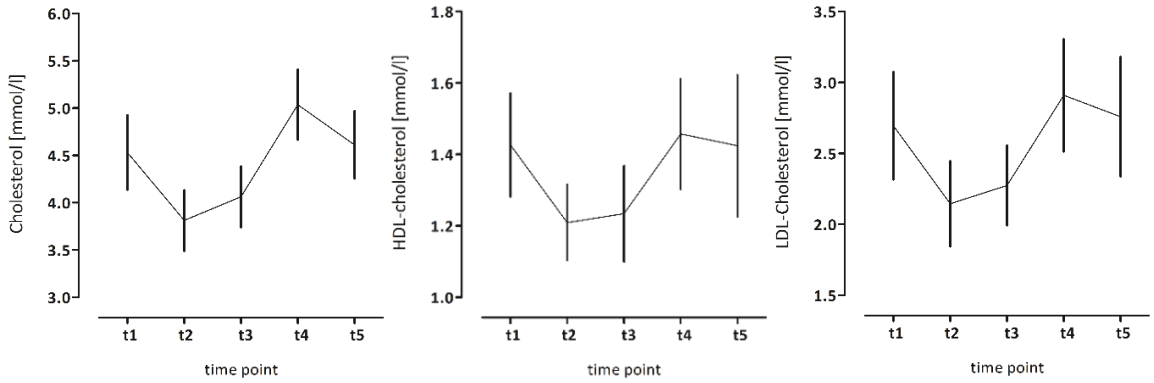

Figure 5 Serum concentration of cholesterol, HDL-cholesterol, and LDL-cholesterol during the study period (mean values with 95 % confidence intervals).

Since SHBG is known to be altered in level in thyroid dysfunction there was an expected increase in protein concentration from baseline (t1) to 4 and 8 weeks (t2 and t3) after treatment (30.16 mmol/l to 50.59 mmol/l and 55.93 mmol/l, respectively). The same holds true for CYTC showing an increase in concentration during the administration of levothyroxine (0.68 mg/l to 0.79 mg/l and 0.86 mg/l). Both proteins returned to baseline levels within 4 weeks after termination of L-T_4 intake (Figure 6).

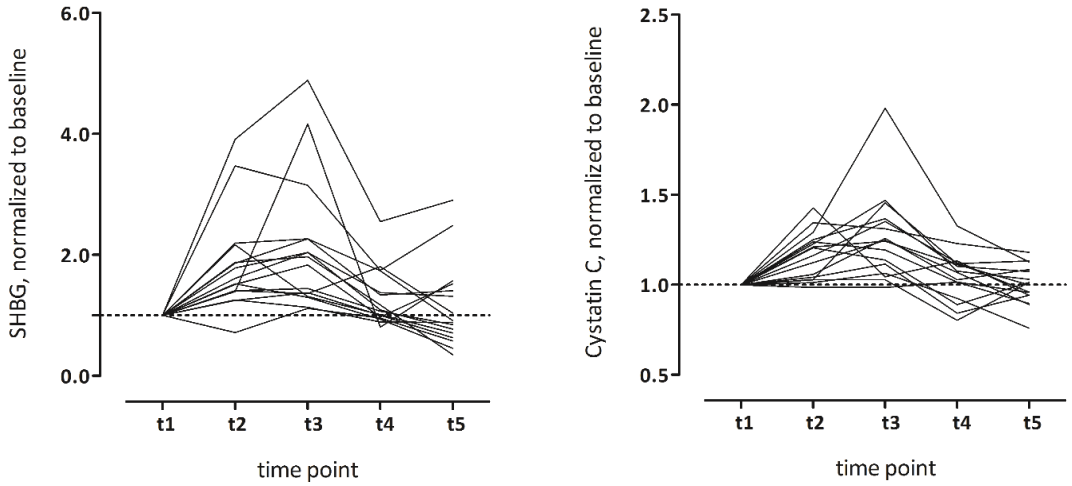

Figure 6 Individual plasma levels normalized to baseline (t1) of sex hormone-binding globulin (SHBG) and cystatin C for each time point during the study period of experimental thyrotoxicosis.

Protein identification

All plasma samples were depleted for six highly abundant proteins using multi affinity removal column (MARS6, Agilent Technologies). Remaining proteins were precipitated using trichloroacetic acid and subsequently proteolytically digested. Prior to mass spectrometric analysis, peptides were desalted and subjected to liquid chromatography. The analysis was performed in 80 single LC-MS/MS runs. The recorded raw data were processed using the Refiner MS software. After chromatogram alignment, isotope group specific clusters were extracted and submitted to a MASCOT database search. Summation of annotated clusters was done using Genedata Analyst software. In total, 2374 *unique* peptides were identified, representing 497 human proteins. Only proteins identified in more than 60 % of all samples (n= 437) were considered for quantification (s.a. Supplementary table S1). Despite affinity depletion to remove high abundant proteins 283 proteins were identified with one peptide only.

Impact of the T4 administration onto plasma protein levels

Prior to statistical analysis, raw protein intensities have to be normalized and corrected for several reasons. To exclude protein changes which occur as a result simply of aging or differences in weight of study participant, protein abundances were adjusted. In addition, due to the size of the sample set and the long measurement time, samples were processed batch-wise. Prior to adjustment for BMI, age and experimental batch all protein intensities were $\log_{10}$ transformed and normalized to the median. Subsequently, free T4 levels and protein abundances of the 437 proteins were correlated according to Pearson. Disregarding the study kinetic the *Pearson correlation coefficient* is a measure of linear dependence between two variables given by free T4 and protein abundances. The aim was to identify protein alterations aligning with free T4 levels, independently of the current state during the study period.

A large subset of proteins (n = 138) demonstrated a correlation coefficient $|r| \geq 0.8$ revealing a strong influence of the levothyroxine treatment on the plasma proteome of male volunteers. Two thirds (n = 91) of correlated proteins revealed a positive correlation whereas 47 proteins were negatively correlated to free T4 levels. Restricting the threshold to $r \geq |0.9|$ 55 proteins were positively correlated and 21 proteins negatively correlated,

respectively. The corresponding correlation coefficients for all proteins can be found in Supplementary table S2. The 10 strongest correlations (positive and negative) between proteins and measured TH are displayed in Table 16.

Table 16 Strongest positive and negative correlation between proteins and free T4 in the study of experimental thyrotoxicosis. Correlation was done according to Pearson. Subcellular location was derived from the Uniprot/Swissprot database.

Swissprot annotation	Protein names	Subcellular location	*r* (Pearson)
CAMP_HUMAN	Cathelicidin antimicrobial peptide	Secreted	-0.990
INSC_HUMAN	Protein inscuteable homolog	Cytoplasm	-0.982
ANKS6_HUMAN	Ankyrin repeat and SAM domain-containing protein 6	Cytoplasm	-0.981
PLMN_HUMAN	Plasminogen	Secreted	-0.976
IF140_HUMAN	Intraflagellar transport protein 140 homolog	Cytoplasm, Cytoskeleton	-0.963
S10A8_HUMAN	Protein S100-A8	Secreted, Cytoplasm	-0.952
CC043_HUMAN	Single-pass membrane and coiled-coil domain-containing protein 1	Cell membrane	-0.948
TTK_HUMAN	Dual specificity protein kinase TTK	Cytoplasm	-0.945
APOD_HUMAN	Apolipoprotein D	Secreted	-0.939
RIMS1_HUMAN	Regulating synaptic membrane exocytosis protein 1	Cell membrane	-0.937
FETUB_HUMAN	Fetuin-B	Secreted	0.982
IC1_HUMAN	Plasma protease C1 inhibitor	Secreted	0.982
PRG4_HUMAN	Proteoglycan 4	Secreted	0.982
MLL3_HUMAN	Histone-lysine N-methyltransferase 2C	Nucleus	0.983
ZA2G_HUMAN	Zinc-alpha-2-glycoprotein	Secreted	0.985
CFAH_HUMAN	Complement factor H	Secreted	0.988
VASN_HUMAN	Vasorin	Cell membrane	0.989
ITIH1_HUMAN	Inter-alpha-trypsin inhibitor heavy chain H1	Secreted	0.990
F13B_HUMAN	Coagulation factor XIII B chain	Secreted	0.991
PEDF_HUMAN	Pigment epithelium-derived factor	Secreted	0.997

The correlation previously mentioned for SHBG and CYTC assessed by laboratory assays was also observable in the untargeted proteome approach with $r = 0.8616$ for SHBG and $r = 0.9525$ for CYTC, respectively (see 2.3.1). Functional categorization of correlated proteins for canonical pathways using Ingenuity Pathway Analysis revealed different categories of proteins influenced by levothyroxine administration (Figure 7).

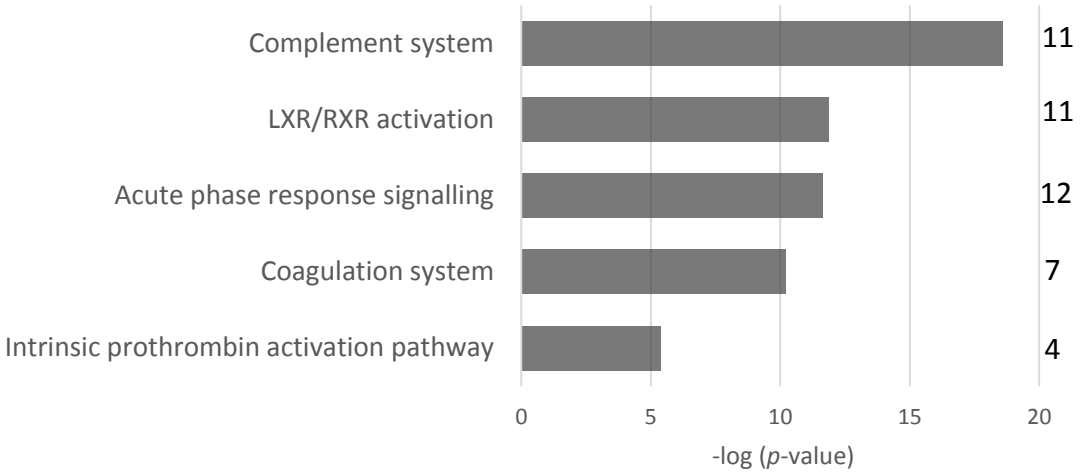

Figure 7 Functional categorization of proteins correlated with free T4 levels. 76 proteins (correlation coefficient $|r| \geq 0.9$) were analyzed using IPA. Numbers behind bars represent the number of assigned proteins for the particular pathway.

From 35 proteins assigned to the coagulation cascade, 24 proteins (almost 70%) were detected by mass spectrometric analysis, out of which 7 showed a significant correlation ($|r| \geq 0.9$) with free T4 levels. The majority of coagulation proteins displayed a positive correlation with coagulation factor XIII subunit B (F13B) ($r = 0.991$) showing the strongest correlation. F13B protein level returned to baseline quickly after discontinuation of LT_4-application. Moreover, coagulation factor IX (F9) could be found with an $r = 0.938$, whereas the correlation and significance of F5 ($r = 0.816$), F2 ($r = 0.813$) and F11 ($r = 0.811$) were slightly lower but showed the same trend (Figure 8).

Additionally, conventional ELISAs were performed for F9 and F13 (Figure 9) to confirm the results from proteome profiling. The results for both proteins confirmed the increase in concentration during the peak of induced thyrotoxicosis as observed by LC-MS/MS measurements. When comparing the levels at time point t1 and t2 significantly different levels were found for F9 ($p = 0.0023$) and F13 ($p < 0.0001$) using Welch's t-test. Other detected coagulation factors (F7, F10, F12, F13A) showed no significant correlation with free T4 whereas protein C inhibitor (SERPINA5), antithrombin III (SERPINC1) and α_2-antiplasmin (SERPINF2) as representatives of the serpin peptidase inhibitor family all revealed positive correlations. In contrast, plasminogen was the only protein among the coagulation cascade detected with a negative correlation and consequently showed a decreased abundance upon L-T_4 treatment ($r = -0.976$).

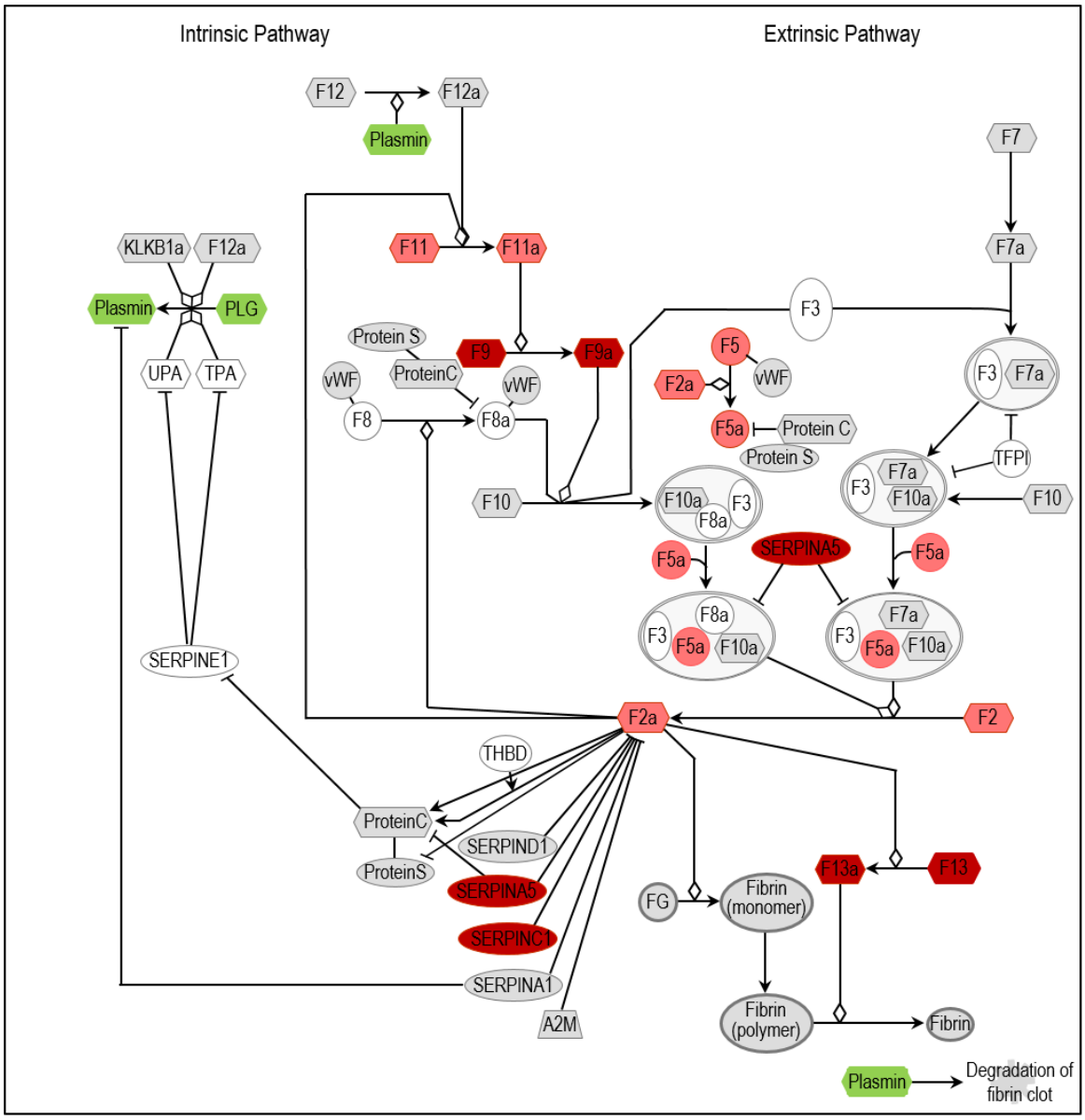

Figure 8 Schematic view of the coagulation cascade. Colored boxes highlight proteins with $r \geq 0.9$ (dark red); $r \geq 0.8$ (light red); $r \leq -0.9$ (green). Gray boxes: proteins were covered by the analysis, but displayed no significant correlation ($0.8 \geq r \geq -0.8$). *A2M* α_2–macroglobulin, *F2* coagulation factor II, *FG* fibrinogen, *KLKB1a* plasma kallikrein, *PLG* plasminogen, *SERPINA1* α_1–antitrypsin, *SERPINA5* protein C inhibitor, *SERPINC* antithrombin III, *SERPIND1* heparin cofactor II, *TFPI* tissue factor pathway inhibitor, *THBD* thrombomodulin, *TPA* tissue plasminogen activator, *UPA* urokinase plasminogen activator, *VWF* von Willebrand factor. The figure is published in Engelmann *et al*., 2015 [83].

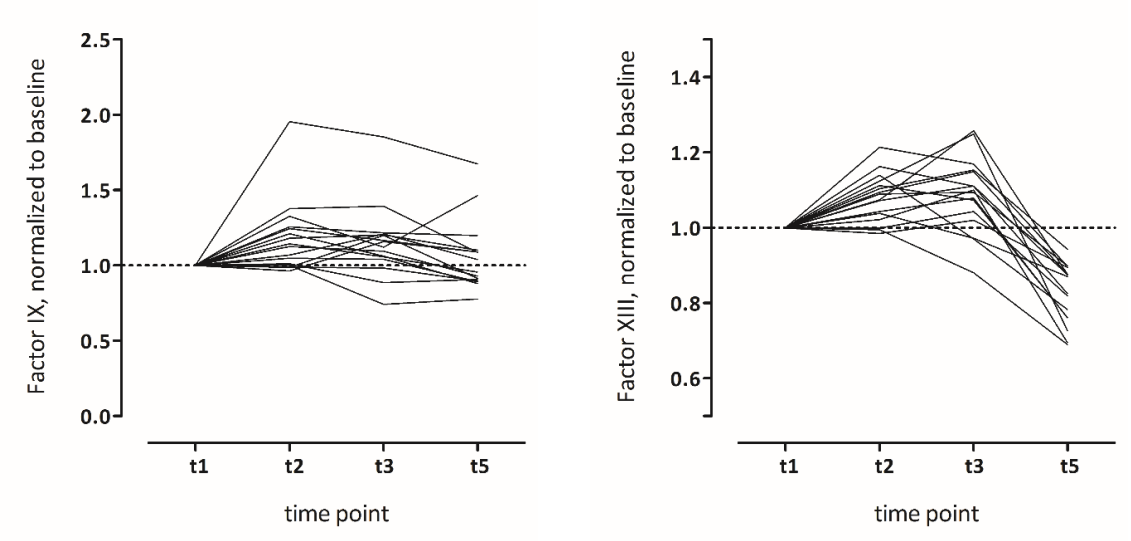

Figure 9 Individual plasma levels determined via ELISA normalized to baseline of coagulation factor IX and XIII for four time points during the study period of experimental thyrotoxicosis. Time point t4 was skipped due to the experimental setup situation.

Besides proteins assigned to the coagulation cascade, 11 proteins with $r \geq 0.9$ and additionally 3 proteins with $r \geq 0.8$ of the complement system were correlated with free T4 (Table 17). All of them showed positive correlation demonstrating a rather moderate but significant increased abundance during the T4 administration.

Table 17 Proteins assigned to the Complement System (IPA) and showing a correlation of $r \geq |0.9|$ according to Pearson.

Swissprot annotation	Protein names	*r* (Pearson)
CFAH_HUMAN	complement factor H	0.9879
IC1_HUMAN	plasma protease C1 inhibitor	0.9822
CO7_HUMAN	complement component 7	0.9760
C1QB_HUMAN	complement C1q subcomponent subunit B	0.9736
CO8G_HUMAN	complement component C8 gamma chain	0.9699
C1QA_HUMAN	complement C1q subcomponent subunit A	0.9575
MBL2_HUMAN	mannose-binding protein C	0.9520
CO8B_HUMAN	complement component C8 beta chain	0.9513
CO8A_HUMAN	complement component C8 alpha chain	0.9351
CO3_HUMAN	complement component 3	0.9189
CO2_HUMAN	complement component 2	0.9051
CFAB_HUMAN	complement factor B	0.8957
CO9_HUMAN	complement component 9	0.8780
C1S_HUMAN	complement component 1, s subcomponent	0.8208

Pearson correlation analysis led to data reduction because the mean value of every protein at one time point was calculated beforehand to correlate it with the free thyroxine levels. Furthermore, simple correlation analysis does not account for the repeated measurement character of the study design and hence further decreases the statistical power to detect significant associations

To overcome these drawbacks, mixed-effect linear regression models accounting for the repeated measurements were subsequently considered. Consequently, the same data set was used for this analysis approach using the mixed-effect linear regression model with serum free T4 concentrations as exposure and protein abundances as outcome controlling for age, BMI, and batch (see 2.3.7). Application of this model on the $\log_{10}$ transformed protein intensities exhibited significant associations with free T4 for 63 out of 437 detected proteins (14 %). The majority (n = 47) was positively associated while 16 proteins exhibited an inverse association.

Consistently, even the reference proteins CYTC and SHBG showed significant inverse associations with free T4 in the new modelling approach.

The significant results are summarized in Figure 10, where three functional groups of proteins are separately marked. The corresponding estimates and FDR values from regression analysis can be found in Supplementary table S3.

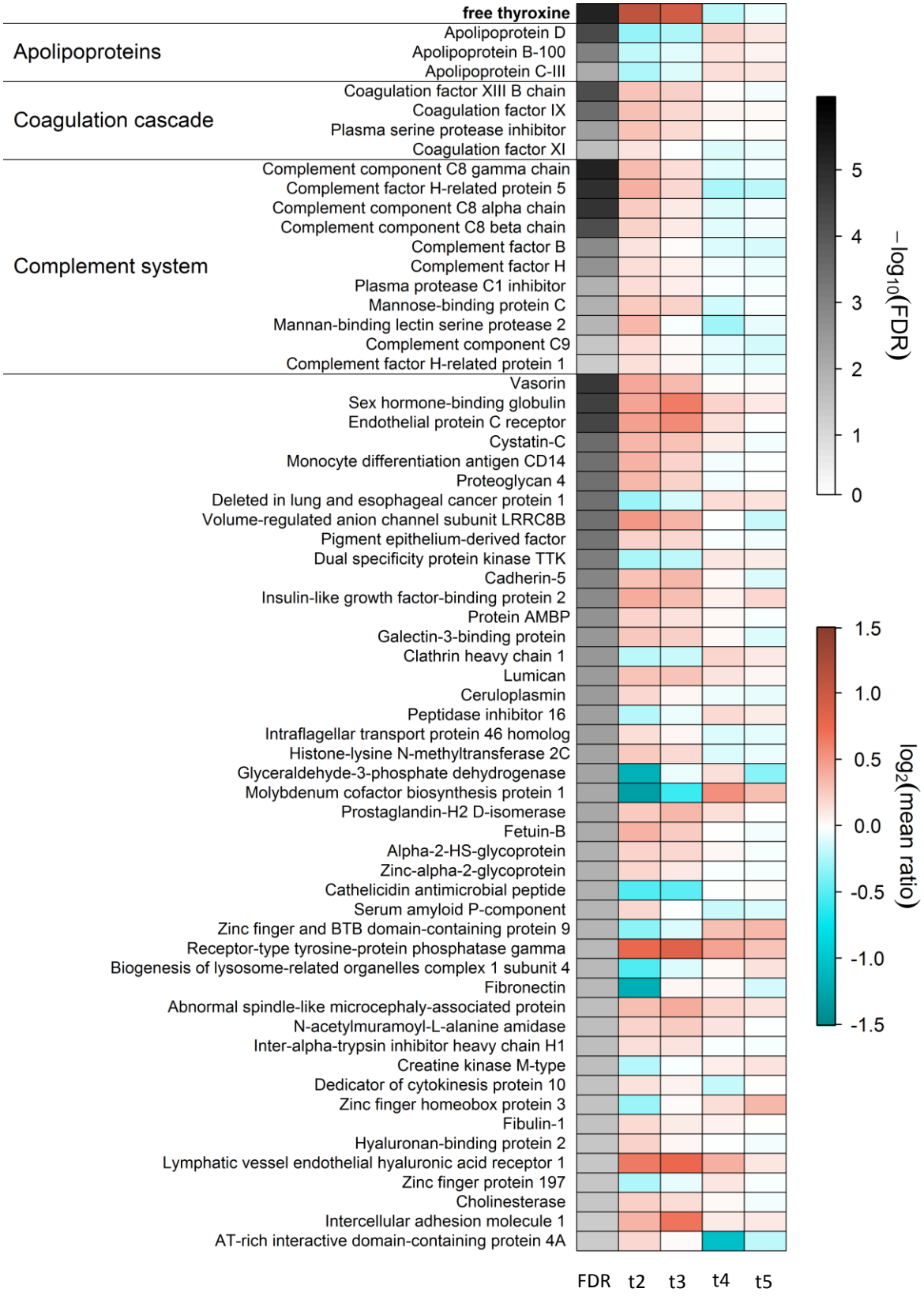
free thyroxine
Apolipoproteins
Apolipoprotein D
Apolipoprotein B-100
Apolipoprotein C-III
Coagulation cascade
Coagulation factor XIII B chain
Coagulation factor IX
Plasma serine protease inhibitor
Coagulation factor XI
Complement system
Complement component C8 gamma chain
Complement factor H-related protein 5
Complement component C8 alpha chain
Complement component C8 beta chain
Complement factor B
Complement factor H
Plasma protease C1 inhibitor
Mannose-binding protein C
Mannan-binding lectin serine protease 2
Complement component C9
Complement factor H-related protein 1
Vasorin
Sex hormone-binding globulin
Endothelial protein C receptor
Cystatin-C
Monocyte differentiation antigen CD14
Proteoglycan 4
Deleted in lung and esophageal cancer protein 1
Volume-regulated anion channel subunit LRRC8B
Pigment epithelium-derived factor
Dual specificity protein kinase TTK
Cadherin-5
Insulin-like growth factor-binding protein 2
Protein AMBP
Galectin-3-binding protein
Clathrin heavy chain 1
Lumican
Ceruloplasmin
Peptidase inhibitor 16
Intraflagellar transport protein 46 homolog
Histone-lysine N-methyltransferase 2C
Glyceraldehyde-3-phosphate dehydrogenase
Molybdenum cofactor biosynthesis protein 1
Prostaglandin-H2 D-isomerase
Fetuin-B
Alpha-2-HS-glycoprotein
Zinc-alpha-2-glycoprotein
Cathelicidin antimicrobial peptide
Serum amyloid P-component
Zinc finger and BTB domain-containing protein 9
Receptor-type tyrosine-protein phosphatase gamma
Biogenesis of lysosome-related organelles complex 1 subunit 4
Fibronectin
Abnormal spindle-like microcephaly-associated protein
N-acetylmuramoyl-L-alanine amidase
Inter-alpha-trypsin inhibitor heavy chain H1
Creatine kinase M-type
Dedicator of cytokinesis protein 10
Zinc finger homeobox protein 3
Fibulin-1
Hyaluronan-binding protein 2
Lymphatic vessel endothelial hyaluronic acid receptor 1
Zinc finger protein 197
Cholinesterase
Intercellular adhesion molecule 1
AT-rich interactive domain-containing protein 4A
FDR
t2
t3
t4
t5
5
4
3
2
1
0
$-\log_{10}$(FDR)
1.5
1.0
0.5
0.0
-0.5
-1.0
-1.5
$\log_2$(mean ratio)

Figure 10 Heat map of plasma proteins significantly associated with free thyroxine (FT4) in mixed effect linear regression models. The first column (grey) displays the values of the mean false discovery rate (FDR) for the FT4 effect across 101 subsamples of the data. Other columns indicate the mean log2-ratio from baseline (t1) compared to 4 and 8 (t2 and t3) weeks of treatment as well as 4 and 8 weeks (t4 and t5) after stopping the treatment. The time course of free T4 concentrations is shown on the top of the map as reference. Orange shading denotes an increase and blue shading a decrease compared to baseline (t1). The figure was published in Pietzner *et al*., 2017 [81].

First, a significant drop in different apolipoproteins could be observed. Abundances of apolipoprotein D (ApoD), apolipoprotein B-100 (ApoB-100), and apolipoprotein C3 (ApoC3) decreased significantly during the treatment with L-T_4 with ApoD showing the strongest association with free T4.

Functional categorization of significantly associated proteins highlighted also proteins of the complement system. Eleven proteins were involved; including complement factors, mannose-binding protein C (MBL) and mannan-binding lectin serine protease 2 (MASP-2) all positively associated with free T4. Similar associations for four complement-factor H related proteins were observed.

Several proteins assigned to the coagulation cascade exhibited significant association with free T4 levels. Coagulation factor XIII B chain (F13B), factor IX (F9) and XI (F11) as well as SERPINA5, an inhibitor of activated protein C, were positively associated with free T4.

However, no significant association with free T4 of TH transport protein thyroxine-binding globulin (THBG) and thyroid hormone-binding protein transthyretin (TTR) could be found.

All described changes during the peak of induced thyrotoxicosis normalized after stopping the application of L-T_4.

3.1.2 Human study of hypothyroidism

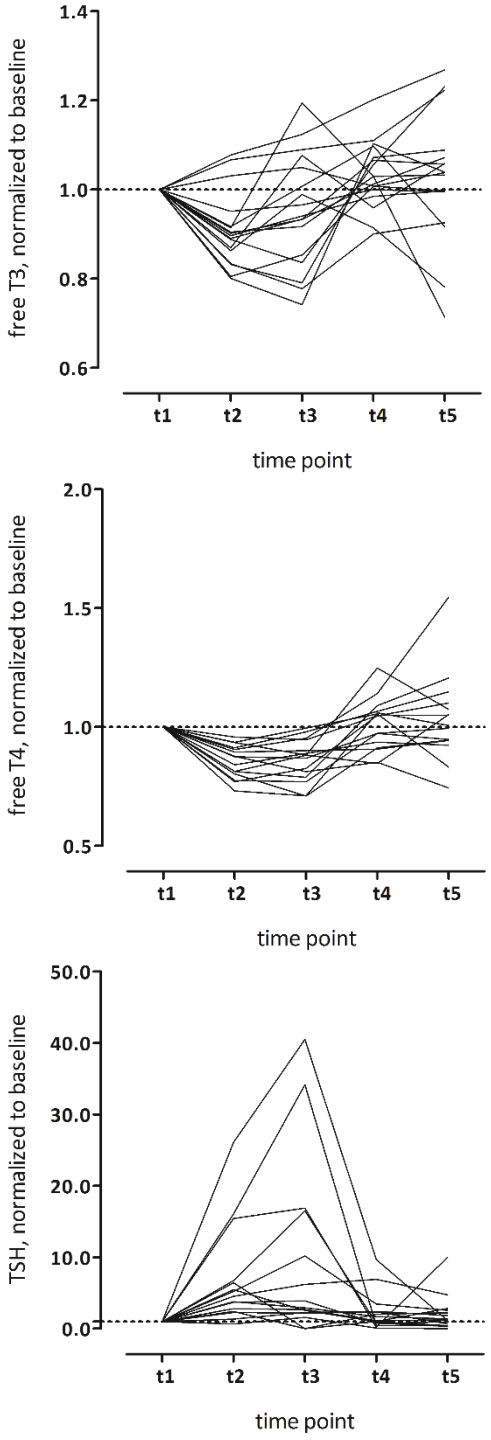

Figure 11 Individual serum levels of thyroid hormones (TH) and TSH for each time point during the human study of hypothyroidism normalized to baseline (t1-baseline, t2 and t3-4 and 8 weeks under thyroxine dose reduction, t4 and t5- 4 and 8 weeks after returning to normal medication).

The second study included 15 patients (n(female) = 13, n(male) = 2) suffering from manifested hypothyroidism. The study design was equivalent to the human model of experimentally induced thyrotoxicosis. Since the patients received their L-T_4 medication on a daily basis to maintain a euthyroid state, they were instructed to reduce their doses to 70 % for a period of 8 weeks. Blood samples were taken before the patients restricted their medication (t1, baseline), after 4 and 8 weeks under reduction (t2 and t3) as well as 4 and 8 weeks (t4 and t5) after returning to previous medication.

Individual time courses of thyroid hormones T4 and T3 as well as TSH, all normalized to baseline (t1) are depicted in Figure 11. As expected after reduction of L-T_4 medication, the level of free T4 dropped in mean values from 16.29 pmol/l ± 2.31 pmol/l (SD) to 13.96 pmol/l ± 2.31 pmol/l after 4 weeks and to 14.12 pmol/l ± 2.43 pmol/l after 8 weeks. Mean concentration normalized at the latest after 8 weeks after returning to normal medication (16.75 pmol/l ± 3.17 pmol/l). As is apparent from Figure 11, levels of free T3 were characterized by a huge variance between the study participants ranging from a slight decrease at time point t2 with an overshooting increase at time point t3 to slightly

increase during the whole study period. Mean concentration of TSH showed an increase from 2.14 mU/l ± 2.32 mU/l at baseline (t1) to 11.08 mU/l ± 20.95 mU/l after 4 weeks (t2) and 14.87 mU/l ± 24.2 mU/l after 8 weeks (t3). Effect sizes differed markedly, ranging from 1.34fold to 26fold after 4 weeks compared to baseline (t2 *vs.* t1).

The previously introduced peripheral markers of TH action SHBG and CYTC showed no consistent alterations during the time course (Figure 12).

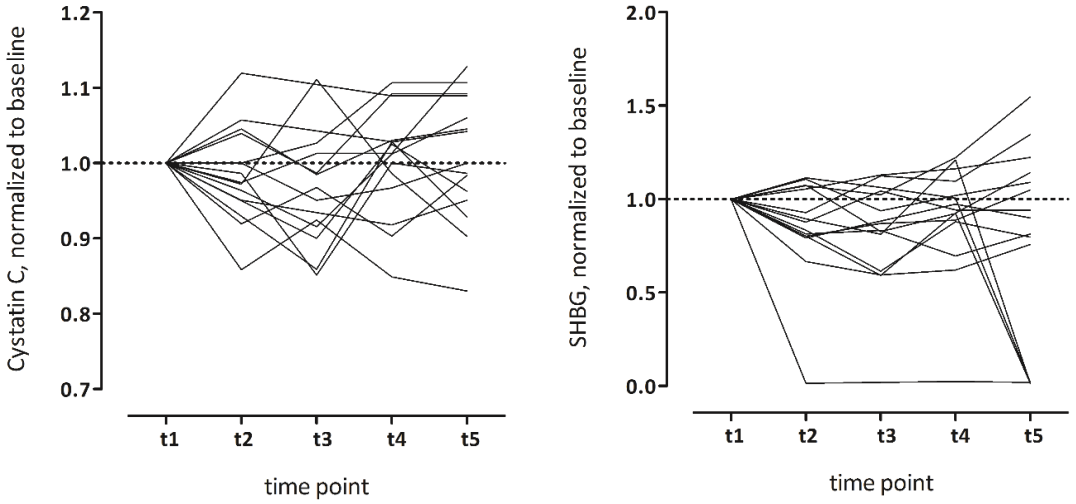

Figure 12 Individual plasma levels normalized to baseline of sex hormone-binding globulin and cystatin C for each time point during the study period of hypothyroidism.

Prior to mass spectrometric analysis of the plasma proteome a metabolome analysis of all samples (N = 75) was performed. Due to huge diversity in the response pattern of metabolites across all patients during the study period no consistent effect regarding the influence of induced hypothyroidism on the metabolome profile in plasma was observable.

Based on these metabolomics findings and the already known time course of CYTC and SHBG which do not reveal consistent response to the reduction in medication, a mass spectrometric measurement to evaluate the plasma proteome was not performed. To provide insights in the changes on protein levels during hypothyroidism obtained findings regarding changes of coagulation proteins in the study of induced thyrotoxicosis were used. Thereupon plasma levels of F9 were determined using an ELISA. Protein concentrations normalized to baseline (t1) are displayed in Figure 13 A.

After exclusion of one outlier, Welch's t-test was applied to compare t2 and t1 protein levels resulting in a significant decrease of F9 after 4 weeks of levothyroxine reduction (p = 0.0123). However, F9 levels rose strongly in many patients after restoration of euthyroidism.

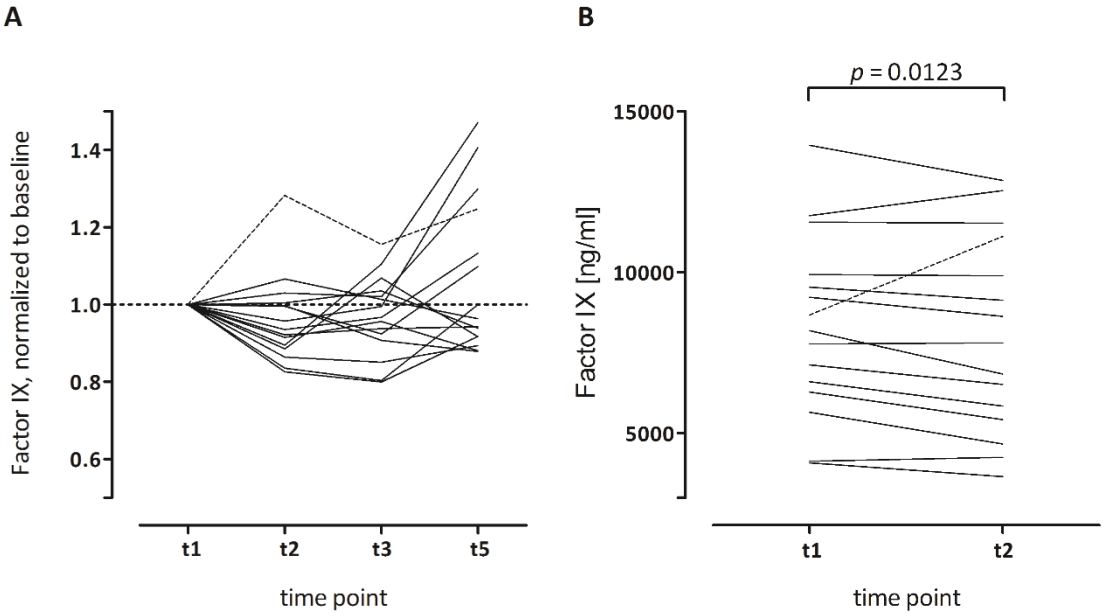

Figure 13 (A) Individual plasma levels normalized to baseline values of coagulation factor IX (F9) for each time point during the study period of hypothyroidism (one patient (dashed line) was considered as outlier and excluded from the analysis) **(B)** Measured F9 concentrations for t1 and t2 (Welch's t-test, p = 0.0123).

Besides the different time courses of the protein in hyper- and hypothyroidism the comparison of F9 concentrations at t1 revealed significantly different baseline levels showing higher abundances of F9 in patients suffering from hypothyroidism (Figure 14).
In comparison with the previously introduced experimental model of thyrotoxicosis which relied on a tightly defined set of male participants, the set up for experimental hypothyroidism was characterized by huge phenotype diversity. The sample set comprised both males and females, covering a wide age range as well as different aetiologies of hypothyroidism (e.g. autoimmune disease and thyroidectomy). In general, this led to greater interindividual variability in the response to induced hypothyroidism, including alterations in protein and metabolite levels.

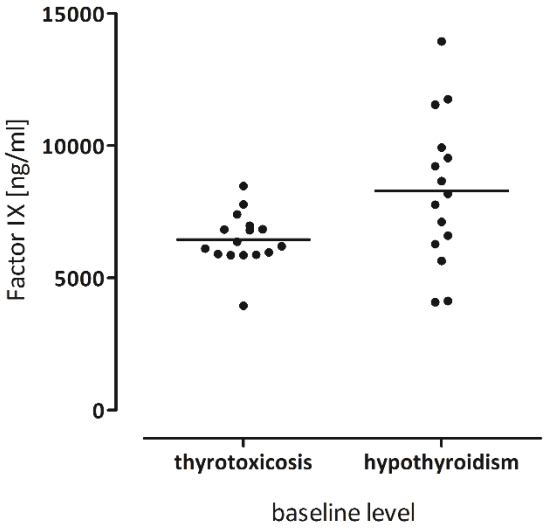

Figure 14 F9 protein concentrations at baseline (t1) of participants of the experimental thyrotoxicosis study (N = 16) and of patients suffering from hypothyroidism (N = 15), respectively. Data was determined *via* ELISA.

3.2 Analysis of murine models of hyper-and hypothyroidism

Experimental studies in humans were complemented by corresponding mouse models. Working with animal models has the opportunity to examine tissues besides easily accessible plasma and connect results with each other. Human biopsy material is mostly not available due to ethical concerns and potential risk for patients and study participants. Within the framework of the mouse studies, not only the plasma proteome was investigated. In addition, the study also explored the influence of T4 on the liver proteome using liver tissue samples derived from the same animals (The corresponding liver tissue samples were analyzed within the framework of the master thesis of Vanessa Kracke and are not part of the thesis.) In the following, two murine studies are described analyzing the influence of thyroid disease on the plasma protein pattern.

3.2.1 Mouse model of transient thyrotoxicosis

The design of the murine study investigating transient thyrotoxicosis was similar to the human study of experimental thyrotoxicosis. However, each blood sample represented an individual animal because repeated blood sampling was not feasible. Mice were randomly assigned to a control, T4, and T4 recovery group of 8 animals each and treated according to the scheme displayed in Figure 15 (N = 24). Total T4 and total T3 measured in all samples are illustrated in Figure 16.

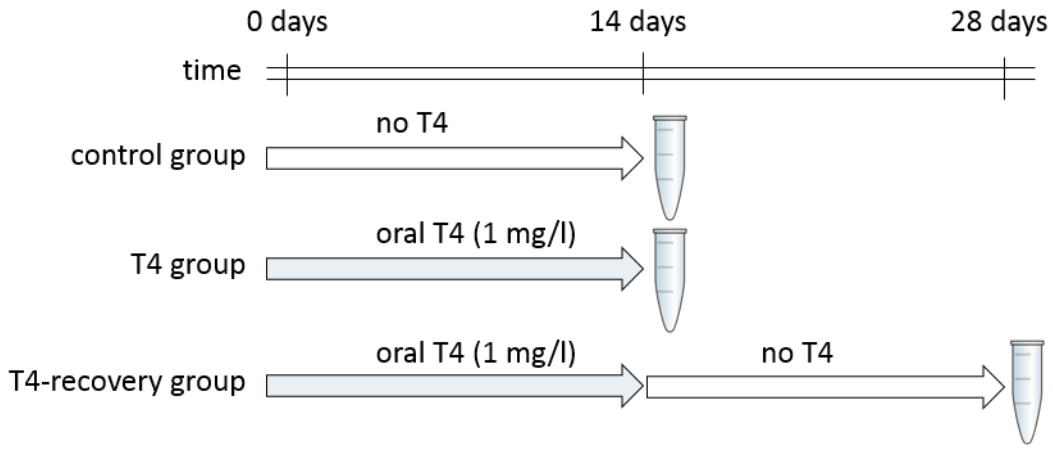

Figure 15 Design of the murine study investigating transient thyrotoxicosis. T4-dosage by T4-containing drinking water (1 mg/l in 0.1 % in BSA containing tap water).

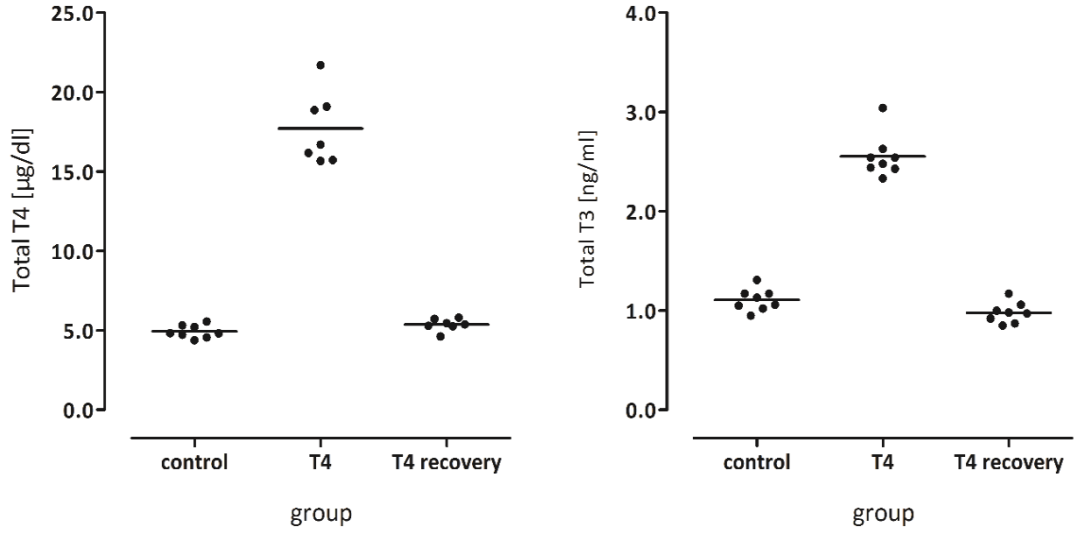

Figure 16 Individual plasma levels and mean values (line) of total T4 and total T3 in the different mice groups.

Total T4 levels in serum were elevated more than 3fold after two weeks of hormone exposure (4.93 µg/dl ± 0.40 µg/dl in the control group and 17.63 µg/dl ± 2.26 µg/dl in the T4 group). The recovery group showed comparable mean total T4 levels (5.37 µg/dl) as in the control group. Similar results were observed for total T3 levels. Control and recovery group showed mean total T3 levels of 1.11 ng/ml ± 0.11 ng/ml and 0.98 ng/ml ± 0.10 ng/ml, respectively. The T4-group showed clearly elevated total T3 levels (2.55 ng/ml ± 0.22 ng/ml).

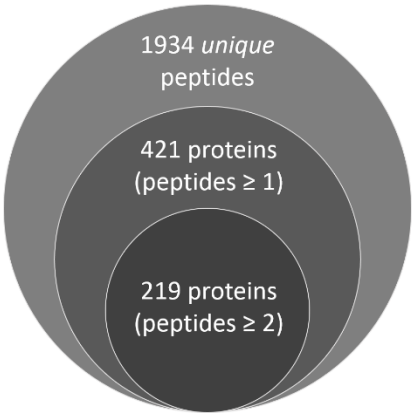

Figure 17 Identifications across all samples of the sample set 'transient thyrotoxicosis in mice'.

All plasma samples were depleted using a multi affinity removal column (MARS3, Agilent) removing the three highly abundant proteins serum albumin, serotransferrin and immunoglobulin G in murine plasma. Depleted plasma samples were analyzed *via* mass spectrometric measurement.

Obtained MS raw data were processed using Genedata Refiner MS software

where cluster annotations and intensities were extracted. Filtering and summation of annotated clusters in Genedata Analyst yielded 1934 *unique* peptides, representing 421 murine proteins (s.a. Supplementary table S5), out of which 219 proteins were identified with at least two peptides (Figure 17). Relative quantification was carried out with 363 proteins which were identified with one or more peptides and had more than 50 % valid values per group. Unsupervised principal component analysis (PCA) of the plasma proteome data was done to gain an impression of the variation within the groups and the differences between the three groups. Figure 18 depicts the first two principal components covering 54 % of variance in the data set.

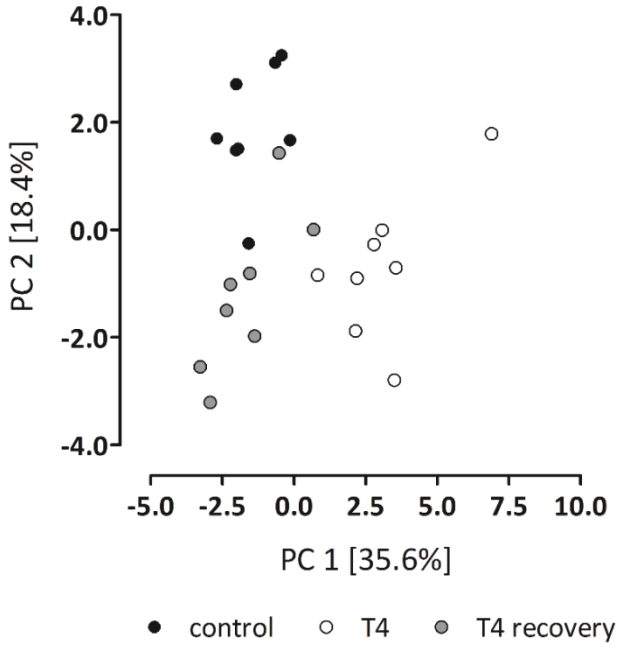

Figure 18 Principal component analysis of all samples included in the analysis of transient thyrotoxicosis. Performance was done using median normalized protein intensities with at least 50 % valid values across all samples. *PC* Principal component

Each dot in the plot represents one mouse and colors indicate the groups. Close proximity in the plot indicates small overall variation of the protein pattern of mice during the study. A separation between the control/recovery animals and mice of the T4 group can be observed in the first principal component. On the other hand, control group and T4 recovery group can be fairly well distinguished along the second principal component, thus already indicating that albeit showing very similar T4 and T3 levels, both groups still significantly differ in their protein pattern.

Significantly altered proteins across all groups were detected using analyses of variance (ANOVA) while accounting for multiple testing using the Benjamini-Hochberg procedure. Proteins exhibiting a false discovery rate (FDR) below 5% were considered significantly altered. Subsequently, single group comparisons of the 218 differently abundant proteins were performed *via* Welch's t-test (s.a. Supplementary table S6). In comparison with the human study, far more alterations in the murine plasma proteome were observed. Mouse models as genotypic identical animals should be yet better suited to identify protein changes. Thus, the number of proteins significantly changed due to T4 administration was even larger.

At all, 120 proteins (28 %) with a fold change ≥ |1.5| differed significantly between T4-treated and control group (Figure 19). The majority of proteins (n = 88) showed decreased abundance upon T4 treatment whereas 32 proteins demonstrated higher abundance (T4 mice group *vs.* controls). Concerning the comparison between T4-treated and T4-recovery group, 129 proteins significantly differed. The majority of proteins (n = 91) showed increased abundance whereas 38 showed decreased abundance.

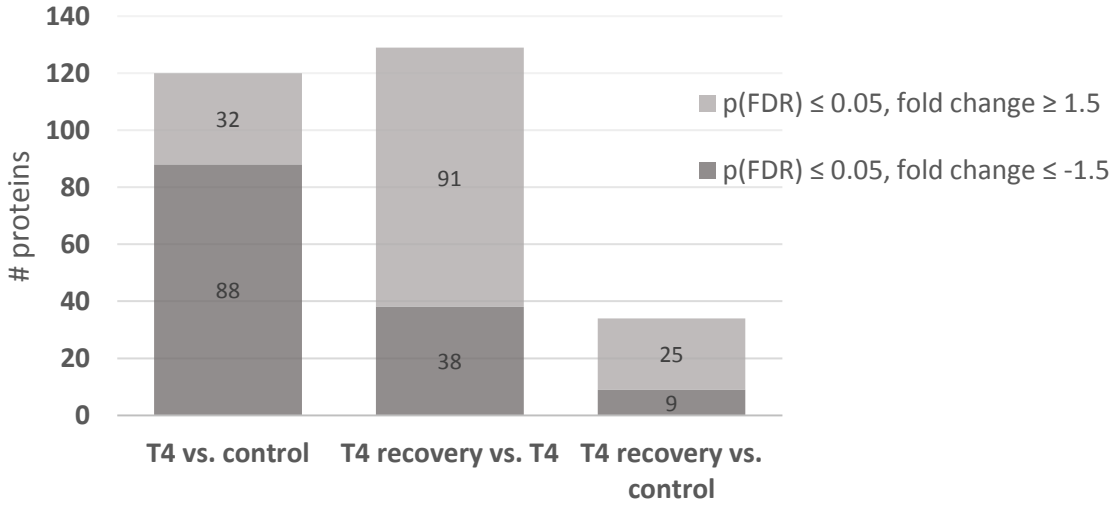

Figure 19 Number of significantly differential abundant proteins in group comparisons using Welch's t-tests (*p*(FDR) ≤ 0.05, fold change ≥ |1.5|).

Assuming a transient influence of thyroxine on the plasma protein level we expected hardly any difference between the T4 recovery group and the controls. However, 25 out of 34 still significantly different proteins showed higher abundance and 9 lower abundance in the recovery group.

Ninety proteins displayed an inverse alteration upon T4 treatment and during recovery phase and illustrate a transient influence of thyroxine administration (Figure 20). The majority of those proteins demonstrated a transient decline upon thyroxine application – 75 % of all significantly different proteins showed a lower abundance in the T4 group compared to the control group.

Considering a less stringent cut-off by neglecting the fold change leaded to an increase in consistent changes and to an larger overlap of proteins significantly altered upon T4 treatment. In detail, 13 proteins out of 30 proteins solely significant in the comparison between T4 treated mice and the controls still showed moderate alterations. The same holds true for 7 proteins out of the 39 proteins of the T4 recovery *vs.* T4 group comparison. The fold changes ranged from 1.3 up to 1.48.

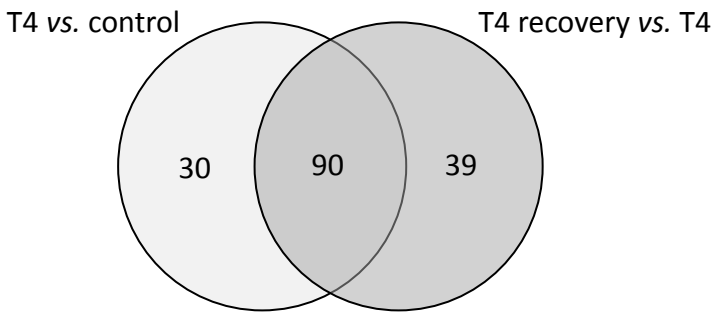

Figure 20 Overlap of proteins significantly altered upon T4 treatment (T4 *vs.* control group) and during depletion of T4 (T4 recovery *vs.* T4 group), *p*(FDR) ≤ 0.05, fold change > |1.5|. All 90 significantly different proteins showed only transient alterations.

Proteins differentially abundant between the T4 group and controls (n = 120) were analyzed using IPA to explore a possible enrichment in specific protein categories (Figure 21). It hase to be noted, that the analysis was done with the whole murine genome database as background. This might lead to biased results due to the lower number of protein classes detected in plasma in comparison to a cell lysate proteome analysis. With the identified protein set as reference, less significantly enriched categories were displayed.

Most proteins were assigned to the functional entities *LXR/RXR activation* and *Acute Phase Response Signaling* (both n = 19). It has to be noted, that a large number of proteins was assigned to more than one pathway as indicated in Figure 21. One protein group

(n = 7) comprised apolipoproteins (ApoD, ApoH, ApoB-100, ApoM, ApoA2, ApoC4, ApoE) showing decreased abundance in the T4-treated mice group compared to the controls. Those proteins were assigned to various categories all marked with a star in Figure 21. Proteins belonging to the complement system (n = 6) dropped in intensity after T4 administration and normalized after 14 days of recovery.

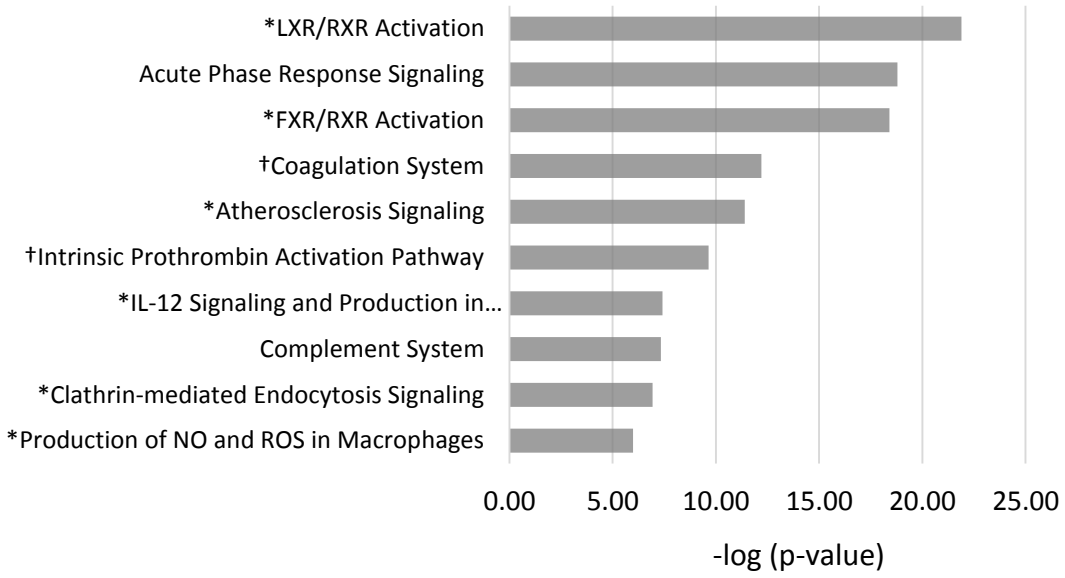

Figure 21 Functional categorization of proteins using Ingenuity Pathway Analysis. 120 proteins (p(FDR) ≤ 0.05, fold change ≥ |1.5|were analyzed. (*), (†): large overlap of proteins assigned to the category. *NO* nitride oxide, *ROS* reactive oxygen species

Exemplarily, Figure 22 illustrates the altered intensities of two proteins belonging to the complement system during the study period. Coagulation factors and associated proteins (n = 9) were also found decreased in the T4-treated mice compared to the controls. Proteins displaying different abundances between the T4 recovery group and the T4-treated group were – as expected – assigned to similar canonical pathways in IPA. Consistently and also as expected, those differences exhibited the reverse direction.

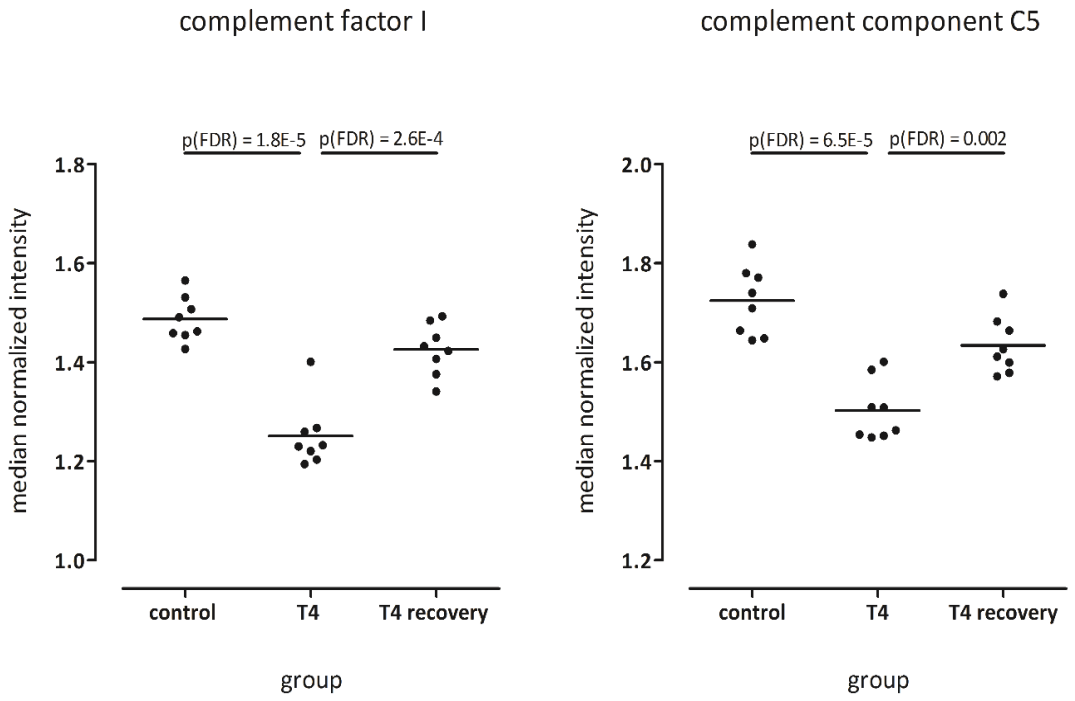

Figure 22 Alteration of complement factor I and complement component C5 during the study period. Significant decrease in protein levels upon T4 exposure and normalization after removal of T4 after 2 weeks.

With respect to the comparison between the T4 recovery group and the controls 34 proteins displayed significantly different levels between these two groups. Illustration of different patterns of proteins until the recovery phase is shown in Figure 23. Only 2 proteins showed significant alterations in all three comparisons (T4 *vs.* controls, T4 recovery *vs.* T4, T4 recovery *vs.* controls), namely α-centractin (ACTZ) and thrombospondin-4 (TSP-4). While ACTZ abundance decreased during T4 administration it increased significantly in the T4 recovery group compared to the controls. The opposite happened for thrombospondin-4 showing increasing abundance in the T4 group which dropped below the baseline level in the recovery group. For both proteins an overcompensatory reaction after stopping the L-T_4 application was observed.

Many of the 34 proteins already revealed different abundances when comparing the T4 recovery mice group with the T4 treated mice (n = 17) or comparing T4 treated mice with the controls (n = 7) including fibrinogen β chain which significantly decreased between T4 treated mice and controls and followed the same trend displaying further reduction in protein levels after 2 weeks of LT_4 withdrawal (T4 recovery). *Vice versa*, it has been

observed for the cytoplasmic malate dehydrogenase that protein levels still increased after stopping the treatment.

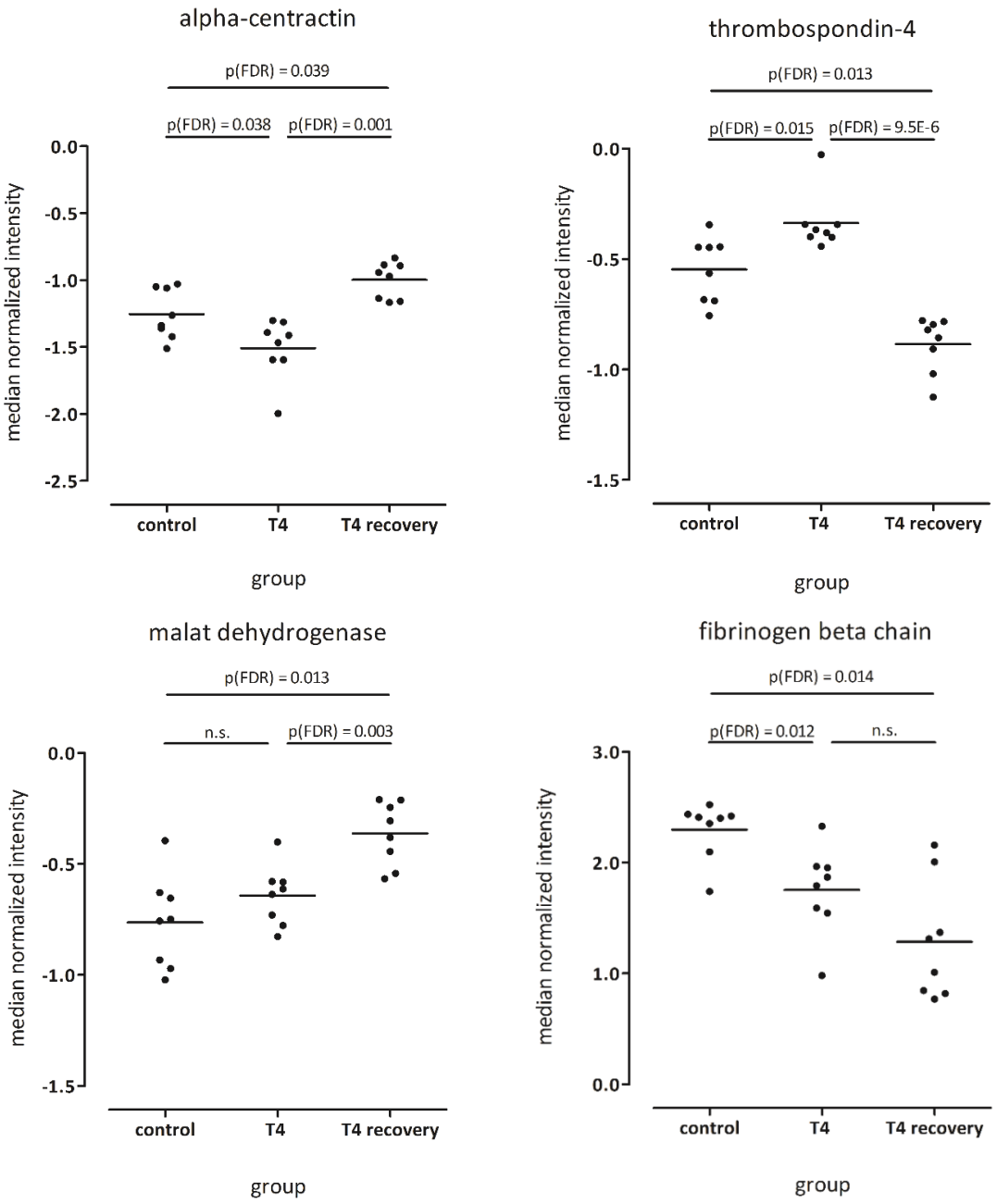

Figure 23 Various proteins significantly changed in the T4 recovery group compared to the controls but showing inconsistent pattern during the study period.

3.2.2 Mouse model analyzing T4, T3 and MMI/$KClO_4$-induced alterations in the murine plasma proteome

The second murine study augmented the previously introduced study design using additionally a T3 treated group as well as hypothyroid group. The last group was rendered hypothyroid by treatment with MMI/$KClO_4$ (methimazole/potassium perchlorate). The study design is depicted in Figure 24.

Total T4 and total T3 measurements in all four groups of mice are depicted in Figure 25. As expected, total T3 rose from 1.66 ng/ml ± 0.44 ng/ml (SD) to 8.36 ng/ml ± 0.51 ng/ml in the T3 administrated group whereas total T4 levels were completely suppressed (0.12 µg/dl ± 0.05 µg/dl). Total T4 increased from 1.83 µg/dl ± 0.87 µg/dl to 10.42µg/dl ± 1.15 µg/dl in the T4 administered group compared to the controls. Total T3 also increased to 3.42 ng/ml ± 0.57 ng/ml in that group. MMI/KClO4 mice group showed a significant drop in total T4 levels (0.10 µg/dl± 0.01 µg/dl) while the decrease of total T3 (0.92 ng/ml ± 0.29 ng/ml) in the hypothyroid mice was not significant compared to the controls.

Quality controls of LC chromatograms exhibited a different profile in two samples probably due to strong hemolysis during blood sampling. Excluding these samples from further analysis led to the following group sizes: control group n = 4, T4 group n = 3, T3 group n = 3, MMI/$KClO_4$ n = 4.

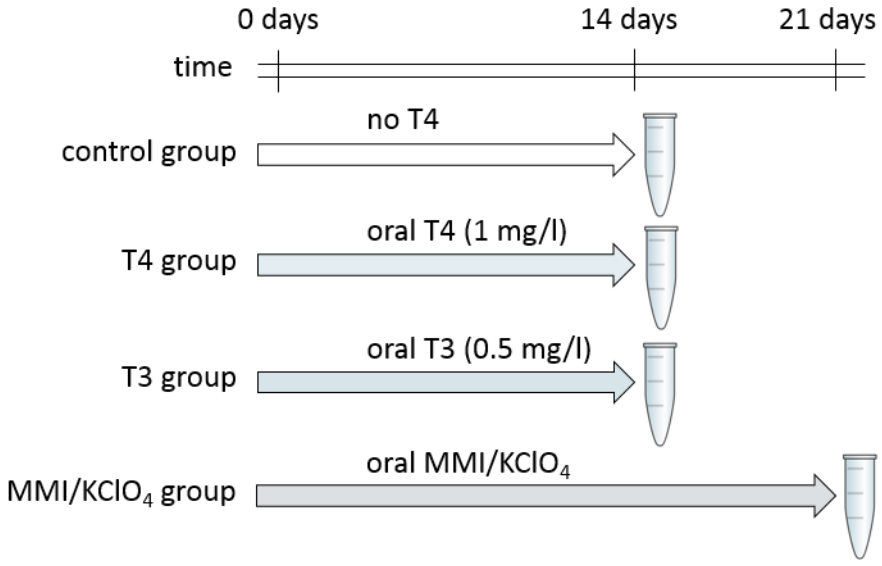

Figure 24 Study design of the second murine study investigating different interventions of the thyroid hormone system. *MMI* methimazole, 0.1 %; *$KClO_4$* potassium perchlorate, 0.2 %; *T4* thyroxine; *T3* triiodothyronine

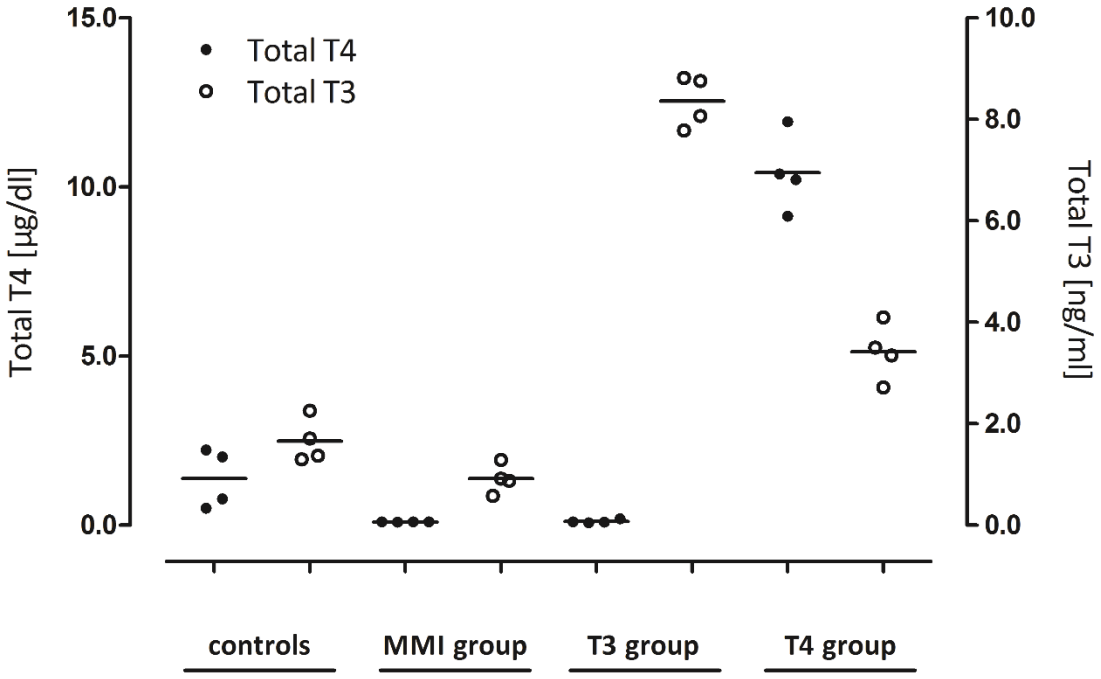

Figure 25 Individual plasma levels and mean values (line) of each total T4 and total T3 in the four treatment groups.

Relative protein quantification was done in Genedata Refiner. In total, 428 proteins (251 proteins with peptides ≥ 2) were considered for analysis (s.a. Supplementary table S7). PCA based on median normalized protein intensities with at least 50 % valid values across all samples sets provided an initial overview about the variability across samples and groups (Figure 26). The first two principle components already covered 46.3 % of the variance in the data set. Mice belonging to the control group showed the largest variation along the first principle component. In general, a clear separation between all groups became apparent along using linear combinations of the first two principle components, indicating the strong effects of the treatments. Furthermore, separation may occurs in accordance to the TH levels revealing a greater distance of T3 treated mice to the MMI/$KClO_4$ treated mice than to the controls, for example. The T4 treatment seems to have a lesser impact on the plasma proteome than the T3 treament.

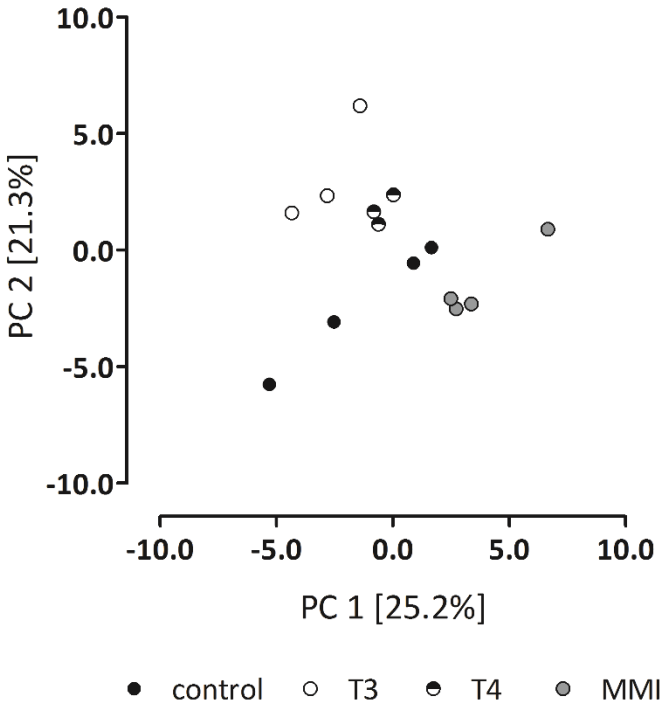

Figure 26 Principal component analysis of all samples. Analysis was done using median normalized protein intensities with at least 50 % valid values across all samples. *PC* Principal component

Differently abundant proteins between the groups were detected using Welch's t-test (s.a. Supplementary table S8). Proteins were considered as significantly different if the *p*-value was ≤ 0.05 (Figure 27). The data set revealed higher variation between the samples in the different groups compared to the first murine study which influences the fold change calculated based on group's mean. In order to assess the consistent changes between the different inductions compared to the controls, we considered only the *p*-value < 0.05 as the threshold of significance.

Most proteins in the group comparisons with controls exhibited a trend for decreased abundances. More alterations were found in T3 *vs.* control (n = 49) than in T4 *vs.* control (n = 36). The comparison of MMI/$KClO_4$ treatment *vs.* control revealed 52 differentially abundant proteins. Among the significantly altered proteins 48 and 26 showed a fold change greater than |1.5| in the T3-treated and T4-treated groups, respectively.

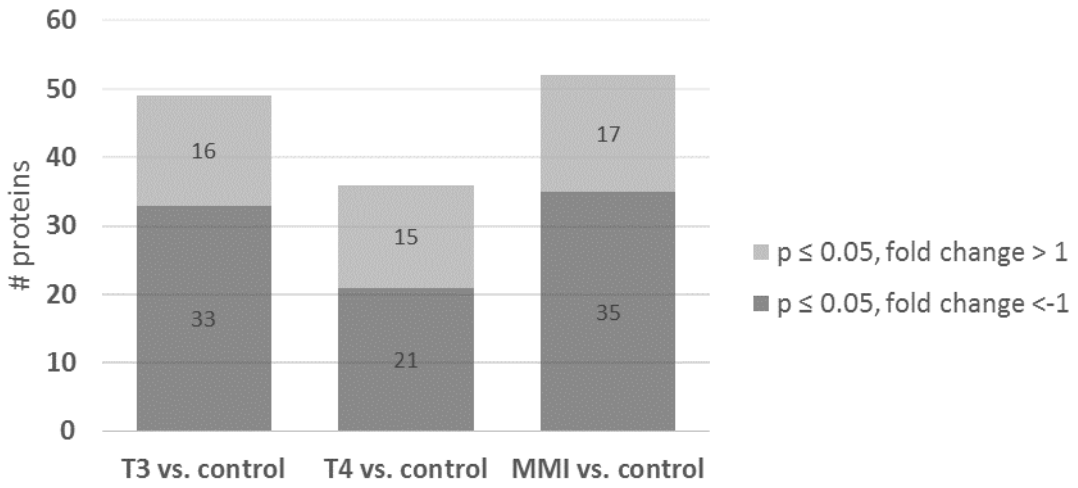

Figure 27 Number of significant differentially abundant proteins between induction groups and controls. Results obtained from Welch's test ($p \leq 0.05$).

The overlap of the proteins displaying alterations in level after T3 and T4 treatment, respectively, consisted of 20 proteins (Figure 28). Many proteins displayed significantly altered abundance only in the T3 *vs.* control and T4 *vs.* control comparison, respectively. Almost all of them showed the same direction in alteration in the respective other group comparison, but missed the threshold of significance.

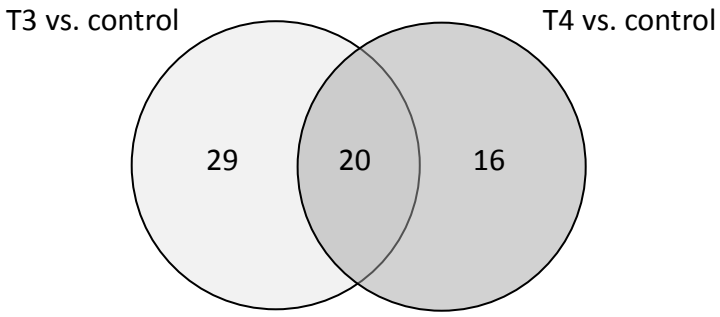

Figure 28 Overlap of proteins significantly altered by T3 or T4 treatment in comparison to non-treated control group ($p \leq 0.05$).

The proteins significantly altered in both T4 group and T3 group compared to the controls are illustrated in Table 18. Reflecting the results from the single group comparisons most proteins (15 out of 20) showed decreased abundance under hyperthyroid conditions. It has to be noted, that effect sizes of changes in the induced hyperthyroidism by T3 are more prominent compared to changes in the induced hyperthyroidism by T4.

Table 18 List of proteins displaying significantly altered levels between T3 and controls- as well as T4-treated animals ($p \leq 0.05$). Positive fold changes indicate increased abundance in the T3/T4 group compared to controls. Negative fold changes indicated decreased abundance in the T4/T3 group compared to controls. Fold change ≥ |2| is indicated in bold.

Annotation	Protein names	T3 *vs.* control		T4 *vs.* control	
		p value	fold change	*p value*	fold change
Hyaluronan metabolic process					
ITIH3_MOUSE	Inter-alpha-trypsin inhibitor heavy chain H3	0.0008	**-8.61**	0.0196	**-3.03**
ITIH2_MOUSE	Inter-alpha-trypsin inhibitor heavy chain H2	0.00001	**-2.90**	0.0311	-1.92
ITIH1_MOUSE	Inter-alpha-trypsin inhibitor heavy chain H1	0.0244	**-2.49**	0.0421	-1.44
Apolipoproteins – cholesterol efflux and more					
APOC1_MOUSE	Apolipoprotein C1	0.0065	**-4.09**	0.0450	**-2.06**
APOB_MOUSE	Apolipoprotein B-100	0.0021	**-3.34**	0.0392	-1.83
APOA2_MOUSE	Apolipoprotein A2	0.0018	**-2.86**	0.0139	-1.88
Complement system					
C4BPA_MOUSE	C4b-binding protein	0.0086	**-2.80**	0.0344	-1.50
CFAI_MOUSE	Complement factor I	0.0083	**-2.51**	0.0306	-1.73
CO3_MOUSE	Complement C3	0.0244	**-2.07**	0.0081	-1.82
Inflammatory responses					
KNG1_MOUSE	Kininogen-1	0.0390	-1.82	0.0406	-1.52
CD5L_MOUSE	CD5 antigen-like	0.0166	**4.57**	0.0235	1.83
Divergent tasks within the organism					
DUS2L_MOUSE	tRNA-dihydrouridine	0.0111	**-6.00**	0.0264	**-2.18**
AMBP_MOUSE	Protein AMBP	0.0003	**-4.44**	0.0070	**-2.19**
CHLE_MOUSE	Buturylcholine esterase	0.0005	**-2.17**	0.0202	**-2.14**
PHLD_MOUSE	Phosphatidylinositol-glycan-specific phospholipase D	0.0067	**-2.15**	0.0115	-1.72
AFAM_MOUSE	Afamin	0.0027	**-2.72**	0.0291	-1.67
PSB6_MOUSE	Proteasome subunit beta type-6	0.0266	1.52	0.0149	1.46
TKT_MOUSE	Transketolase	0.0283	**3.14**	0.0499	**2.82**
VGFR3_MOUSE	Vascular endothelial growth factor receptor 3	0.0041	**3.78**	0.0149	**2.33**
MUP6_MOUSE	Major urinary protein 6	0.0083	**8.12**	0.0132	**5.65**

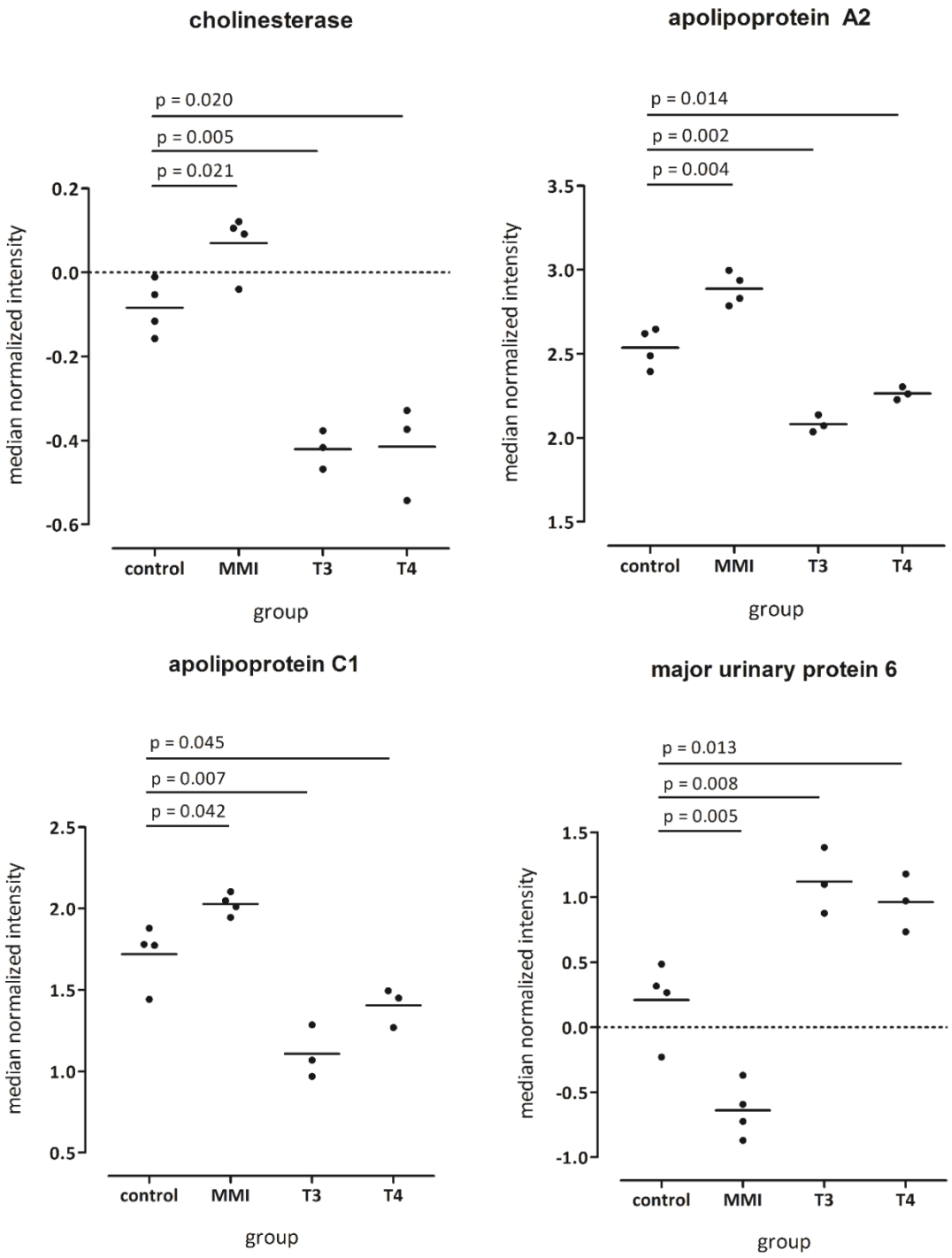

Figure 29 Protein levels of cholinesterase, apolipoprotein A2 and C1 as well as major urinary protein 6 in all four different groups. Levels are plotted as median normalized intensities with mean value (line) and *p* value derived from Welch's t-test.

Proteins displaying significant alterations in level after each treatment, and hence likely reflecting thyroid state, were apolipoprotein A2 (ApoA2), apolipoprotein C1 (ApoC1), buturylcholine esterase (BChE) and major urinary protein 6 (MUP-6). The alterations

showed a reverse trend between T4/T3 *vs.* control and MMI/$KClO_4$ *vs.* control, respectively (Figure 29). The strongest effect on the plasma proteome was noted when the animals received metabolically active hormone T3.

Significantly changed proteins ($p \leq 0.05$, fold change 1.5) in the hyperthyroid and hypothyroid groups compared to the control group were categorized *via* Ingenuity Pathway Analysis (IPA). Enrichment results are depicted in Table 19.

Table 19 Functional categorization of proteins using IPA. Significantly altered ($p \leq 0.05$, fold change $\geq |1.5|$) proteins of single group comparisons *via* Welch's t-test were used. (*) same proteins assigned to the pathway; (†) huge overlap of proteins assigned to the pathway.

Canonical pathway	T3 *vs.* control		T4 *vs.* control		MMI *vs.* control	
	p-value	#proteins	*p*-value	#proteins	*p*-value	#proteins
Acute Phase Response Signaling	2.62E-12	10	1.78E-06	5	2.89E-04	4
Complement System	1.68E-10	6	9.46E-04	5	7.85E-09	5
***†LXR/RXR Activation**	2.00E-10	8	1.02E-10	7	8.00E-05	4
***†FXR/RXR Activation**	2.77E-10	8	1.36E-10	7	9.36E-05	4
†Atherosclerosis Signaling	8.18E-06	5	1.68E-05	4	1.37E-07	6

Selected examples of proteins assigned to the category *LXR/RXR activation* or *Complement system* are displayed in Figure 30. Similar enriched pathways could be detected by IPA across the three group comparisons. However, regarding the three different inductions, different proteins were significantly altered and accountable for the observed enrichment. Additionally, the alterations in level of proteins belonging to the same functional category were not inverse in general. An inverse fold change comparing the hyperthyroid and hypothyroid state can be observed for apolipoproteins, but not for complement components and factors.

In total, 11 apolipoproteins were detected *via* mass spectrometric analysis, but only 3 (ApoA2, ApoC1, ApoB-100) of them were significantly altered and dropped in both hyperthyroid conditions compared to the controls. However, all others showed at least a tendency of decreased intensities. Under hypothyroid conditions, apolipoprotein A2 and C1 increased more than 2fold. Even if not significant, the majority of all other quantified apolipoproteins also demonstrated a trend to increased levels under hypothyroid conditions.

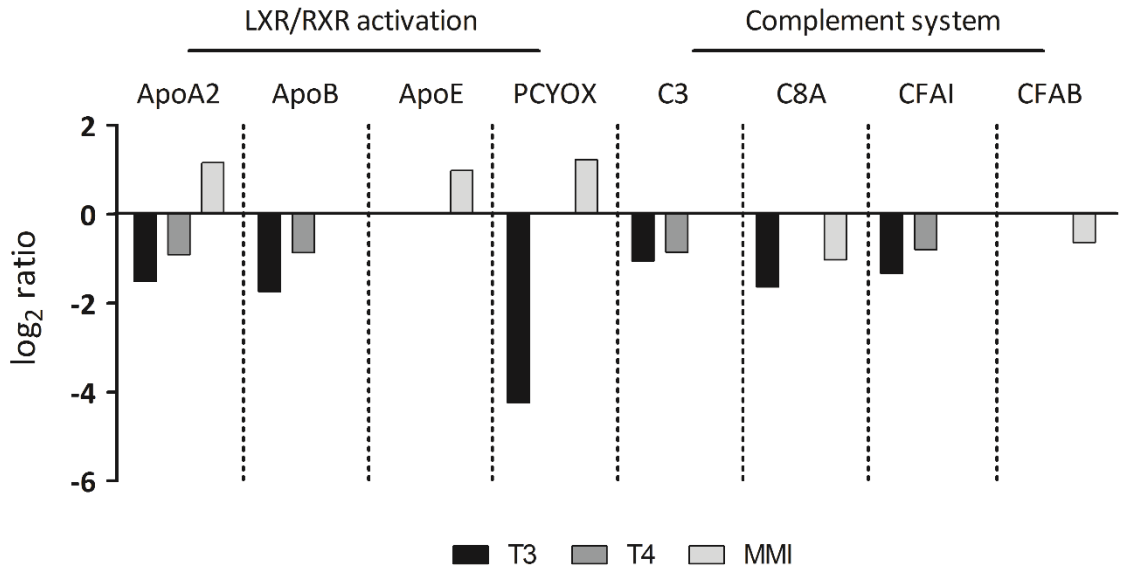

Figure 30 Selected proteins of the canonical pathways *LXR/RXR activation* and *Complement system* derived from the functional categorization of IPA (see table 19). Log_2 ratio demonstrates the alteration in abundance in the respective induction group compared to the control mice group. *ApoA2* apolipoprotein A2; *ApoB* apolipoprotein B-100; *ApoE* Apolipoprotein E; *PCYOX* prenylcysteine oxidase; *C3* complement component C3; *C8A* complement component C8 α chain; *CFAI* complement factor I; *CFAB* complement factor B

Complement factors seemed to be influenced by T3 and dropped in intensity (C3, C5, C8A, CFAD and CFAI) while mannose binding-protein C (MBL) as another protein assigned to this pathway increased in the hyperthyroid group (fold change 1.75). Little response was seen after T4 administration. Only 2 complement factors demonstrated decreased abundance in this hyperthyroid group compared to the control (CFAI and C3). Furthermore, minor effect sizes could be observed. Interestingly, levels of complement system associated proteins also significantly decreased in the hypothyroid mice group, but in part other components than in the hypothyroid group (CFAB, C8A, C8B, C8G and C1QC).

No enrichment with respect to the coagulation cascade was observable. At least kininogen-1 showed a decreased abundance in both hyperthyroid mice groups and no change in protein level in hypothyroid mice (T3 *vs.* control $p = 0.039$, fold change -1.82; T4 *vs.* control $p = 0.041$, fold change -1.52).

Transthyretin as thyroid hormone-binding protein decreased remarkably in the hyperthyroid groups as seen for T3 ($p = 0.0344$, fold change -6.82) and showed a clear

tendency towards dropped intensity in the comparison T4 *vs.* control (p = 0.0893, fold change -3.95) while in the MMI/$KClO_4$ group a reverse trend with increased abundance of transthyretin compared to the controls (p = 0.0522, fold change 5.47) was observed. Additionally, a substantial depletion of thyroid hormone-binding globulin (THBG) was noted in the presence of increased levels of T3 and T4. Thus, THBG could not be identified in the T3 group at all and only detected at low levels in the T4 group. In contrast, the hypothyroid mice group receiving MMI/$KClO_4$ showed a strong significant increase of THBG levels compared to the control group (p = 1.3E-6, fold change = 31.3).

3.3 Comparison of both murine studies

Within this work two different proteome studies using murine plasma samples were carried out. The first study (**set 1**) investigated merely the influence of T4 on the plasma proteome indicating a transient effect of experimental thyrotoxicosis. Mice were assigned to three separate groups. Besides the untreated control group and the T4-treated group a third group of mice who recovered from T4 administration was included.

The second study (**set 2**) contained various induction groups which were compared to an untreated control group. As previously, hyperthyroidism was induced by T4 administration in the first group of mice. A second hyperthyroid group served to investigate the influence of the metabolically more active T3 on the plasma proteome. A third group represented induced hypothyroidism achieved by the administration of MMI/$KClO_4$. The study did not include recovery groups for the different induction groups. Both studies were performed using male C57BL/6 mice. Husbandry situation was the same for all animals and TH or MMI/$KClO_4$ were administered through drinking water. In both studies, T4 was used for inducing experimental hyperthyroidism and the duration of T4 administration was kept equal. Only the hypothyroid group was conditioned longer due to the delayed impact of MMI/$KClO_4$.

Both studies aimed to elucidate the influence of thyroid dysfunctions on the murine plasma proteome. Experimental processing of all plasma samples was equal consisting of the depletion of three high abundant proteins *via* immunoaffinity chromatography, followed by precipitation and tryptic digestion of the remaining proteins. Measurements were performed on two widely used mass spectrometers for proteomic analysis.

The first set focusing on transient thyrotoxicosis was recorded on a LTQ-Orbitrap Velos™ mass spectrometer whereas the second study investigating hyper- and hypothyroidism was measured on a Q Exactive™ Orbitrap mass spectrometer. All data sets were acquired in data-dependent acquisition mode (DDA). This is a process driven by an automated instrument control routine that schedules the MS/MS acquisition depending on the signal intensities in the preceding MS scan starting with the highest signal. Unfortunately, this often results in lower abundant signals being left out unanalyzed and therefore unidentified. For the LTQ-Orbitrap Velos™ the 20 most intense peaks were selected for fragmentation in the ion trap while for the Q Exactive a Top10 method was chosen.

On the LTQ-Orbitrap Velos™, the precursor mass spectra were acquired with an orbitrap whereas the MS/MS data were acquired with the ion trap using collision induced dissociation. At the Q Exactive™ the orbitrap is used for both MS and MS/MS data acquisition. Former study showed that acquisition on a Q Exactive™ mass spectrometer resulted in a higher number of unique peptides summarized in more protein identifications most likely due to a faster scan rate, improved sensitivity and higher resolution [84]. Looking at the two murine studies presented in this thesis, data dependent acquisition mode using one instrument or the other led to comparable results regarding peptide and protein identifications. Both analyses yielded in a similar number of peptides with 1934 unique peptides for the data set of transient thyrotoxicosis and 2034 unique peptides for the second set which is only an increase of 5 % regarding the total number. When comparing the mean peptide identifications per protein there was no major difference with 4.78 peptides per protein for Q Exactive™ data and 4.59 peptides per protein for LTQ-Orbitrap Velos™ data. The analysis of both study sets resulted also in similar counts for protein identifications. The first study of transient thyrotoxicosis with a size of 24 samples revealed 421 proteins compared to 428 proteins in the second murine study from a total of 14 included samples. Protein identifications are depicted in Figure 31.

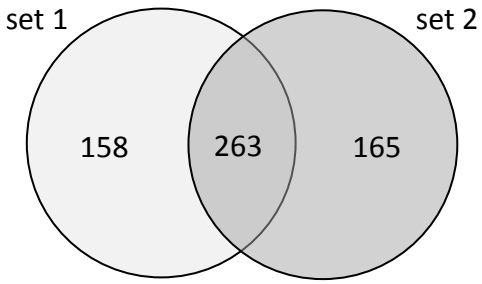

Figure 31 Venn diagrams displaying the number of protein identifications in both murine data sets. *Set 1:* study of experimental thyrotoxicosis, *Set 2:* study of hyper- and hypothyroidism induced by TH or MMI/$KClO_4$

In total, 263 distinct proteins (60 %) were found in both studies. The proportion of classical plasma proteins found within the overlap was close to 62 %. Proteins identified with two or more peptides showed a greater overlap between both data sets. The proportion of secreted proteins out of these 188 proteins is closely to 73 %.

Looking at the studies separately, the proportion of secreted proteins of the total number of identified proteins is rather similar in set 1 and 2 with 40 % and 44 %, respectively

(Figure 32). 53 % and 54 % (set1 and set 2) of protein intensities correspond to secreted proteins emphazising that classical plasma proteins are more abundant in both sets than leakage proteins.

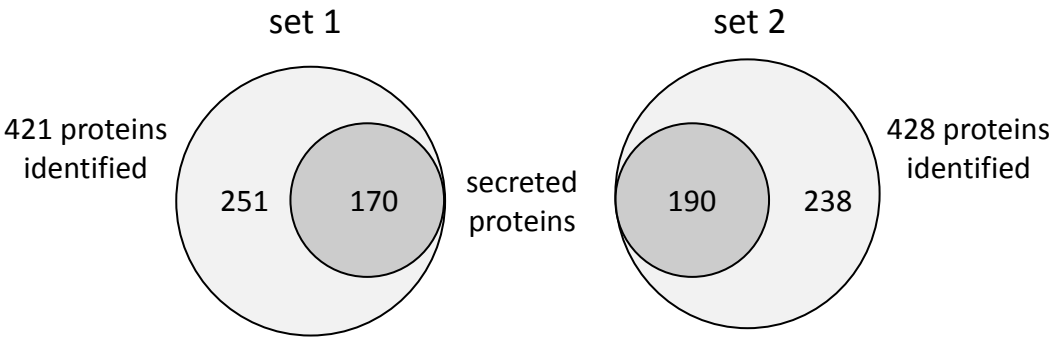

Figure 32 Proportion of secreted proteins (dark circles) of total protein identifications in both murine study sets. *Set 1:* study of experimental thyrotoxicosis; *Set 2:* study of hyper- and hypothyroidism induced by TH or MMI/$KClO_4$

According to the multiplicity of similarities, it is possible to compare both studies and their results. As illustrated in Figure 33 A, the analysis of the transient thyrotoxicosis study set resulted in 120 proteins with a fold change ≥ |1.5|. A similar statistical testing approach applied to the second murine data set revealed only 36 significant changes even without a fold change restriction. Only 26 proteins showed an alteration ≥ |1.5| between the T4 and control group. Comparison of significantly changed proteins which were also detected of the respective other analysis, led to 72 proteins in set 1 and 21 in set 2 (Figure 33 B).

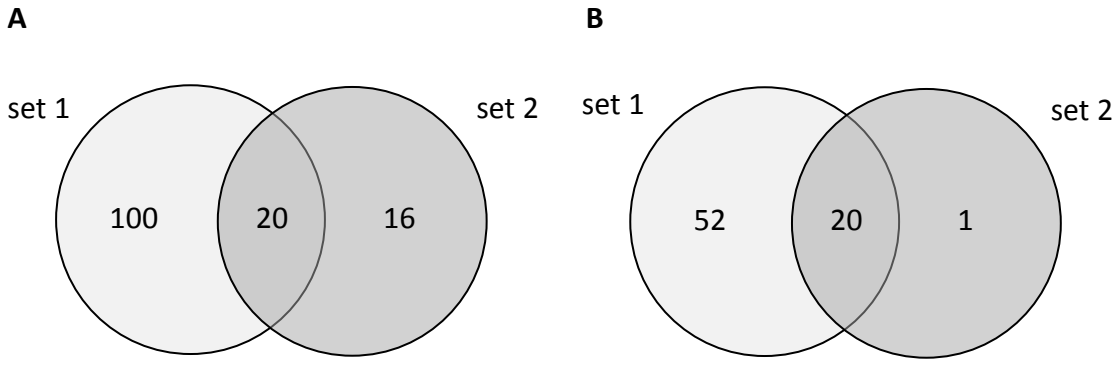

Figure 33 Overlap of significantly altered proteins between T4 treated mice compared to the control group in both murine data sets; **(A)** *Set 1:* 120 proteins differentially abundant (T4 group *vs.* controls, Welch's t-test, *p*(FDR) ≤ 0.05, FC ≥ |1.5|; *Set 2*: 36 proteins differentially abundant (T4 group *vs.* controls, Welch's t-test, p ≤ 0.05); **(B)** same comparison but only considering proteins which were detected in both sample sets. *Set 1:* 72 proteins, *Set 2:* 21 proteins

Proteins covered in the overlap are presented in Table 20. The majority are classical plasma proteins like various apolipoproteins and proteins belonging to the complement system. Just two proteins (VCAM1_MOUSE, VGFR3_MOUSE) are described as leakage proteins located in the cell membrane. Except of α2-antiplasmin all proteins showed the same trend across both data sets, mostly revealing larger changes in the data set of transient thyrotoxicosis, probably due to the higher variance in the control group in set 2 lowering the mean values per group used for fold change calculations.

The observed deviations between both studies could be due to various reasons. First, different group sizes were considered, leading to a restricted statistical power in the second murine study. The transient thyrotoxicosis study had twice as much samples per group (n = 8). Hence, differences in protein abundances between separate groups are better accessible and indicate statistical significance even after accounting for multiple testing (Benjamini-Hochberg). Another reason might be the higher variance between control animals in the second set as obvious from the PCA (Figure 26) hampering statistical testing.

Table 20 Common differentially abundant proteins in both murine studies (T4 group *vs.* controls, Welch's t-test). *Light grey* significant differentially abundant proteins in set 1; even though missing the significance threshold in set 2, they showed the same trend.

Swissprot Annotation	Description	Set 1		Set 2	
		p(FDR)	fold change	*p*-value	fold change
Apolipoproteins					
APOB_MOUSE	Apolipoprotein B-100	2.74E-08	-2.80	3.92E-02	-1.83
APOA2_MOUSE	Apolipoprotein A2	3.54E-07	-3.46	1.39E-02	-1.88
APOC1_MOUSE	Apolipoprotein C1	3.63E-05	-3.76	4.50E-02	-2.06
APOE_MOUSE	Apolipoprotein E	2.23E-08	-2.96	0.0842	-1.48
Complement system					
CO3_MOUSE	Complement C3	5.81E-07	-2.36	8.11E-03	-1.82
CFAI_MOUSE	Complement factor I	1.85E-05	-1.72	3.06E-02	-1.73
C4BPA_MOUSE	C4b-binding protein	5.23E-04	-1.64	3.44E-02	-1.50
Hyaluronan metabolic process					
ITIH3_MOUSE	Inter-alpha-trypsin inhibitor heavy chain H3	2.64E-05	-3.53	1.96E-02	-3.03
ITIH1_MOUSE	Inter-alpha-trypsin inhibitor heavy chain H1	6.27E-04	-1.70	4.21E-02	-1.44
ITIH4_MOUSE	Inter alpha-trypsin inhibitor, heavy chain 4	4.84E-03	-1.54	3.39E-02	-1.44
Coagulation					
A2AP_MOUSE	Alpha-2-antiplasmin	3.61E-04	-2.12	1.97E-02	1.17
KNG1_MOUSE	Kininogen-1	3.67E-04	-1.54	4.06E-02	-1.52
Divergent tasks in the organism					
PHLD_MOUSE	Phosphatidylinositol-glycan-specific phospholipase D	6.39E-08	-2.00	1.15E-02	-1.72
AFAM_MOUSE	Afamin	1.80E-06	-2.09	2.91E-02	-1.67
CLUS_MOUSE	Clusterin	7.08E-06	-1.75	2.72E-02	-1.33
PON1_MOUSE	Serum paraoxonase	1.36E-05	-1.84	2.63E-02	-1.85
CHLE_MOUSE	Cholinesterase	1.05E-04	-8.11	2.02E-02	-2.14
VCAM1_MOUSE	Vascular cell adhesion protein 1	1.28E-03	1.52	3.03E-02	1.32
CD5L_MOUSE	CD5 antigen-like	9.48E-03	1.77	2.35E-02	1.83
AMBP_MOUSE	Protein AMBP	1.18E-02	-1.62	7.02E-03	-2.19
VGFR3_MOUSE	Vascular endothelial growth factor receptor 3	1.50E-02	6.38	1.49E-02	2.33
A2M_MOUSE	Pregnancy zone protein	2.97E-07	-2.69	0.0687	-1.81
MUP2_MOUSE	Major urinary protein 2	9.83E-03	2.14	0.0601	2.72
TRFL_Mouse	Lactotransferrin	7.77E-03	-1.83	0.0857	-1.45

3.4 Comparison of results from human and murine studies

A summary of the workflows and the data of the human plasma proteome study investigating experimentally induced thyrotoxicosis and the analogous murine proteome study of transient thyrotoxicosis is provided in Table 21.

Table 21 Summary of the human study of experimentally induced thyrotoxicosis and the murine study of transient thyrotoxicosis and recovery.

Species	Human	Mice
Data set	N = 80	N = 24
Design	Longitudinal study, 16 subjects, 5 time points per subject	Case-and-Control samples, 3 groups, 8 samples per group
Depletion	Immunoaffinity chromatography Human MARS6 column,Agilent	Immunoaffinity chromatography Mouse MARS3 column,Agilent
Digestion	• Reduction and alkylation • Tryptic proteolysis	• Reduction and alkylation • Tryptic proteolysis
Measurement	LTQ-Orbitrap Velos™ mass spectrometer	LTQ-Orbitrap Velos™ mass spectrometer
Date	2013/12	2015/04
Data preparation and analysis	Genedata Refiner MS and Analyst software	Genedata Refiner MS and Analyst software
Peptide/Protein identification	2374/512 (437 considered for quantification)	1934/421 (363 considered for quantification)

In the human study investigating experimentally induced thyrotoxicosis, 16 healthy young male volunteers were administered L-T_4 over 8 weeks and blood was sampled at different time points covering baseline and peak concentration of T4 after 4 and 8 weeks of administration as well as time points after the application stopped.

The following mouse study was inspired by the human T4 intervention study and had an analogous design. The mouse control group reflected the baseline levels and the T4 group mimicked the influence of L-T_4 treatment. Samples of an additional group referred to as T4 recovery group were taken 2 weeks after stopping the L-T_4 treatment.

The great benefit of the human study was a study design which implemented repeated measurements of the same subjects. In the murine study, repeated measurements could not be achieved because blood sample collection is final in rodents, thus each blood sample represented an individual animal.

Apart from this aspect, both studies are comparable. For the sample measurement, an Orbitrap Velos™ mass spectrometer operated in data dependent acquisition mode was used. Following data analysis of both raw data sets contained equal steps with similar settings for all parameters. Annotated isotope peak clusters were summed up to peptides. After filtering, *unique* peptides per protein were summed up to generated protein intensities. In total, 512 human proteins were identified out of which 437 were considered for quantification (60 % valid values per protein across all samples). The data analysis of the murine plasma set yielded in 421 proteins of which 363 proteins were identified in at least 50 % of all samples per group. The comparison of identified proteins is displayed in Figure 34 and is based on the Uniprot/Swissprot annotation. All proteins were verified manually since homologue proteins in mouse and human can have different identifiers.

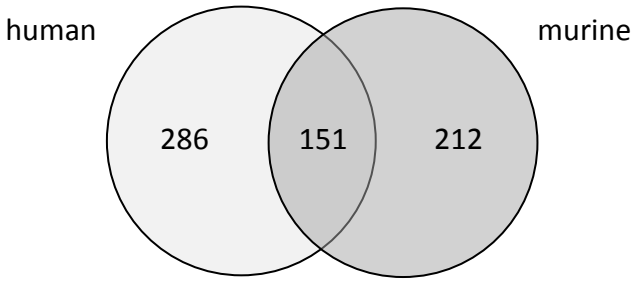

Figure 34 Overlap of protein identifications between the human and the murine data set. 437 proteins (at least 60 % valid values) considered for quantification in the human study (n=80) compared to 363 proteins considered for quantification (at least 50 % valid values per group) in the murine study (n=24). 151 proteins were identified in both studies.

Impact of thyroid hormones on both the murine system and humans

T4 administration for 4 weeks (t2 compared to t1) resulted in a total of 91 proteins with significant different level in plasma (p-value ≤ 0.05) of human subjects. Results of the performed paired t-test are summarized in Supplementary table S4. In the murine system, 120 proteins displaying significantly altered levels were detected with a Welch's t-test with a corrected p-value ≤ 0.05 and an additional fold change threshold of 1.5. The

number increased up to 168 proteins without restriction on the extent of change (see table S7 for further information). Comparison of both studies is shown in Figure 35 with an overlap of 30 proteins identified as differentially abundant due to T4 treatment in both humans and mice.

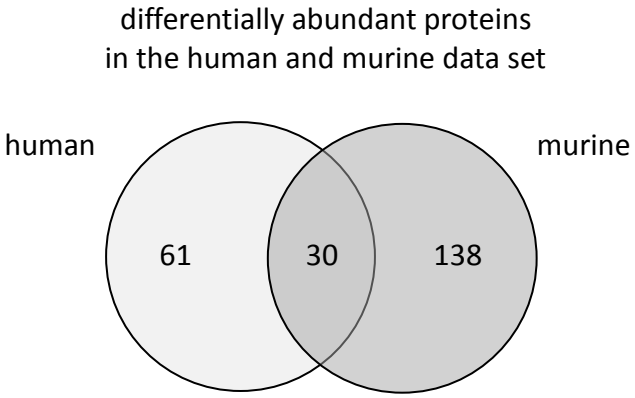

Figure 35 Overlap of significantly altered proteins upon T4 administration between the human and the murine data set. Significantly changed proteins in the human study detected using a paired t-test (t2 vs. t1, *p*-value ≤ 0.05). Significantly changed proteins in the murine study were detected by a Welch's t-test (*p*(FDR) ≤ 0.05, fold change ≥ |1.5|).

An overview of individual proteins comprised in the Venn diagram overlap is given in Table 22. Effect sizes of T4-induced alterations observed in humans were smaller than in the murine samples. Even with wisely chosen male volunteers, of the same age and BMI, they still revealed larger interindividual differences than mice. The animals were of the same genotype and were living in a controlled environment. In essence for most of the proteins demonstrating alterations in both systems the direction was inversed. This was observed for proteins assigned to the complement system and proteins involved in coagulation which increased in amount upon T4 administration in humans but displayed a reduction in mice. As a group, only the apolipoproteins were influenced by T4 administration in both humans and mice in the same way, i.e. decrease in levels following treatment.

Table 22 Common differentially abundant proteins associated with free T4 across the human study of experimental thyrotoxicosis and the murine study of transient thyrotoxicosis and recovery. *Human plasma study: p*-value received from paired T-test, *t1* baseline level, *t2* T4 administration for 4 weeks; *Murine plasma study: p*(FDR) received from Welch's t-test. *Light grey* proteins showing inverse trend in abundance due to T4 administration.

Protein description	Human *p*-value / t2 *vs.* t1	Murine *p*(FDR) / T4-group *vs.* controls
Apolipoproteins		
Apolipoprotein B-100	1.09E-02 ↓	2.74E-08 ↓
Apolipoprotein C3	2.67E-02 ↓	3.87E-04 ↓
Apolipoprotein C4	4.20E-02 ↓	1.52E-03 ↓
Apolipoprotein D	3.68E-04 ↓	5.76E-05 ↓
Complement system		
Complement component C8 α chain	1.27E-03 ↑	4.36E-05 ↓
Complement component C8 β chain	3.32E-03 ↑	2.74E-05 ↓
Complement component C8 γ chain	1.89E-04 ↑	2.91E-04 ↓
Complement factor H	1.18E-02 ↑	6.02E-03 ↓
Mannan-binding lectin serine protease 2	7.40E-04 ↑	2.19E-03 ↓
Coagulation		
Coagulation factor XIII B chain	1.53E-04 ↑	1.09E-02 ↓
Coagulation factor IX	9.90E-05 ↑	3.91E-02 ↓
Kininogen-1	6.85E-03 ↑	3.67E-04 ↓
Plasma protease C1 inhibitor	1.55E-02 ↑	1.54E-05 ↓
Antithrombin-III	3.08E-03 ↑	5.01E-04 ↓
Fibulin-1	1.70E-02 ↑	3.78E-04 ↑
Inflammatory response		
Alpha-2-HS-glycoprotein	3.44E-03 ↑	4.57E-02 ↑
Fibronectin	2.86E-04 ↓	1.34E-02 ↑
Vascular cell adhesion protein 1	2.64E-02 ↑	1.28E-03 ↑
Extra cellular matrix proteins		
Extracellular matrix protein 1	3.35E-02 ↓	1.67E-02 ↑
Lumican	1.59E-03 ↑	5.49E-03 ↑
Divergent tasks within the organism		
Adiponectin	1.81E-03 ↓	3.71E-05 ↓
Protein AMBP	8.62E-04 ↑	1.18E-02 ↓
Buturylcholine esterase	4.69E-02 ↑	1.05E-04 ↓
Inter-alpha-trypsin inhibitor heavy chain H1	2.49E-02 ↑	6.27E-04 ↓
Pigment epithelium-derived factor	3.09E-03 ↑	4.27E-02 ↓
N-acetylmuramoyl-L-alanine amidase	1.94E-03 ↑	3.31E-04 ↑
Sulfhydryl oxidase 1	7.96E-03 ↑	2.10E-03 ↓
Zinc-alpha-2-glycoprotein	1.73E-02 ↑	2.50E-03 ↓
Cathelicidin antimicrobial peptide	5.47E-05 ↓	5.48E-07 ↓
Abnormal spindle-like microcephaly-associated protein	3.24E-03 ↑	1.76E-03 ↑

Comparing depletion efficiencies across different species

As mentioned before, plasma analysis can be challenging regarding the composition of the biofluid. Protein abundances in plasma cover more than 10 orders of magnitude. Additionally, already a few highly abundant proteins comprise more than 90 % of the total protein content in plasma or serum. Overcoming this drawback would allow a better detection of medium and low abundant proteins. Therefore, prior to mass spectrometric analysis, all samples were depleted using a human MARS6 column or mouse MARS3 column for immunoaffinity chromatography with the aim to diminish the level of highly abundant proteins and enhance insights into the plasma proteome.

To evaluate the effects of immunodepletion on the plasma proteome, samples were analyzed *via* LC-MS/MS (LTQ-Orbitrap Velos™ mass spectrometer) before and after this step. For this purpose, baseline samples of all 16 subjects of the human study investigating experimental induced thyrotoxicosis were used. On the other hand, 4 mouse samples were analyzed to assess the impact of depletion.

First, the human depletion strategy was evaluated. Figure 36 illustrates the proportion of the six highest abundant proteins which were diminished *via* immunoaffinity chromatography. In part A the composition found in the literature is depicted [75], whereas in part B the mean intensity values calculated from the actual data set is shown.

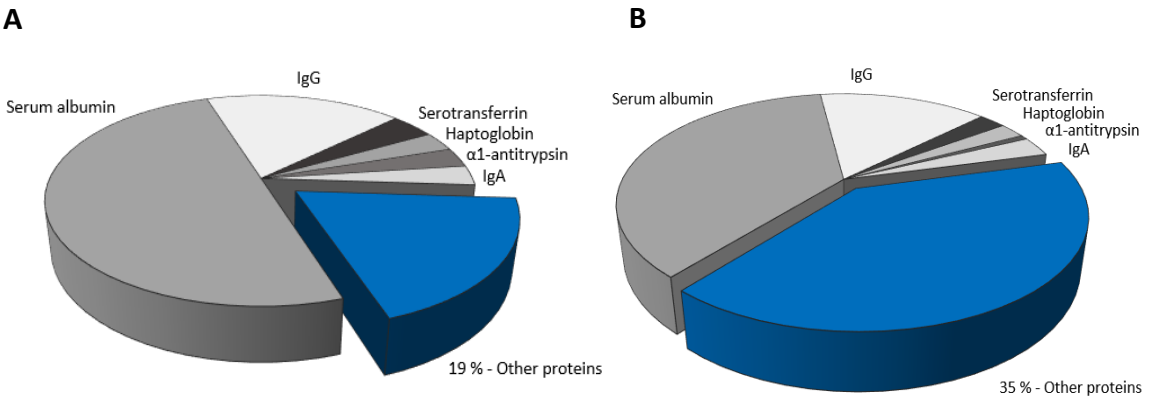

Figure 36 Proportion of the six highest abundant proteins depleted from human plasma *via* MARS6 immunoaffinity chromatography. **(A)** Reference values from literature. **(B)** Calculated mean intensity proportions of proteins from non-depleted plasma of all baseline samples of the study investigating experimentally induced thyrotoxicosis.

It is noteworthy that serum albumin was determined in a lower proportion in the data set than described in the literature. In fact, reference values based on calculated absolute amounts for serum albumin range from 50 - 60 % reflecting the vast range of acceptable, physiological normal levels of the protein. The proportion of serum albumin is calculated according the protein intensity in relation to the summed intensities of all proteins found in the analysis. Amounts of serum albumin ranged from 23 – 53 % with a mean value of 37 %. One reason is certainly the signal saturation reached in the mass spectrometer for serum albumin peptides. Thus, intensities for these peptides are underrepresented and therefore underestimated. On average, serum albumin is depleted by 84 % in the samples. Looking at all six proteins caught by the antibodies on the MARS6 column, the targeted proteins were reduced by 92 % on average.

According to the manufacturer's protocol, 85-90 % of the total protein amount will be depleted. The reference value from literature for the proportion of the six highest abundant proteins in crude plasma is at about 80 %. The data set analyzed in our study provided an amount of 64 % for the total sum of intensities of these six proteins. After depletion, the proportion decreased to 10 % of the total sum of intensities. The depletion efficiency was not equal for all targeted proteins. On average, serum albumin decreased to 7.9 % whereas the portion of all other depleted proteins in the depleted plasma samples was below 1 %. Moreover, the variation of the depletion efficiency in the individual samples was surprisingly high with a range from 2.5 % up to 19 % of total protein intensities taken by the 6 depleted target proteins. The described variance was predominantly caused by the proportion of serum albumin.

After mass spectrometric analysis, identified unique peptides in crude and depleted plasma across all samples were compared (Figure 37). In total, 1446 unique peptides were identified in undepleted plasma, whereas 1910 unique peptides could be found in depleted plasma. The 815 additional unique peptides in the depleted sample set clearly emphasized the necessity of this pre-analytical step. However, 351 peptides were only detected in crude plasma but not after depletion. Nearly 100 of them belong to one of the six depleted proteins and are therefore undesired peptides.

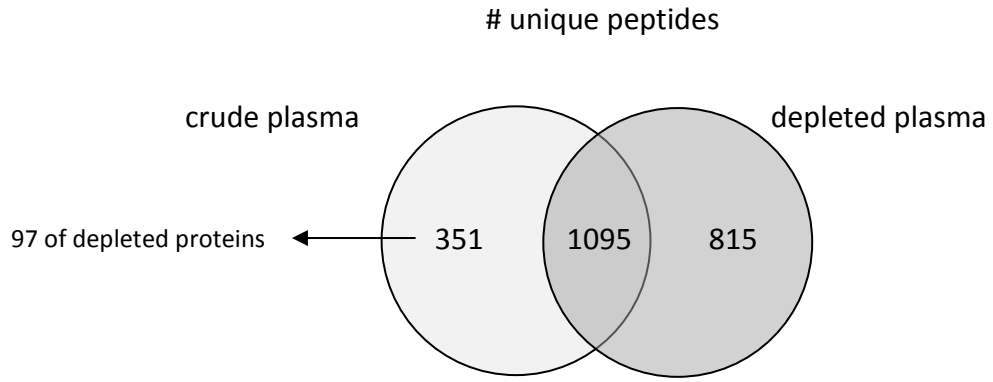

Figure 37 Number of unique peptides identified in depleted and crude human plasma. 1446 peptides were identified in crude plasma; 1910 peptides were identified in depleted plasma. 97 peptides of 351 peptides only identified in crude plasma belong to one of the six depleted proteins.

To reveal the impact of immunodepletion in murine plasma, samples of male adult C57BL/6 mice were analyzed before and after this step. In order to do so, only 4 specimens were sampled. The composition of murine plasma according to the literature [85] and data from the sample set are shown in Figure 38. The pieced-out part displays the remained proteins after depletion of the three high abundant ones.

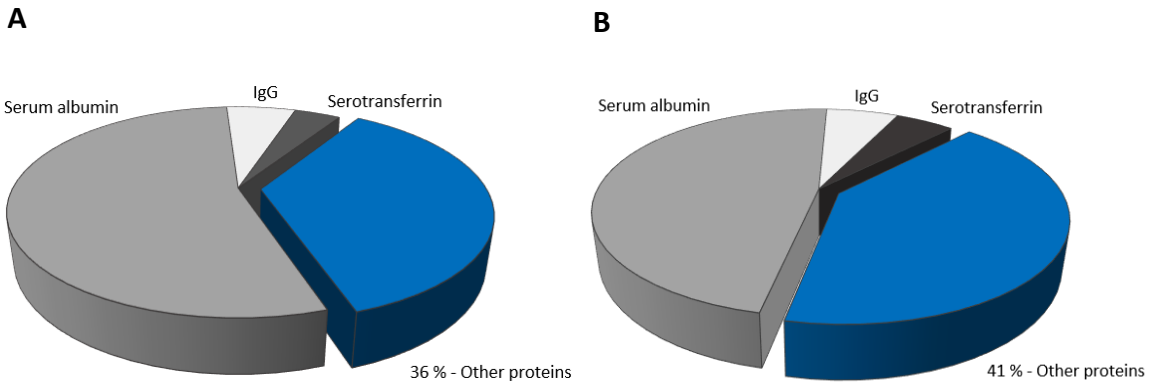

Figure 38 Proportion of the three highest abundant proteins depleted from mouse plasma *via* MARS3 immunoaffinity chromatography. **(A)** Reference values from literature; **(B)** Calculated mean values from 4 undepleted mice samples.

According to the literature, serum albumin, serotransferrin and IgG account for 64 % of the total amount. The manufacturer's protocol indicates a depletion of 80 % of the total plasma protein amount, while the calculated amount of these three abundant proteins

was determined as 59 %. Serum albumin is the highest abundant protein in mice plasma with 54 % according to reference values for C57BL/6 mice. With a mean value for serum albumin in the small data set of 47 %, amount seems to be comparable. Serum albumin was diminished by 95 % in the depleted samples. Taking the mean of all depleted proteins, the efficiency rose to 96 %. Remaining portion of depleted proteins was only 1.5 % of the total sum of protein intensities.

The comparison of identified unique peptides in crude and depleted plasma is displayed in Figure 39. In total, 1524 unique peptides were identified in undepleted plasma, whereas 2221 unique peptides could be found in depleted plasma. The 1005 identified peptides solely detected in the depleted sample sets support the choice of the pre-analytical immunoaffinity depletion.

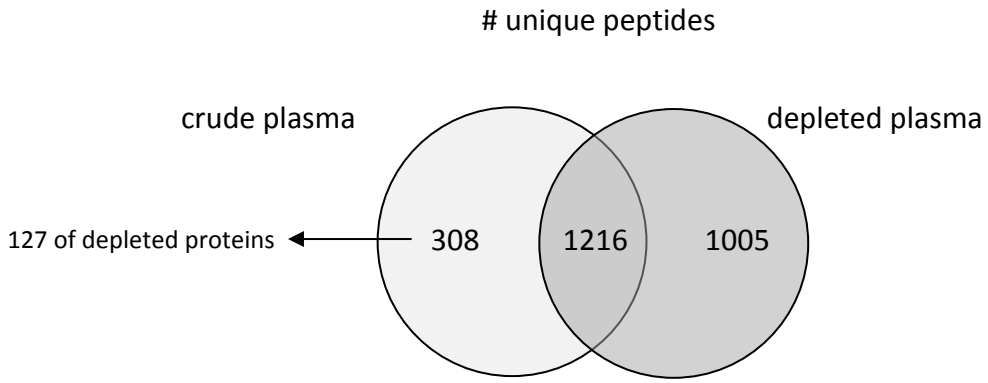

Figure 39 Number of unique peptides identified in crude and depleted murine plasmas. 1524 peptides were identified in crude plasma; 2221 peptides identified in depleted plasma. 127 peptides of 308 peptides only identified in crude plasma belong to one of the three depleted proteins.

Based on these findings depletion efficiency of the targeted proteins seems to be higher when using MARS3 columns for mice in comparison to MARS 6 columns for human plasma.

3.5 Analysis of human primary hepatocytes

The objective of the study was to examine the influence of T4 on the intracellular proteome and secretome of human primary hepatocytes.

The analysis of the plasma proteome of the human study investigating experimental thyrotoxicosis revealed tremendous alterations in protein abundances due to L-T_4 administration. Huge parts of the identified proteins and plasma proteins in general have a hepatic origin. This raised the question whether the alterations of plasma protein levels detected are a direct consequence of effects of T4, or more precisely it's metabolically more active derivative T3, on TH sensitive target genes in hepatocytes.

As a cell of the main parenchymal tissue of the liver, hepatocytes make up 70-85 % of the liver mass. Hepatocytes serve as a suitable *in vitro* model to reflect metabolism in the human liver [86]. They are valuable to identify compounds that are potentially toxic to humans. The disadvantage is the shortage of available human liver material which can be overcome with cryopreserved hepatocytes. However, primary hepatocytes do not proliferate and lose their metabolic activity after a short time span which has to be considered when planning the duration of experiments.

In this study, primary human hepatocytes of three individual donors were incubated in absence (controls) or presence of T4 (induced condition). To decide about the final experimental design regarding the concentration of T4, the application of 10 nM and 100 nM T4 was tested. As incubation times 24 h, 48 h, and 72 h were considered.

T4 and T3 levels within the cells could not be determined. However, gene expression of different known TH responsive genes was investigated using quantitative real-time PCR. Besides known T3 target genes like *Thrsp* encoding thyroid hormone-inducible hepatic protein and *Serpine7* encoding plasminogen activator inhibitor 1, housekeeping genes (*Hprt1*) which do not differ in expression over time and are not regulated by the supplied T4, were considered in the PCR.

The preliminary tests revealed 72 h induction with 10 nM T4 as supplement in the cell culture medium as the most promising approach. *Dio1*, converting the pro-hormone T4 in the more potent T3, showed a 2.4fold increase in mRNA abundance under those inducing conditions.

For the main experiment, total RNA and total proteins were prepared from all samples. For the corresponding analysis of secreted proteins, supernatant was also collected every 24 h paralleled by media change. In total, 8 samples could be used for analysis (Figure 40). Samples were labeled as follows: Do1-3 for the different donor cells, Co/T4 to distinguish between control and induction and further either 1 or 2 when two T4-supplied samples per control were available.

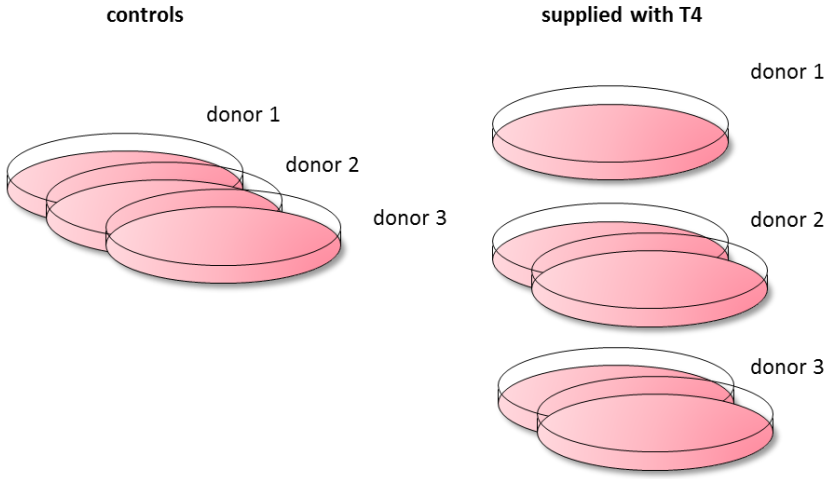

Figure 40 Number of samples generated for the analysis of human primary hepatocytes. To each control a minimum of one T4 treated sample was obtained (for donor 2 and donor 3 two T4 supplied samples (T4-1 and T4-2) were available). Besides preparation of total protein for the analysis of the intracellular proteome, supernatants were collected for secretome analysis.

Morphology of cells

In order to gain a first ompression of the impact of T4 treatmetn the primary human hepatocytes were analyzed by microscopy. The picture in the upper left corner of Figure 41 displays the cells directly 6 h after seeding. After attachment to the collagen layer they developed the typical cubic cell shape and often contained two nuclei (day 1 in culture). Within 24h they reached confluence of more than 50 % before T4 was applied.

The two images in the lower row show the same cells after 4 days in culture, but in different conditions. While the lower left image shows an untreated control, the lower right image represents cells after induction for 72 h with levothyroxine *via* T4-supplemented medium. No major phenotypical differences could be found between controls and treated cells.

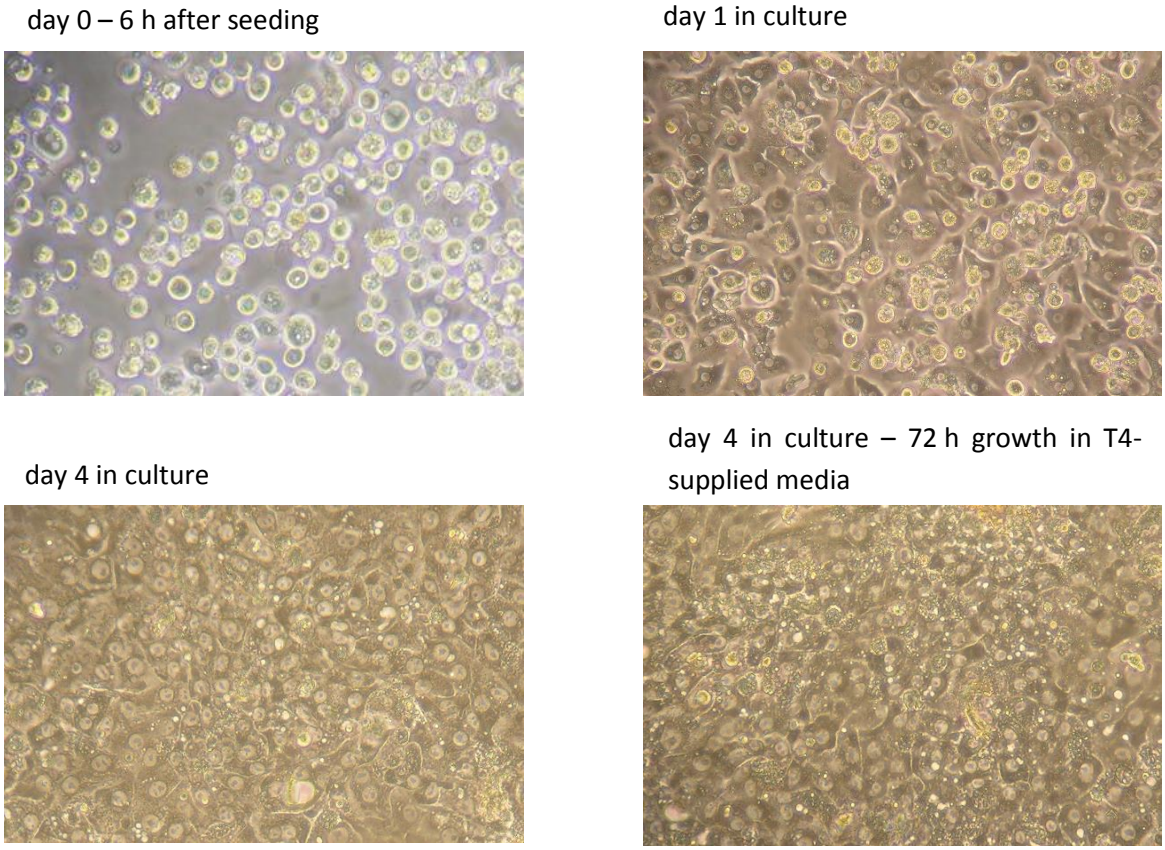

Figure 41 Light microscope images of human primary hepatocytes 6 h after seeding, at day 1 in culture and day 4 (72 h after induction). Cells were grown in T4-supplemented medium. Cultures without T4 served as controls.

Intracellular proteome analysis

After protein extraction using TRIzol® preparation and in-solution digestion, the intracellular proteome was measured with a Q Exactive™ Orbitrap mass spectrometer. MS raw data were subjected to database search and intensities extracted to generate median normalized protein values. In total, 12403 unique peptides could be identified yielding in total 2747 proteins (Figure 42, s.a. Supplementary table S9). Moreover, 2679 proteins had no missing values across all samples. When only looking at proteins identified with two or more peptides, 1881 proteins remained.

Since only three biological replicates were available, statistical testing was rather inappropriate leading to the idea to build ratios for the comparison of the T4 induced cells with the controls.

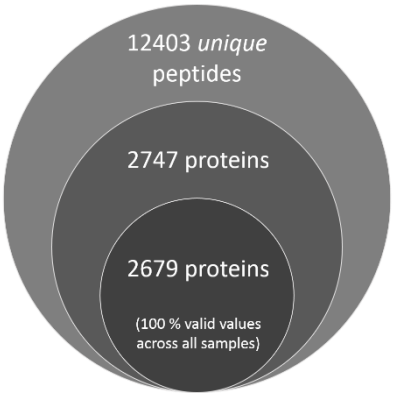

Figure 42 Identifications of the intracellular proteome of human primary hepatocytes across all samples.

PCA based on median normalized protein intensities with at least 50 % valid values across all samples sets provided an initial overview about the variability across the different donors and the control/T4 induction situation (Figure 43). The first two principle components covered almost 80 % of the variance in the data set. In general, a clear seperation between the bioreplicates became apparent. Furthermore, the marginal differences between the controls and the treated cells indicate only small effects of the treatment.

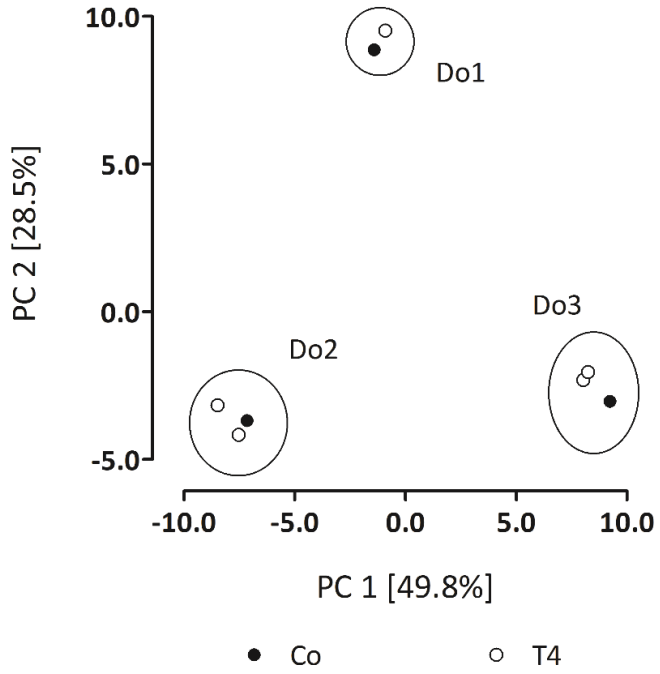

Figure 43 Principal component analysis of the intracellular samples of human primary hepatocytes. Analysis was done using median normalized protein intensities with at least 50 % valid values across all samples. *Do1-3:* indicating the different donors; *Co:* controls; *T4:* thyroxine induction; *PC* Principal component

Despite observing changes induced by T4 compared to the controls, no consistent influence on proteins became visible (s.a. Supplementary table S10). General alterations were expected to be found in proteins regarding carbohydrate and lipid metabolism, cell proliferation, cytoskeletal proteins, ribosomal proteins as well as apoptosis-associated proteins. These protein groups were identified to be under TH control by Feng *et al.* and Weitzel *et al.* in hepatic gene expression studies upon T3 treatment [87,88].

In none of these categories consistent changes between T4 induced condition and controls throughout the three bio-replicates could be reported. Furthermore, proteins which were known to be regulated by T3 were not identified (e.g. thyroid hormone-inducible hepatic protein (Spot14)) or did not show any alteration due to T4 exposure (e.g. phosphoenolpyruvate carboxykinase).

T3 induction is reported to mediate more explicit changes reflecting the higher affinity of T3 to nuclear TH receptors compared to T4 [89]. Lin and colleagues published data on the effect of T3 treatment on target gene regulation in a hepatocellular carcinoma cell line HepG2 with an overexpressed TH receptor α (TRα1) [90,91]. T3 modulated the expression of multiple genes encoding plasma protein in the cell line. Among them apolipoproteins of the C family, several inflammatory proteins (e.g. complement component 1, s subcomponent) and proteins involved in coagulation (F10, F2, prothrombin and fibrinogen) [90]. Comparison of the HepG2 and HepG2-TRα1 transcriptome demonstrated that the positive regulation of several plasma proteins depends on the level the TH receptors, namely TRα. This is likely an explanation for the missing alterations as primary hepatocytes lacked an overproduced α-receptor.

In contrast, a study of Yen *et al.* investigated TR-specific hepatic gene expression profiles using *Thra* and *Thrb* knock-out mice showing a similar expression pattern in both knock-out strains and the wild type mice. This would rather indicate a co-regulation of hepatic genes [48]. Protein signatures revealed in the human plasma proteome study included proteins involved in coagulation and inflammation originating from the liver. Proteins of the coagulation cascade and the complement system were barely identified in the analysis of the intracellular proteome of primary hepatocytes leaving the possibility to detect these in the secretome analysis.

Secretome analysis

Secreted proteins constitue an important subset of plasma proteins. Due to technical limitations of detecting low abundant proteins in the background of serum containing media the analysis of the secretome usually proves rather to be difficult in normal FCS-containing medium. Therefore, human primary hepatocytes were cultured in FCS-free medium, but in the presence of human serum albumin to maintain the viability of the cells. Proteins which were secreted by the hepatocytes were prepared from the supernatant. The enrichment of proteins in the supernatant using ethanol precipitation had the additional benefit of partly diminishing bovine serum albumin included in the cell culture media. Extraction of LFQ values from MaxQuant analysis yielded in a total number of 944 proteins across all samples. For relative quantification only proteins with 2 or less missing values were considered resulting in a total protein count of 735 across all samples out of which 138 are classically secreted proteins or proteins which are secreted under specific circumstances (s.a. Supplementary table S11). Detailed information for single replicates is listed in Table 23.

Table 23 Protein identifications and proportion of secreted proteins for each single sample of the sample set. Do1-3: three different donors, Co/T4: control and T4 induced condition, T4-1/T4-2: technical replicates of the same donor sample.

sample	**Do1**		**Do2**			**Do3**		
	Co	T4	Co	T4-1	T4-2	Co	T4-1	T4-2
# proteins identified	703	715	804	763	776	887	887	836
# secreted proteins	129	127	150	151	151	146	147	143
Proportion of secreted proteins [%]	18.35	17.76	18.66	19.79	19.46	16.46	16.57	17.11
Fraction of intensity accounted for secreted proteins [%]	54.51	53.94	68.85	70.10	70.03	50.32	49.82	55.20

PCA of the secretome data was done to gain an impression of the variation between the different donors as well as the control and T4 induction (Figure 44). The first two principal components covers 79.3 % of the variance of the data set depicting a similar picture for the secretome compared to the intracellular proteome. Close proximity of the dots belonging to one donor indicates small variation between the treated and untreated cells wheras a clear separation and therefore large variance is visible between the individual human donors.

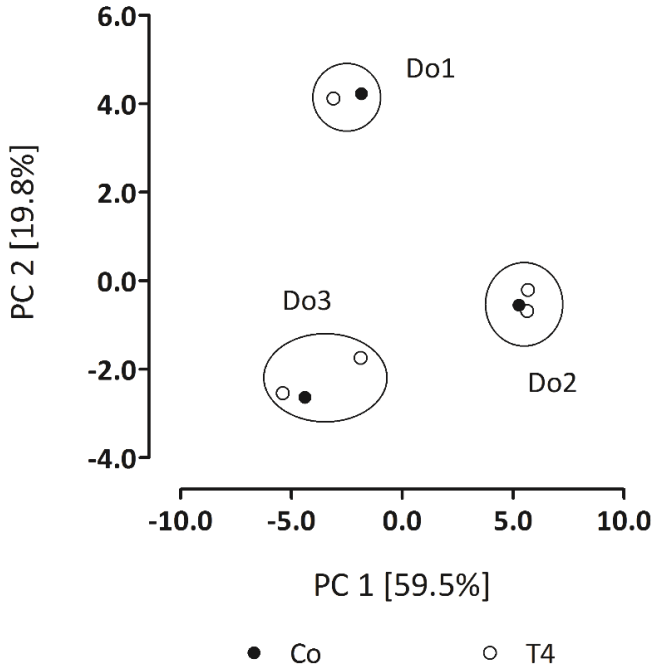

Figure 44 Principal component analysis of the extracellular samples of human primary hepatocytes. Analysis was done using the LFQ values of the MaxQuant analysis. *Do1-3:* indicating the different donors; *Co:* controls; *T4:* thyroxine induction; *PC* principal component

Although many proteins seemed to be affected by the T4 treatment only a few proteins revealed consistent alterations due to T4 exposure throughout the three biological replicates (s.a. Supplementary table S12). Fibronectin, collagen alpha-2(I) chain, and coagulation factor XIIIB showed increased abundance in the supernatant of T4 treated cells compared to the controls without T4. Follistatin revealed the strongest differences between the hyperthyroid statuses *vs.* controls with a fold change of -1.4 up to -2.4, displaying reduced levels of that protein in the secretome of T4 treated hepatocytes. A study of Tseng *et al.* documented a positive association of follistatin levels with free T4 levels in serum of patients with hyperthyroidism compared to euthyroid subjects [92]. Opposed to the results demonstrated from the supernatant the reasons may the different analyzed compartment and time points.

To ensure the comparability between the study of human primary hepatocytes and the human plasma studies culture media was supplemented with T4 and not T3. In all reported studies, the induction of a hyperthyroid status was done *via* T3 with the advantage of adding the active hormone instead of the pro-hormone T4, which might also be a reason for the different results of our experiments in comparison to published data.

4 DISCUSSION

The thyroid as the thyroid hormone (TH) producing gland plays a vital role for almost all tissues. Therefore, TH imbalances result in many different clinical symptoms. Most of these are caused by TH excess or insufficient TH amounts, namely hyperthyroidism and hypothyroidism. Current assessment of the TH status is based on the determination of TSH or the log ratio of TSH and free T4, which is defined as the gold standard for diagnostic tests. Under specific physiological conditions, the additional determination of free T3 is used for clinical diagnosis. However, the exclusive use of TH measurement has limitations in the clinical context. Owing the negative feedback regulation of the HPT axis, there is a tightly controlled individual setpoint for TSH and free TH in every individual [93,94]. Additionally, wide reference ranges for TSH and TH levels exist [95,96] making it difficult to detect subclinical thyroid dysfunctions. However, this is crucial since already milder forms of hormonal imbalances were found to be associated with an increased risk for cardiovascular events and pathological changes in bone structure.

Another problem concerns different assay specificities [97,98]. Apart from these challenges the identification of rare clinical conditions which cannot be detected *via* determination of TSH and TH would fail. All these reasons emphasize the need for novel diagnostic clinical biomarkers of thyroid dysfunction, encouraging appropriate systematic screens.

OMICS technologies are currently not frequently used for analysis of the general thyroid hormone action on the metabolism. Hitherto, most OMICS studies were restricted to animal models and analyzed T3 mediated changes in the gene expression pattern [87,88,99]. Other investigators used the well described hepatoma cell line HepG2 or even human muscle biopsies to study the effect of TH [100,101]. Based on these studies an

increasing number of TH targets genes could be discovered by transcriptome analyses. However, especially in liver transcript levels do not consequently correlate with the amounts of synthesized proteins which emphasizes the utility of proteome analyses. One example is the shotgun proteomic study of Silvestri *et al.* identifying T3 mediated alterations in the liver proteome of hypothyroid rats [70].

The analysis of the animals' biofluids like serum and urine using metabolomics approaches highlighted the extensive impact of TH in other body compartments [102–104]. In humans, most analyses of serum or plasma were performed more targeted. As one example, healthy volunteers received levothyroxine to investigate the effects of TH excess on coagulation and fibrinolysis [32]. The comprehensive impact of thyroid hormones on the plasma proteome has not been addressed yet.

To gain insights into this compartment, a human study of experimental thyrotoxicosis was conducted. Young healthy male volunteers were treated with 0.25 mg/d levothyroxine for 8 weeks to induce thyrotoxicosis. Sampling was done before the application started, during the treatment after 4 and 8 weeks and additionally 4 and 8 weeks after withdrawal of levothyroxine. The model of experimentally induced thyrotoxicosis presents a variety of advantages. Compared to the study of endogenous hyperthyroidism the extent and duration of thyroxine exposure is defined. Furthermore, the potential impact of comorbidities and any other potentially interfering influences on the plasma proteome was excluded using healthy and young subjects. In thyroid autoimmune diseases, it is difficult to distinguish between TH dependent effects and those related to the underlying autoimmune process. Therefore, in Graves' disease, the analysis of hyperthyroidism is frequently complicated by disease specific effects of autoantibodies.

As described previously, the application of levothyroxine clearly induced biochemical thyrotoxicosis with increased free TH levels and strongly suppressed TSH [105]. With the disturbance of the hormonal balance a large number of molecular alterations could be characterized [81]. Among them, increased levels of the known markers for TH action, sex hormone-binding globulin (SHBG) and cystatin C were detected.

SHBG is a circulating protein binding the two sex hormones androgen and estrogen [106], long known to show increased plasma levels in hyperthyroidism [107]. SHBG levels in the circulation were described to be increased in hyperthyroidism in several studies [108–110]. SHBG serum levels were also found to be elevated in children with Graves' disease

[111]. On the other hand, no alteration in protein levels can be observed in patients with familial thyroid hormone resistance, despite their increased blood TH levels [112]. TH indirectly increase the SHBG production via hepatocyte nuclear factor 4α (HNF4α), which is a direct hepatic target gene of T3 [89]. The T3-induced increase in cellular HNF4α levels thereby finally drives *SHBG* transcription [113] resulting in increased SHBG plasma levels, even though the SBHG promotor lacks a typical thyroid hormone response element.

Coincident with SHBG increased levels of cystatin C were found in hyperthyroidism [114,115]. Indeed, both proteins were confirmed to be up-regulated in our plasma proteome analysis. However, as already mentioned, the usability of both proteins as biomarkers of peripheral thyroid function is limited: Besides their response to TH imbalances they are also influenced by non-thyroidal effects. It cannot be ruled out, that detected SHBG level alterations are caused by type 2 diabetes, non-alcohol fatty liver disease or polycystic ovary syndrome instead of enhanced thyroid function [116,117]. On the other hand, increased cystatin C levels were linked to renal dysfunctions [118,119].

Besides SHBG and cystatin C, our plasma analysis revealed further remarkable alterations of the plasma proteome. Pearson correlation analysis detected 76 proteins whose levels significantly changed under thyrotoxicosis. Not surprisingly, the correlation analysis confirmed the strong impact of TH on proteins assigned to the coagulation cascade. Pathway analyses based on the IPA software assigned 35 proteins to the coagulation cascade, out of which 24 proteins were detected *via* LC-MS/MS analysis. Ten proteins showed a significant increase owing the direct impact of TH on coagulation-associated proteins. Among these were pro-coagulation factors XIII subunit B (F13B), II (F2), XI (F11) and IX (F9). Exemplarily, conventional ELISAs were performed for F9 and F13 yielding the same pattern as the proteomics derived data and thus also confirming the results.

Many studies investigated the effect of TH imbalances on specific proteins involved in coagulation and fibrinolysis, but none of them did so using an untargeted approach [32,120-122]. Furthermore, measurement of variables refers often to activities and not protein abundance. The study of van Zaane *et al.* assessed the influence of thyrotoxicosis on coagulation and fibrinolysis by treatment of healthy volunteers for 14 days with a daily dose of 0.45 mg or 0.6 mg levothyroxine depending on the body weight. With 0.25 mg/d and a treatment period of 8 weeks, the study presented here differs in duration and dose of medication. Van Zaane *et al.* found increased levels of pro-coagulative factors including

F9 [32] which was confirmed by higher protein levels in our study, too. However, some observations could be confirmed by our analysis. Von Willebrand factor which was described several times to be increased in either protein levels or activity in a hyperthyroid state compared to the normal situation did not change in level in the proteome study presented here. Observed differences might be due to exposure time or levothyroxine dosing and possibly reflect different stages of thyrotoxicosis and assay specificities.

Besides increased protein levels of clotting factors, lower levels of plasminogen were inversely correlated to higher free T4. Plasminogen is a proenzyme converted to its active form plasmin which in turn promotes fibrinolysis. Consequently, increased free T4 levels may induce a hypercoagulative state by interfering with the synthesis of clotting factors in the liver.

Recently, it was demonstrated that patients with pathologic high free T4 levels have an up to 2fold risk for venous thrombosis and pulmonary embolism [120]. Therefore, lower levels of plasminogen may also indicate a hypofibrinolytic state. Stuijver *et al.* also demonstrated elevated plasminogen activator inhibitor I (PAI-I) levels in patients with endogenous hyperthyroidism. This supports the thesis of reduced fibrinolysis. Increased PAI-I blocks fibrinolysis, but decreased plasminogen levels may have the same effect, thereby contributing to the hypofibrinolytic state. PAI-I was not detected in our proteome analysis which unfortunately does not permit any further conclusions.

Another interesting finding is the positive correlation of protein C inhibitor with free T4. As a potent inhibitor of activated protein C which prevents clot formation it does not display a typical protein addressed in studies with a focus on coagulation and fibrinolysis. By an increase of the inhibitor clot lysis by activated protein C is lowered and contributes to a pro-hemostatic role of elevated free T4 levels. More compact clots in hyperthyroid patients support this hypothesis [33].

In contrast, levels of antitrypsin, antithrombin-III, and α2-antiplasmin correlated positively with free T4 and may mirror anticoagulatory compensatory mechanisms. So far, increased levels of these proteins in hyperthyroid states have not been demonstrated.

Up-regulation of various plasma proteins including clotting factors and other assigned proteins was documented in different studies using the differentiated hepatocellular carcinoma cell line HepG2 with an overproduced TRα1 [90,91]. Lin *et al.* observed increased RNA levels of fibrinogen-α, prothrombin, F2 and F10 using cDNA array analysis

[90]. Moreover, they demonstrated induced expression of genes encoding apolipoproteins of the C family whose levels were all found to be decreased in murine plasma. Shih and co-workers also demonstrated the ability of T3 to modulate the expression of genes coding for proteins involved in coagulation in HepG2 cells with overexpressed TRα [91]. They reported up-regulation of fibrinogen-α, prothrombin, α1-acid glycoprotein and F10 after T3 treatment.

Fibrinogen was the primary analyzed target of many previous studies all demonstrating an increase of its hepatic gene expression after addition of T3 [123–125]. Compared to the plasma protein changes in fibrinogen-γ and -β which were observed in the transient thyrotoxicosis, the former investigations mainly addressed changes in the α-chain. As the different chains are linked to each other by disulfide bonds and contribute equally to the formation of the final hexamers, there is no obvious explanation for the different results in the discussed studies.

A molecular mechanism for the increase of proteins involved in coagulation is currently not clear, but a plausible hypothesis is gain of protein stability due to TH stimulation or enhanced expression of the respective genes. The latter hypothesis is supported by a recent study of patients with resistance in TRβ presenting with elevated free T4 levels but unaltered coagulation conditions and protein levels. Hence, the pro-coagulative effects observed in thyrotoxicosis and hyperthyroidism might be mediated through TRβ [126].

A regulatory effect of HNF4α on blood coagulation was described for mice [127]. The use of liver-specific HNF4α-null mice provided evidence for the dependence of the gene expression of F5, F11, F12 and F13B on hepatic HNF4α. In turn, the levels and activity of HNF4α are regulated by several hormonal and signaling pathways among them thyroid hormones [128]. It could be demonstrated in hepatocytes, that TH increase the HNF4α mRNA and protein level [89]. In summary, increase of pro-coagulant clotting factors and enhanced inhibition of the protein C pathway might support a hypercoagulable state during thyrotoxicosis.

After seeing such a substantial influence of TH on the plasma proteome pattern *via* the rather simple *Pearson* correlation analysis, a more sophisticated statistical approach was used. Implementation of the mixed effect linear regression model to detect free T4 associated changes in the plasma proteome led to identification of 63 differentially abundant proteins. Besides the already discussed protein signature of augmented

coagulation, another striking signature comprised decreased apolipoprotein levels, namely ApoB-100, ApoD, and ApoC3.

The influence of TH on the levels of apolipoproteins and other associated proteins has been shown before [23,129,130]. Already 1992, Muls *et al.* investigated the role of TH on lipid and apolipoprotein metabolism in 33 hyperthyroid patients before and after treatment. The data obtained with the data were compared with healthy volunteers. This study revealed lower levels of ApoB-100 in the untreated and treated hyperthyroid group as compared to the control group. While ApoA2 levels were identical through all patients, ApoA1 levels were lower before the treatment. The post-treated time point was not different from the levels in healthy subjects. In the untreated hyperthyroidism, the alterations in apolipoprotein levels were accompanied by a decrease of HDL-cholesterol, LDL-cholesterol and total cholesterol measured by clinical assays compared to both treated and control situation [23]. DeBruin *et al.* confirmed the findings regarding apolipoprotein B-100 when treating hypothyroid patients with levothyroxine and observing a decrease in total plasma ApoB-100 [130]. Another study including 18 hypothyroid patients and 5 hyperthyroid patients showed that HDL-cholesterol, total cholesterol, ApoA1 and additionally ApoE decreased with the treatment of hypothyroidism while ApoA2 levels remained unaltered. *Vice versa*, it could be observed that lipid parameters and ApoA1 increased with the treatment of hyperthyroidism along with no change in ApoA2 and ApoE levels [129].

The strongest association with free T4 levels was found for ApoD which represents a rather atypical apolipoprotein [131]. It is structurally similar to proteins of the lipocalin family transporting lipids and small hydrophobic ligands. Circulating ApoD is mainly bound to HDL particles which mediate the reverse cholesterol transport (RCT) from peripheral tissues to the liver. As mentioned in the introduction, stimulation of the RCT through TH is mediated *via* the increased expression of genes encoding proteins involved in cholesterol transport and metabolism. One of these genes is *SCARB1* encoding for the multi-ligand binding scavenger receptor class B member 1 SRB1 which binds cholesterol-enriched HDL particles, particularly in liver [20]. Therefore, the drop of apolipoprotein D levels in plasma might be explained by the TH stimulated increase of hepatic HDL cholesterol uptake.

On the other hand, the decrease of ApoB-100 levels represents a direct consequence of TH stimulated LDL uptake from the circulating blood: ApoB-100 is mostly associated with VLDL and LDL particles essentially mediating systemic transport of lipids from liver to peripheral tissues. ApoB-100 is also the primary ligand of the LDL receptor [132]. The uptake of LDL particles *via* ApoB dependent LDL receptor binding and endocytosis is TH mediated. Expression of *LDLR* is also positively regulated by SREBP-2 which is in turn also induced by TH at the gene expression level [133–135].

The third down-regulated apolipoprotein ApoC3 is localized on the surface of mature triglyceride rich chylomicrons and VLDL particles. It is also associated with HDL particles and thereby contributes to the reverse cholesterol transport, too [132]. The uptake of VLDL particles is mediated *via* the VLDL receptor. In rodents, Jokinen *et al.* demonstrated that the gene encoding the receptor is under positive TH control [136]. Therefore, lower ApoC3 levels in thyrotoxicosis are part of the TH-mediated gene expression stimulation of VLDL receptor and SRB1.

Besides apolipoproteins a significant drop in HDL-cholesterol, LDL-cholesterol and total cholesterol plasma levels could be determined in the study group by clinical standard laboratory measurements, thereby supporting the findings of the proteome analysis.

Besides plasma proteome profiling untargeted metabolome analysis was performed [81]. In line with the known TH-mediated stimulation of lipid metabolism, lipid-related compounds cover the largest portion of metabolites. The increased levels of free fatty acids and glycerol in hyperthyroidism are explained by TH-induced induction of lipolysis in white adipose tissue [137].

Another protein group altered during thyrotoxicosis includes proteins of the complement system. The complement system consists in over 30 soluble and surface-localized proteins protecting the organism against pathogens as part of the innate immune system [138]. Initiation of the complement activation can occur *via* three different pathways. The *classical way* is activated by the binding of C1q with either IgG or IgM FC regions. Then, C1s component of the C1qrs complex cleaves C4 and C2 into their active forms C4b and C2b subsequently leading to the formation of the C3 convertase. The *lectin pathway* is initiated by MBL binding to suitable bacterial carbohydrate motifs which causes activation of MBL-associated serine proteases, also resulting in the cleavage of C4 and C2 as described above. The third, so-called *alternative pathway* of complement activation is

always in an idle state and continuously activated at a low level. C3 can associate with a water molecule forming C3(H_2O) which in turn recruits Factor D called properdin, cleaving Factor B into an active serine protease able to cleave C3. The resulting C3bBb convertase repeatedly cleaves C3 molecules. Consequently, the amplification of the C3 convertase step is regardless of the initial activation. Further steps include cleavage of C5 which then is able bind C6. The alliance of both components facilitates the subsequent binding of C7, C8, and several molecules of C9, all together forming the membrane attack complex (Figure 45).

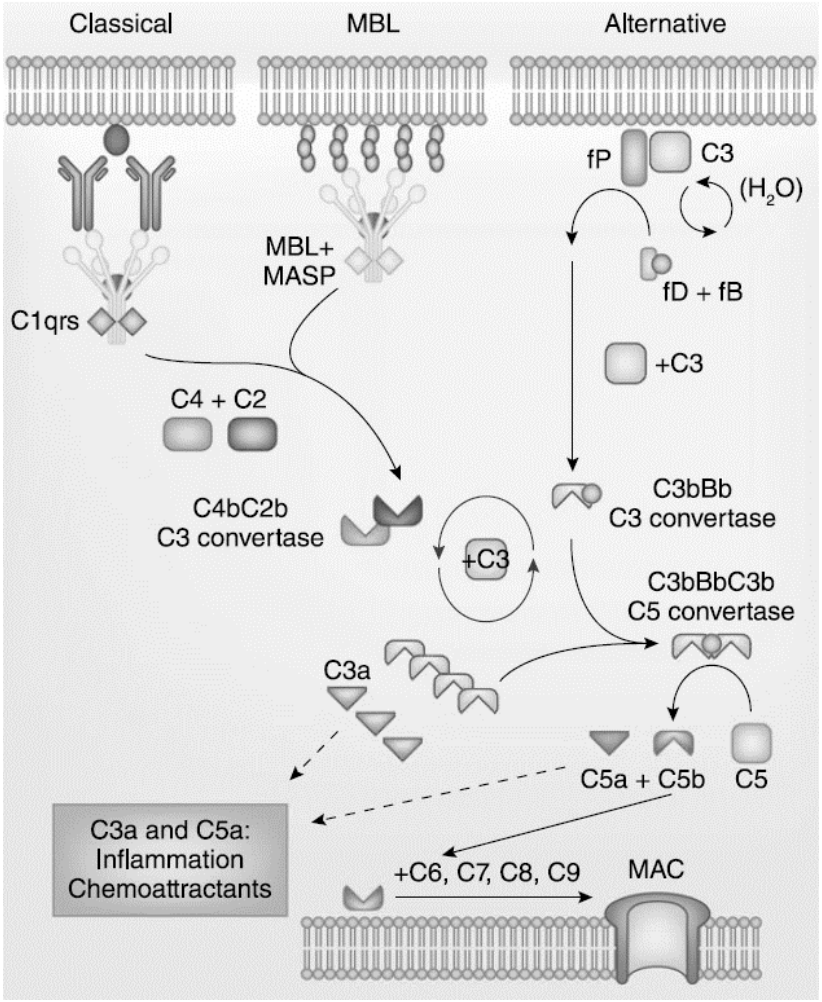

Figure 45 Schematic overview of the complement activation. The figure is copied from Mathern and Heeger [139].

The 11 proteins assigned to the complement system that were significantly positively associated with free T4 levels in the present study represent components of different complement activation pathways. Besides those of different complement components

and the complement factors H and B, the plasma levels of MBL, MASP-2, and plasma protease C1 inhibitor were found to be positively associated with T4. This was also the case for complement factor H related proteins 1 and 5, both able to bind complement component C3b [140]. C3 itself barely missed the statistical threshold of significance in the proteome analysis. However, when measuring the levels of C3 as well as C4 with standard laboratory tests, moderate, but significant increases of both proteins were detected during thyrotoxicosis. In line with the findings of the proteome analysis, one positively associated C3 fragment (HWESASLLR) [141] was detected among the metabolites.

Hooper *et al.* reported ambivalent results regarding C3 [33]. Comparing patients with endogenous hyperthyroidism exhibiting symptoms of thyrotoxicosis for at least 2 months with age- and gender matched controls revealed increased C3 levels. In a short-term model of induced thyrotoxicosis in healthy volunteers, no elevated C3 levels were detected, emphasizing a crucial influence for the duration of hyperthyroidism [33].

Other studies found a 43 % decrease of C3 levels in hyperthyroid patients compared to controls and no C3 changes in hypothyroidism [142]. However, as these results were obtained from Chinese patients, the different ethnicity of the study groups could explain the different findings. Other possible explanations are different platforms for C3 measurement. Jafarzadeh *et al.* demonstrated elevated serum C3 levels in hypothyroid women, but no increase in protein levels in hyperthyroid subjects [143].

The positive correlation found between TH and complement protein levels in both thyroid autoimmune conditions and in non-thyroidal autoimmune diseases suggests an impact of autoantibodies. Zhang *et al.* estimated the thyroid hormone levels in patients with multiple sclerosis and neuromyelitis [144]. Additionally, they determined the levels of C3, C4 and CH_{50} - the latter representing a screening assay which determines the activation of the classical complement pathway. It could be shown that TH levels correlate with C4 levels and with the total complement activity in these patients. In line with these findings the proteome analysis presented here revealed increased levels of C8a, C8b, C8g and C9 as part of the active membrane attack complex. Already earlier, the group of Oleesky *et al.* described increased C9 plasma concentrations in patients with toxic Graves' disease [145]. Though, serum free T4 concentrations did not correlate with measured C9 plasma concentration assuming an impact of autoantibodies in the progress of the membrane

attack complex formation. As part of this study, healthy subjects were treated with 4 daily doses of 20 µg T3 for one week which did not result in a changed C9 concentration in serum. Nevertheless, the possibility of chronic thyroid dysfunction due to Graves' disease which caused the alterations in C9 levels could not be excluded. The investigated mid-term model of thyrotoxicosis is not compliant with a chronic condition, but the effects of TH seem to be time course dependent. Weetman *et al.* also could determine significantly increased terminal complement complex concentrations in patients with untreated Graves' disease [146]. As mentioned before, changes in proteins assigned to the complement system did not seem to be related to hormonal alterations but rather to the appearance of autoantibodies since an increase in the terminal complement complex could also be observed in Hashimoto's thyroiditis.

MBL2 encodes for the mannose binding lectin (MBL) initiating the first step in the lectin pathway. In 2005, it was demonstrated that TH have a stimulating effect on the plasma levels of this protein [147]. Sørensen *et al.* used the hepatoma cell line HuH-7 to study the effects of T3 and T4. Treatment for 3 days resulted in significantly increased levels of MBL in the culture supernatant whereby T3 provided a more potent response than T4. In line with the protein amounts, *MBL2* mRNA levels increased within 48 h of T3 application. These findings underline a frequently described direct effect of TH on the liver [148]. A more recent study reported a tight correlation between the serum levels of MBL and TH, indicating increased and decreased amounts of MBL in hyperthyroidism and hypothyroidism, respectively [149]. *MBL2* represents a direct PPARα target [150,151]. PPARα itself belongs to a group of transcriptional co-regulators which interact with TH receptors after binding of TH to the latter, which might explain the increased circulating MBL2 levels in hyperthyroidism. The same mechanism might apply for other complement system proteins.

Independent of these extensive molecular changes due to increased free T4 levels, none of the volunteers noticed any subjective symptoms regarding thyrotoxicosis [105]. This demonstrates that biochemical alterations are detectable earlier compared to clinical symptoms. If so, the patients with thyroid dysfunctions might not be correctly diagnosed in clinical routine if the disease is not yet fully clinically manifested but only detectable on a molecular basis. This emphasizes the importance of proteome analyses for the

identification of new biomarkers for investigating thyroid status beyond the use of classical TH and TSH.

Derived from the model of experimentally induced thyrotoxicosis, an opposite study design was used for studying mid-term hypothyroidism. All patients included were all treated with L-T_4 to reach an euthyroid state at baseline level. Since a complete withdrawal of levothyroxine was not possible due to medical and ethical aspects, prescription was considerably reduced to achieve a hypothyroid state. After the medication has been discontinued or rather reduced to achieve 70 % of the original doses, TSH levels increased as expected and free TH levels decreased. Therefore, molecular changes anticipated in this study were expected to be more limited and less pronounced than those seen in the thyrotoxicosis model. Another likely reason for the restricted number of effects is the large heterogeneity of the study group based on different age and BMI as well as diseases underlying the respective thyroid dysfunctions.

The results of the measurements of HDL, LDL, as well as total cholesterol were inconclusive (data not shown). In fact, both overt and subclinical hypothyroidism are both well-known causes for hyperlipidemia, most frequently presented as hypercholesterolemia due to increased LDL levels [152–154]. This is often accompanied by elevated levels of VLDL and HDL cholesterol [155]. The expected increase in lipoprotein particle levels could not be confirmed in the present study, underpinning the problems associated with an inhomogeneous study cohort.

In parallel, a comprehensive metabolome analysis was performed in order to identify metabolites influenced by the withdrawal of TH. Only minor alterations were detected, causing us to refrain from the idea of a whole proteome approach due to the missing information from the metabolome analysis.

To get a first impression, known biochemical markers were determined. In the literature inconsistent information was found for cystatin C: In a study cohort of 8126 male participants, both hyperthyroidism and hypothyroidism were reported to be associated with elevated levels of the protein [156]. Small increases during hypothyroidism could also be detected by Goede *et al.* [157]. In contrast, decreased levels were determined after the withdrawal of T4 leading to severe hypothyroid states in 48 patients [158]. Other

studies of hypothyroidism also reported a slight drop in cystatin C [159,160] or the measured levels did not exceed the reference interval even though a trend to lower levels of the protein in hypothyroidism was mentioned [161]. Similar results were obtained in the study of Kotajuma *et al.* [115] where hypothyroidism was rather related to decreased levels of cystatin C but did not reach statistical significance, which correspond to the findings of the current study. The levels of measured cystatin C showed no significant changes when comparing the hypothyroid states (t2 and t3) with the baseline level which is referred to as the euthyroid state under levothyroxine administration, but there was a tendency towards decreased levels.

SHBG which generally shows a strong association with free T4 did not change under hypothyroid conditions in the present study. Hypothyroidism was frequently associated with significantly decreased SHBG levels [108,162]. On the other hand, in female patients with severe hypothyroidism after thyroidectomy, the low TH level was accompanied with increased SHBG levels [163]. It could be demonstrated that under hypothyroid conditions, application of levothyroxine, besides adjusting an euthyroid state, also tuned the SHBG levels to the normal range [164]. However, SHBG shows minor age- and gender-dependent concentrations [165,166] making it difficult to globally judge SHBG levels in thyroid dysfunctions.

Another explanation for the unchanged SHBG level in hypothyroid patients is the basal hepatic secretion of this protein independent of TH [166]. Furthermore, a prolonged half-live of SHBG in hypothyroidism was postulated. Brenta *et al.* characterized SHBG isoforms according to their sialic acid content. In hypothyroidism they found a higher proportion of more acidic SHBG isoforms which might explain the unaltered total levels of SHBG [167].

Fifteen patients were included in the present human hypothyroidism study. Participants were mostly women with different age, BMI and medical history resulting in the large variability of the study group. Since the hypothyroid status is induced by reduced input of levothyroxine but not by complete withdrawal the alterations on molecular levels were rather moderate. Hence, a valid conclusion regarding cystatin C and SHBG protein levels was not easily possible.

One distinct protein signature detected in the model of induced thyrotoxicosis was the indication of augmented coagulation. It was described before that endocrine disorders can influence the hemostatic equilibrium [168]. TH represent one of the many factors

influencing hemostasis. Increased T3 and T4 levels cause coagulative abnormalities ranging from mild deviations in laboratory tests, thrombotic effects, and bleeding up to acquired von Willebrand syndrome [169]. Hyperthyroidism and mild hypothyroidism are reported to be associated with a hypercoagulative state, so patients are more prone to thrombosis. Severity of hypothyroidism plays a significant role regarding the fibrinolytic pattern, too [43]. In contrast, patients suffering from overt hypothyroidism are more vulnerable to bleeding and hypocoagulability. Small case-control studies have shown abnormalities in coagulation and fibrinolysis [170–172]. Increased plasma fibrinolytic activity resulted in decreased levels of e.g. PAI-I [173]. Biondi *et al.* even reported decreased levels of F7 and PAI-I in subclinical hypothyroidism [174], thus contradicting Chadarevian *et al.* [175]. PAI-I was not detected in the proteome analysis of induced thyrotoxicosis and hence we refrained from measuring PAI-I in this study.

Regarding clotting factors in hypothyroidism, studies of Egeberg and Simone *et al.* from 1963 and 1965 respectively described significant decreases in F8, F9, and F11 activities [40,41]. In the following years many other studies confirmed at least parts of these findings [30,176]. The significant abnormalities in clotting activities were often referred to coagulation factor VIII (F8). Alongside with that Marongiu *et al.* reported rare cases with F9 alterations [172]. F9 showed clear level alterations in our study of induced thyrotoxicosis with a mean increase of 18 % in the ELISA measurements. Therefore, analysis of this coagulation factor was also performed with the samples of the hypothyroid patients. The obtained ELISA data revealed an average decrease in F9 levels of 6 % indicating reduced coagulation. However, in summary reports about the influence of hypothyroidism on hemostasis are controversial [175,177]. On the one hand, low levels of free T4 are discussed to be associated with a hypercoagulable state. On the other hand, reported positive correlations between free T3 levels and F9 activities as well as increased levels of antithrombin-III and PAI-I suggest an increased risk of developing thrombosis during hypothyroidism [170]. In summary, the existing data demonstrate a wide range of phenotypes regarding the coagulation status in hypothyroid patients. There is no complete accordance, indicating the need of further analyses using a larger sample set.

Besides the analysis of the human plasma proteome to characterize TH associated physiological changes murine plasma proteome studies were also intended. The use of mouse models and other rodents to analyze complex pathological processes in various biomedical questions is common. Invasive procedures which are frequently restricted to animals allow for investigating organs and organ-specific mechanisms, too.

Since there is strong evidence that TH play an essential role in virtual all tissues and organs, OMICS approaches are of interest in this context. Metabolomics, transcriptomics, and proteomics hold the promise to enable a deeper insight into the physiological networks in which TH are involved. The need to gain more understanding in the complex physiological regulation of the TH system led to increased use of such techniques in the last decade. Nevertheless, only few studies aimed to analyze comprehensive molecular alterations upon induced TH imbalances on a molecular level. As metabolically strongly active tissues known to be subject of TH regulation liver and skeletal muscle are frequently the subject of corresponding OMICS approaches [70,71,87,88,178]. Comparable data cannot be obtained easily in humans due to the necessary medical procedures to receive sample material. Ethical reasons do not permit interventional studies so that animal models remain as a possibility to study TH effects in tissues/ organs.

Transcriptome analyses in rodents treated with T3 revealed a large number of well-known as well as novel T3 target genes [87,88]. Weitzel *et al.* documented 23 hepatic genes out of a panel of 588 distinct hepatic genes as affected by T3 [87]. Among them genes involved in lipid/steroid metabolism and -transport like apolipoproteins were found to be affected by T3. Nevertheless, the majority of genes were not primarily involved in metabolic function. Ribosomal genes were detected to be differentially expressed suggesting a role of TH in the regulation of the translation apparatus. One of the already known TH-regulated genes was that encoding gluthatione S transferase [179] included in xenobiotic detoxification and defense against oxidative stress. Over all, two thirds of the genes significantly differentially expressed after T3 treatment showed increased mRNA levels in rats. In contrast, a murine cDNA microarray study reported 41 and only 14 hepatic genes to exhibit decreased and increased transcript levels, respectively, after TH application [88]. One large portion of significantly differentially expressed genes was assigned to carbohydrate and fatty acid metabolism. These genes include the gene coding for fatty acid binding protein which was already found to be TH-regulated in the study mentioned

earlier. Further genes are assigned to cell proliferation, signal transduction, cellular immunity and cytoskeletal functions.

Species-specific differences as well as a different duration and amount of TH application leading to diverse serum T3 concentrations might be responsible for the partially inconsistent results of the two transcriptome analyses. Silvestri *et al.* performed a proteome analysis to investigate direct T3 effects on the liver as one of the primary target organs [70,71]. Analysis of 600 distinct spots in a 2D-PAGE analysis followed by MALDI-TOF measurement revealed 53 proteins whose abundance changed after TH treatment. Proteins with functions in lipid and energy metabolism, e.g. ATP synthase, α chain), or detoxification, e. g. gluthatione S transferase, were affected. A large portion of these proteins showed decreased levels in hyperthyroid *vs.* hypothyroid state. According to that, the levels of proteins modulating urea and ammonia production in the liver (arginase 1, peroxisomal catalase and ornithine carbamoyltransferase) were found to be negatively TH correlated.

These data supported the transcriptome analysis of Feng *et al.* revealing a prevalent negative effect of TH on gene expression [88]. In contrast, T3 application rather promoted an increase of specific proteins in skeletal muscle tissue [71] (whole cell content of gastrocnemius muscle) including elevated levels of proteins involved in substrate metabolism (pyruvate kinase and malate dehydrogenase) and energy metabolism (creatine kinase M type and ATP synthase β chain). Another prominent group constituted heat shock proteins while the remaining proteins have structural functions or are involved in translation. These differential findings highlights a rather tissue-specific proteomic response on TH imbalances [71].

Proteome analyses based on mass spectrometric measurements provide the opportunity to identify and quantify hundreds of proteins simultaneously. Proteins represent the global players in the cell as they exert all vital functions in the compartment. Proteins which fulfill their tasks in the circulation are referred to as secreted proteins.

In the current work, samples of two studies have been analyzed to elucidate the impact of thyroid dysfunction on the murine plasma proteome. The first had a similar design as the experimentally induced thyrotoxicosis study on humans described here. Mice were randomly assigned to a control group, a T4 receiving group and a T4 recovery group which

first received T4 followed by a subsequent TH withdrawal. This experiment allows the investigation of transient TH-mediated changes on the plasma proteome.

The portion of significantly affected proteins was certainly high with 120 proteins exhibiting different levels between T4 and control group (28 % of all identified proteins). Ninety proteins did not only change during T4 application but also showed the reverse trend after T4 withdrawal (T4 recovery *vs.* T4), thereby displaying transient alterations. The second analysis focused on the impact of hyperthyroidism and hypothyroidism caused by T3 or T4 treatment and MMI/$KClO_4$ application, respectively. The study design provided only a control group but no recovery groups for the different inductions. Obtained data revealed a less extensive impact on the plasma proteome. This was surprising since the thyroxine receiving group reached T3 levels of 3.5 µg/l compared to a T3 peak concentration of 2.5 µg/ l in the study of transient thyrotoxicosis. The T3 treatment group reached hormone levels around 8 µg/ l after two weeks. The differences in the number of significantly differentially abundant proteins as well as in the effect sizes of the changes can be partly explained by different group sizes of 8 animals in the transient thyrotoxicosis study compared to only 4 or 3 animals in the second study. This resulted in a striking loss of statistical power in the second study. When a 50 % smaller sample size is used, outliers will reduce the statistical significance for certain proteins dramatically. Therefore, future studies should focus on a higher number of animals per group to ensure reliable results from animal experiments.

In plasma, the majority of those proteins exhibiting decreased levels during TH application returned to baseline levels after withdrawal of thyroxine. Like in the human study of hyperthyroidism, particular interesting findings comprised the decreased levels of apolipoproteins in the hyperthyroid state reflecting the enhanced reverse cholesterol transport to the liver and impact on HDL-, LDL- and VLDL-particles as described above. Also, other rodent studies support the current results. Thus, apolipoproteins of the C family all represent components of chylomicrons, VLDL and HDL. The VLDL receptor seems to play a role in the metabolic process in muscles, as increased amounts of the receptor were detected in skeletal muscle in hyperthyroid rats [136]. ApoB-100 as a primary ligand of LDL particles demonstrated a decreased abundance, which is explained by a higher T3-dependent expression of the LDL receptor coding gene as explained above in the context of the human thyrotoxicosis proteome study [14] . Indeed, originally a murine study

revealed the impact of the transcriptional SREBP-2 activation on LDL receptor gene expression [134].

Apolipoprotein E which is mainly found within chylomicrons is also bound *via* VLDL receptor. In rats, it could be shown in rats that the hepatic synthesis rate of ApoE decreased 7fold in the hyperthyroid state [180]. The opposite was observed in hypothyroidism were a twofold increase was described. This opposed regulation of apolipoprotein levels was also found in the current study in the hypothyroid mice group and the same underlying regulatory mechanism might therefore be postulated for hypothyroid human patients.

In this regard, also alterations of prenylcysteine oxidase 1 (PCYOX) [181], an LDL-particle bound protein were observed. In line with the observations of HDL- and LDL-particle associated proteins described above, low PCYOX levels were found in the group of T3 induced hyperthyroidism and inverse effects in the hypothyroid group. Since TH stimulate *LDLR* expression, the observed drop in protein abundance could be explained by increased uptake of LDL particles from the circulation in peripheral tissues. The protein is also found within VLDL particles [182] whose receptor is also under positive transcriptional regulation of TH. In summary, the influence of TH on apolipoproteins in mice seems to be similar to the human response, as decreased apolipoprotein levels are observed after treatment in both species. The opposite can be seen for hypothyroidism revealing increased levels.

In contrast, proteins of the complement system displayed invers behavior in the murine as compared to the human model. The murine study of transient thyrotoxicosis revealed decreased levels of several complement components and factors in the hyperthyroid state. However, in the T3 group of the second murine study less clear alterations could be detected and even only marginal changes after T4 induction. Furthermore, the MMI/$KClO_4$-induced hypothyroidism also led to a reduction of several proteins assigned to the complement system, although other components and factors seemed to be affected. In contrast, components of the different complement activation pathways were found to be increased in human samples (see above).

Various analyses of the hepatic transcriptome in different murine models before and after T3 application failed to demonstrate differentially expressed genes encoding proteins assigned to the complement system [87,88,99]. One reason for this might be that the

immune systems of mice and humans generally differ significantly [183]. Remarkable discrepancies between humans and mice regarding the production of complement components and the regulation of complement activation were already described, which provides a possible explanation for inconsistent results [184].

A comparison of the effects of T3 and T4 on the murine plasma proteome based on the 20 proteins altered upon both treatment conditions revealed more prominent changes when mice were treated with T3. This seems to reflect the greater bioavailability of T3 compared to the pro-hormone thyroxine which has to be deiodinated before full biological activity is gained [89].

Besides the apolipoproteins A2 and C1 which were discussed in detail before, only two other proteins, namely buturylcholine esterase (BChE) and major urinary protein 6 (MUP- 6) exhibited a significant inverse trend in hyperthyroidism and hypothyroidism.

BChE and MUP-6 are two secreted proteins that are very different. BChE is a classical liver protein whose use as a prognostic marker was discussed previously as its serum level decreased in several clinical conditions including inflammation and liver damage [185]. Hepatocellular impairment leads to the reduction of its enzymatic activity in serum, resulting from a drop of the plasma protein levels in acute and chronic liver damage and cirrhosis. In contrast, increased activity of the enzyme which hydrolyzes both choline and aliphatic esters was documented e.g. in obesity, diabetes and hyperlipoproteinemia [186,187]. Hyperlipoproteinemia is a disorder yielding in the disability to break down lipids, especially cholesterol and triglycerides. If there is no plausible genetic background the reasons for secondary hyperlipoproteinemia are the result of certain health conditions including hypothyroidism [188]. BChE showed significantly higher levels in the hypothyroid group compared to the controls, while in opposite to that, abundance of BChE decreased in all hyperthyroid states either in the T4 group in transient thyrotoxicosis or in the T3 and T4 group in the second murine study.

BChE activity was also described to be positively correlated with serum concentrations of cholesterol and triglycerides [189]. In humans, cholesterol levels decreased significantly during thyrotoxicosis, supporting the thesis of reduced protein levels in mice. However, BChE protein abundance in the human study was positively associated with free T4 levels, showing the opposite trend as in the murine study.

In contrast, the major urinary protein 6 (MUP-6) displayed increased abundances in both hyperthyroid states induced by either T3 or T4 and reduced protein levels in the hypothyroid state. MUPs are members of the lipocalin superfamily with 21 distinct genes in mice encoding MUP proteins and additionally 21 pseudogenes [190]. Proteins of this family act as transport proteins, as modulators of behavior by acting as pheromone-binding proteins, allergens to humans and so called kairomones - signaling information between species. Already in 1983, a connection of MUP abundance and thyroid levels was reported revealing a prominent effect of hormonal changes on *Mup* RNA levels [191]. Hepatic transcription of the *Mup* genes is dependent on both thyroxine and growth hormones, whereby T4 is also known to mediate transcriptional stimulation of growth hormone encoding genes [192]. TH withdrawal therefore leads to reduced growth hormone levels and influences *Mup* expression both directly and indirectly. However, the physiological functions remain to be elucidated for several MUP family members. Lately, the association of MUPs with the regulation of energy expenditure in mice was reported [193]. Data suggest that MUP-1 enhances the mitochondrial function in skeletal muscle causing beneficial effects on energy metabolism. Hui *et al.* described that induced obese, diabetic mice have significantly decreased levels of hepatic *Mup1* mRNA compared to their lean littermates accompanied with reduced circulating protein concentration. Although MUP-1 was not detected in both data sets of the studies presented here, MUP-2, MUP-3 and MUP-6 could be identified and quantified in at least one of the murine studies. Besides Mup-6, Mup-2 was shown to be elevated in the T4 group of transient thyrotoxicosis and the T3 group with a trend of increased abundance in the corresponding T4 group. Feng *et al.* reported an almost 4fold T3-mediated increase of *Mup2* RNA in the liver *via* a cDNA array [88].

The association of coagulative and fibrinolytic proteins with thyroid dysfunction has already been described in human systems or human hepatocellular carcinoma cell line HepG2 as well as in rodent models [32,121,122,170,194]. In the study of transient hyperthyroidism, TH seems to have predominantly negative regulatory effects on proteins of the coagulation cascade in mice (see Table 18). Several coagulation factors and other accompanied proteins all exhibited decreased abundance during thyrotoxicosis. Only two proteins (kininogen-1 and α2-macroglobulin) revealed consistent alterations in the T3

group of the second murine study, only kininogen-1 remained in the T4 group and no protein changes could be reported in the hypothyroid mice group.

Salloum-Asfar *et al.* investigated the immediate and long-term effects of TH on plasma coagulation and hepatic gene transcription of proteins of the coagulation and found reduced mRNA levels of the genes encoding fibrinogen- γ, antithrombin-III, as well as protein C and protein Z already after 4 h of a single T3 injection [194]. Prolonged T3 application led to a reduction of the latter three proteins and additionally led to down-regulation of F2 (prothrombin), F9, and F10 which coincided with increased levels of F11 and F12. Genes encoding these two proteins are established targets of HNF4α which in turn is transcriptionally positively regulated by TH [127]. The role of HNF4α in TH-mediated regulation of F11 was also described by Safdar *et al.* [195]. In the current murine study protein levels of the coagulation factor XII showed no significant change in the hyperthyroid state compared to controls. F11 was not detected whereas the observed changes with decreased levels for F2, F9, and F10, correspond to the results in the plasma proteome study. The reduced levels of fibrinogen- γ and antithrombin-III monitored after 4 h of T3 injection [194] were also detected after two weeks of T4 administration while no change was seen for protein C and protein Z. This data points towards bleeding tendency rather than to higher risk of thrombosis as it is more frequently described for hyperthyroid conditions in rodents and particularly in humans.

Higher abundance of various plasma proteins including clotting factors and other assigned proteins was demonstrated in different studies using the differentiated hepatocellular carcinoma cell line HepG2 with an overproduced TRα1 [90,91].

Literature-based findings regarding a T3-mediated induction of genes encoding proteins involved in coagulation were all described for cell lines or rats. The only exception was the murine study of Salloum-Asfar *et al.* also describing a potential transcriptional suppression of these genes mediated by TH resulting in decreased mRNA levels and finally enzymatic activities of clotting factors and other related proteins [194]. This mechanism is rather poorly understood, but represents a possible explanation for observed results like those described in the murine study of transient hyperthyroidism presented here.

Independent of inconsistent results in the numerous studies, an important role of TH in the process of blood coagulation can be underlined. Rodent studies provide a very divergent picture of TH action in general. Study designs of animal models are very

sensitive to external influences and should be well thought through to prevent inconsequential and meaningless results. As outlined in table 18, TH administration mostly led to inverse changes in mice and humans as displayed by proteins involved in the coagulation cascade and in the complement system. However, the T4 mediated influence on apolipoproteins in mice is comparable with the protein response in humans.

In summary, possible reasons for inverse outcomes regarding the influence of TH in mice and human plasma might be based on species-specific differences. In this context, one problem could be the different time courses of disease recovery in humans and mouse. Recently, Burhardt and Zlotnik briefly discussed the limitations of mouse models in inflammation as research tools [196]. The usefulness of mouse models has been questioned more frequently, but inbred mice are a well-established model to conduct disease research because the ability of studying the underlying disease mechanisms of complex diseases and efficiencies of administered drugs [197]. On the other hand, it is exactly this complexity of human diseases, the inbred nature of mouse models as well as the evolutional distance making translational considerations sometimes difficult.

5 REFERENCES

1. Vanderpump MPJ (2011) The epidemiology of thyroid disease. British medical bulletin 99: 39–51.
2. British Thyroid Association, Royal College of Physicians (Perros P, ed) (2007) Guidelines for the management of thyroid cancer. London: Royal College of Physicians. 83 p.
3. Chiasera JM (2013) Back to the Basics: Thyroid Gland Structure, Function and Pathology.
4. Krassas G, Rivkees S, Kiess W, editors (2006) Diseases of the Thyroid in Childhood and Adolescence. Basel: KARGER.
5. Yen PM (2001) Physiological and Molecular Basis of Thyroid Hormone Action. Physiological Reviews 81 (3): 1097–1142.
6. Brent GA (2012) Mechanisms of thyroid hormone action. The Journal of clinical investigation 122 (9): 3035–3043.
7. Brix K, Führer D, Biebermann H (2011) Molecules important for thyroid hormone synthesis and action - known facts and future perspectives. Thyroid research 4 Suppl 1: S9.
8. PITTMAN JA, BROWN RW, REGISTER HB (1962) Biological activity of 3,3',5'-triiodo-DL-thyronine. Endocrinology 70: 79–83.
9. Mullur R, Liu Y, Brent GA (2014) Thyroid hormone regulation of metabolism. Physiological Reviews 94 (2): 355–382.
10. Ortiga-Carvalho TM, Sidhaye AR, Wondisford FE (2014) Thyroid hormone receptors and resistance to thyroid hormone disorders. Nature reviews. Endocrinology 10 (10): 582–591.
11. Hodin RA, Lazar MA, Chin WW (1990) Differential and tissue-specific regulation of the multiple rat c-erbA messenger RNA species by thyroid hormone. The Journal of clinical investigation 85 (1): 101–105.
12. Lazar MA (1993) Thyroid hormone receptors: multiple forms, multiple possibilities. Endocrine reviews 14 (2): 184–193.

13. Lopez D, Abisambra Socarrás, Jose F, Bedi M, Ness GC (2007) Activation of the hepatic LDL receptor promoter by thyroid hormone. Biochimica et biophysica acta 1771 (9): 1216–1225.
14. Shin D, Osborne TF (2003) Thyroid hormone regulation and cholesterol metabolism are connected through Sterol Regulatory Element-Binding Protein-2 (SREBP-2). The Journal of biological chemistry 278 (36): 34114–34118.
15. Lammel Lindemann, Jan A, Angajala A, Engler DA, Webb P, Ayers SD (2014) Thyroid hormone induction of human cholesterol 7 alpha-hydroxylase (Cyp7a1) in vitro. Molecular and cellular endocrinology 388 (1-2): 32–40.
16. Dedecjus M, Masson D, Gautier T, de Barros, Jean-Paul Pais, Gambert P et al. (2003) Low cholesteryl ester transfer protein (CETP) concentration but normal CETP activity in serum from patients with short-term hypothyroidism Lack of relationship to lipoprotein abnormalities. Clinical endocrinology 58 (5): 581–588.
17. Potenza M, Via MA, Yanagisawa RT (2009) Excess thyroid hormone and carbohydrate metabolism. Endocrine practice : official journal of the American College of Endocrinology and the American Association of Clinical Endocrinologists 15 (3): 254–262.
18. Park EA, Song S, Vinson C, Roesler WJ (1999) Role of CCAAT enhancer-binding protein beta in the thyroid hormone and cAMP induction of phosphoenolpyruvate carboxykinase gene transcription. The Journal of biological chemistry 274 (1): 211–217.
19. Suh JH, Sieglaff DH, Zhang A, Xia X, Cvoro A et al. (2013) SIRT1 is a direct coactivator of thyroid hormone receptor β1 with gene-specific actions. PloS one 8 (7): e70097.
20. Sinha RA, Singh BK, Yen PM (2014) Thyroid hormone regulation of hepatic lipid and carbohydrate metabolism. Trends in endocrinology and metabolism: TEM 25 (10): 538–545.
21. Oetting A, Yen PM (2007) New insights into thyroid hormone action. Best practice & research. Clinical endocrinology & metabolism 21 (2): 193–208.
22. Brent GA (2008) Clinical practice. Graves' disease. The New England journal of medicine 358 (24): 2594–2605.
23. Muls E, Blaton V, Rosseneu M, Lesaffre E, Lamberigts G et al. (1982) Serum lipids and apolipoproteins A-I, A-II, and B in hyperthyroidism before and after treatment. The Journal of clinical endocrinology and metabolism 55 (3): 459–464.
24. Singh SP, Snyder AK (1978) Effect of thyrotoxicosis on gluconeogenesis from alanine in the perfused rat liver. Endocrinology 102 (1): 182–187.
25. Klein I, Danzi S (2007) Thyroid disease and the heart. Circulation 116 (15): 1725–1735.
26. Klein I (2011) Endocrine disorders and cardiovascular disease. In Bonow, RO et al. editors. Braunwald's heart disease, chapter 86. WB Saunders and Company (9th edition): 1829–1843.

27. Klein I, Ojamaa K (2001) Thyroid hormone and the cardiovascular system. The New England journal of medicine 344 (7): 501–509.
28. Biondi B, Palmieri EA, Lombardi G, Fazio S (2002) Effects of thyroid hormone on cardiac function. The relative importance of heart rate, loading conditions, and myocardial contractility in the regulation of cardiac performance in human hyperthyroidism. The Journal of clinical endocrinology and metabolism 87 (3): 968–974.
29. Orwoll ES, Orwoll RL (1987) Hematologic abnormalities in patients with endocrine and metabolic disorders. Hematology/oncology clinics of North America 1 (2): 261–279.
30. Rogers JS, Shane SR, Jencks FS (1982) Factor VIII activity and thyroid function. Annals of internal medicine 97 (5): 713–716.
31. Erem C, Ersoz HO, Karti SS, Ukinç K, Hacihasanoglu A et al. (2002) Blood coagulation and fibrinolysis in patients with hyperthyroidism. Journal of endocrinological investigation 25 (4): 345–350.
32. van Zaane B, Squizzato A, Debeij J, Dekkers OM, Meijers, J C M et al. (2011) Alterations in coagulation and fibrinolysis after levothyroxine exposure in healthy volunteers: a controlled randomized crossover study. Journal of thrombosis and haemostasis : JTH 9 (9): 1816–1824.
33. Hooper, J M W, Stuijver, D J F, Orme SM, van Zaane B, Hess K et al. (2012) Thyroid dysfunction and fibrin network structure: a mechanism for increased thrombotic risk in hyperthyroid individuals. The Journal of clinical endocrinology and metabolism 97 (5): 1463–1473.
34. Ajjan RA, Weetman AP (2015) The Pathogenesis of Hashimoto's Thyroiditis: Further Developments in our Understanding. Hormone and metabolic research = Hormon- und Stoffwechselforschung = Hormones et metabolisme 47 (10): 702–710.
35. Pearce EN, Farwell AP, Braverman LE (2003) Thyroiditis. The New England journal of medicine 348 (26): 2646–2655.
36. Duntas LH, Wartofsky L (2007) Cardiovascular risk and subclinical hypothyroidism: focus on lipids and new emerging risk factors. What is the evidence. Thyroid : official journal of the American Thyroid Association 17 (11): 1075–1084.
37. Biondi B, Klein I (2004) Hypothyroidism as a risk factor for cardiovascular disease. Endocrine 24 (1): 1–13.
38. Dalton RG, Dewar MS, Savidge GF, Kernoff PB, Matthews KB et al. (1987) Hypothyroidism as a cause of acquired von Willebrand's disease. Lancet (London, England) 1 (8540): 1007–1009.
39. Michiels JJ, Schroyens W, Berneman Z, van der Planken, M (2001) Acquired von Willebrand syndrome type 1 in hypothyroidism: reversal after treatment with thyroxine. Clinical and applied thrombosis/hemostasis : official journal of the International Academy of Clinical and Applied Thrombosis/Hemostasis 7 (2): 113–115.

40. EGEBERG O (1964) THYROID FUNCTION AND HEMOSTASIS. Scandinavian journal of clinical and laboratory investigation 16: 511–512.
41. Simone JV, Abildgaard CF, Schulman I (1965) Blood coagulation in thyroid dysfunction. The New England journal of medicine 273 (20): 1057–1061.
42. Vescovi PP, Favaloro EJ, Lippi G, Garofano M, Montagnana M et al. (2011) The spectrum of coagulation abnormalities in thyroid disorders. Semin Thromb Hemost 37 (1): 7–10.
43. Chadarevian R, Bruckert E, Leenhardt L, Giral P, Ankri A et al. (2001) Components of the fibrinolytic system are differently altered in moderate and severe hypothyroidism. The Journal of clinical endocrinology and metabolism 86 (2): 732–737.
44. Akhtar A (2015) The flaws and human harms of animal experimentation. Cambridge quarterly of healthcare ethics : CQ : the international journal of healthcare ethics committees 24 (4): 407–419.
45. Rosenthal N, Brown S (2007) The mouse ascending: perspectives for human-disease models. Nature cell biology 9 (9): 993–999.
46. Seok J, Warren HS, Cuenca AG, Mindrinos MN, Baker HV et al. (2013) Genomic responses in mouse models poorly mimic human inflammatory diseases. Proceedings of the National Academy of Sciences of the United States of America 110 (9): 3507–3512.
47. Takao K, Miyakawa T (2015) Genomic responses in mouse models greatly mimic human inflammatory diseases. Proceedings of the National Academy of Sciences of the United States of America 112 (4): 1167–1172.
48. Yen PM, Feng X, Flamant F, Chen Y, Walker RL et al. (2003) Effects of ligand and thyroid hormone receptor isoforms on hepatic gene expression profiles of thyroid hormone receptor knockout mice. EMBO reports 4 (6): 581–587.
49. Tsang W, Houlden RL (2009) Amiodarone-induced thyrotoxicosis: a review. The Canadian journal of cardiology 25 (7): 421–424.
50. Wilkins MR, Appel RD (2007) Ten Years of the Proteome. In: Wilkins MR, Appel RD, Williams KL, Hochstrasser DF, editors. Proteome Research. Berlin, Heidelberg: Springer Berlin Heidelberg. pp. 1–13.
51. Wilkins MR, Gasteiger E, Sanchez J, Appel RD, Hochstrasser DF (1996) Protein identification with sequence tags. Current Biology 6 (12): 1543–1544.
52. James P (1997) Protein identification in the post-genome era: the rapid rise of proteomics. Quart. Rev. Biophys. 30 (4): 279–331.
53. O'Farrell PH (1975) High resolution two-dimensional electrophoresis of proteins. The Journal of biological chemistry 250 (10): 4007–4021.
54. Klose J (1975) Protein mapping by combined isoelectric focusing and electrophoresis of mouse tissues. A novel approach to testing for induced point mutations in mammals. Humangenetik 26 (3): 231–243.

55. Aebersold R, Mann M (2003) Mass spectrometry-based proteomics. Nature 422 (6928): 198–207.
56. Ong SE, Pandey A (2001) An evaluation of the use of two-dimensional gel electrophoresis in proteomics. Biomolecular engineering 18 (5): 195–205.
57. Domon B, Aebersold R (2006) Mass spectrometry and protein analysis. Science (New York, N.Y.) 312 (5771): 212–217.
58. Gregorich ZR, Ge Y (2014) Top-down proteomics in health and disease: challenges and opportunities. Proteomics 14 (10): 1195–1210.
59. Deracinois B, Flahaut C, Duban-Deweer S, Karamanos Y (2013) Comparative and Quantitative Global Proteomics Approaches: An Overview. Proteomes 1 (3): 180–218.
60. Durbin KR, Fornelli L, Fellers RT, Doubleday PF, Narita M et al. (2016) Quantitation and Identification of Thousands of Human Proteoforms below 30 kDa. Journal of proteome research 15 (3): 976–982.
61. Ross PL, Huang YN, Marchese JN, Williamson B, Parker K et al. (2004) Multiplexed protein quantitation in Saccharomyces cerevisiae using amine-reactive isobaric tagging reagents. Molecular & cellular proteomics : MCP 3 (12): 1154–1169.
62. Gygi SP, Rist B, Gerber SA, Turecek F, Gelb MH et al. (1999) Quantitative analysis of complex protein mixtures using isotope-coded affinity tags. Nature biotechnology 17 (10): 994–999.
63. Ong S, Mann M (2006) A practical recipe for stable isotope labeling by amino acids in cell culture (SILAC). Nature protocols 1 (6): 2650–2660.
64. Ong S, Mann M (2005) Mass spectrometry-based proteomics turns quantitative. Nature chemical biology 1 (5): 252–262.
65. Thompson A, Schäfer J, Kuhn K, Kienle S, Schwarz J et al. (2003) Tandem mass tags: a novel quantification strategy for comparative analysis of complex protein mixtures by MS/MS. Analytical chemistry 75 (8): 1895–1904.
66. Neilson KA, Ali NA, Muralidharan S, Mirzaei M, Mariani M et al. (2011) Less label, more free: approaches in label-free quantitative mass spectrometry. Proteomics 11 (4): 535–553.
67. Patel VJ, Thalassinos K, Slade SE, Connolly JB, Crombie A et al. (2009) A comparison of labeling and label-free mass spectrometry-based proteomics approaches. Journal of proteome research 8 (7): 3752–3759.
68. Liu H, Sadygov RG, Yates JR (2004) A model for random sampling and estimation of relative protein abundance in shotgun proteomics. Analytical chemistry 76 (14): 4193–4201.
69. Chelius D, Bondarenko PV (2002) Quantitative profiling of proteins in complex mixtures using liquid chromatography and mass spectrometry. Journal of proteome research 1 (4): 317–323.

70. Silvestri E, Moreno M, Schiavo L, Lange P de, Lombardi A et al. (2006) A proteomics approach to identify protein expression changes in rat liver following administration of 3,5,3'-triiodo-L-thyronine. Journal of proteome research 5 (9): 2317–2327.
71. Silvestri E, Burrone L, Lange P de, Lombardi A, Farina P et al. (2007) Thyroid-state influence on protein-expression profile of rat skeletal muscle. Journal of proteome research 6 (8): 3187–3196.
72. Anderson NL, Polanski M, Pieper R, Gatlin T, Tirumalai RS et al. (2004) The human plasma proteome: a nonredundant list developed by combination of four separate sources. Molecular & cellular proteomics : MCP 3 (4): 311–326.
73. Poste G (2011) Bring on the biomarkers. Nature 469 (7329): 156–157.
74. Veenstra TD, Conrads TP, Hood BL, Avellino AM, Ellenbogen RG et al. (2005) Biomarkers: mining the biofluid proteome. Molecular & cellular proteomics : MCP 4 (4): 409–418.
75. Putnam FW, editor (1984) The plasma proteins. Structure, function and genetic control. New York: Academic P. xvi, 420 s p.
76. Anderson NL (2002) The Human Plasma Proteome: History, Character, and Diagnostic Prospects. Molecular & Cellular Proteomics 1 (11): 845–867.
77. Tiwari RP, Jain A, Khan Z, Kohli V, Bharmal RN et al. (2012) Cardiac troponins I and T: molecular markers for early diagnosis, prognosis, and accurate triaging of patients with acute myocardial infarction. Molecular diagnosis & therapy 16 (6): 371–381.
78. Colantonio DA, Dunkinson C, Bovenkamp DE, van Eyk JE (2005) Effective removal of albumin from serum. Proteomics 5 (15): 3831–3835.
79. Bradford MM (1976) A rapid and sensitive method for the quantitation of microgram quantities of protein utilizing the principle of protein-dye binding. Analytical biochemistry 72: 248–254.
80. Cox J, Hein MY, Luber CA, Paron I, Nagaraj N et al. (2014) Accurate proteome-wide label-free quantification by delayed normalization and maximal peptide ratio extraction, termed MaxLFQ. Molecular & cellular proteomics : MCP 13 (9): 2513–2526.
81. Pietzner M, Engelmann B, Kacprowski T, Golchert J, Dirk A et al. (2017) Plasma proteome and metabolome characterization of an experimental human thyrotoxicosis model. BMC medicine 15 (1): 6.
82. Silva JC, Gorenstein MV, Li G, Vissers, Johannes P C, Geromanos SJ (2006) Absolute quantification of proteins by LCMSE: a virtue of parallel MS acquisition. Molecular & cellular proteomics : MCP 5 (1): 144–156.
83. Engelmann B, Bischof J, Dirk A, Friedrich N, Hammer E et al. (2015) Effect of Experimental Thyrotoxicosis onto Blood Coagulation: A Proteomics Study. European thyroid journal 4 (Suppl 1): 119–124.
84. Sun L, Zhu G, Dovichi NJ (2013) Comparison of the LTQ-Orbitrap Velos and the Q-Exactive for proteomic analysis of 1-1000 ng RAW 264.7 cell lysate digests. Rapid communications in mass spectrometry : RCM 27 (1): 157–162.

85. Zaias J, Mineau M, Cray C, Yoon D, Altman NH (2009) Reference values for serum proteins of common laboratory rodent strains. Journal of the American Association for Laboratory Animal Science : JAALAS 48 (4): 387–390.
86. Wilkening S, Stahl F, Bader A (2003) Comparison of primary human hepatocytes and hepatoma cell line Hepg2 with regard to their biotransformation properties. Drug metabolism and disposition: the biological fate of chemicals 31 (8): 1035–1042.
87. Weitzel JM, Radtke C, Seitz HJ (2001) Two thyroid hormone-mediated gene expression patterns in vivo identified by cDNA expression arrays in rat. Nucleic acids research 29 (24): 5148–5155.
88. Feng X, Jiang Y, Meltzer P, Yen PM (2000) Thyroid hormone regulation of hepatic genes in vivo detected by complementary DNA microarray. Molecular endocrinology (Baltimore, Md.) 14 (7): 947–955.
89. Selva DM, Hammond GL (2009) Thyroid hormones act indirectly to increase sex hormone-binding globulin production by liver via hepatocyte nuclear factor-4alpha. Journal of molecular endocrinology 43 (1): 19–27.
90. Lin K, Lee H, Shih C, Yen C, Chen S et al. (2003) Plasma protein regulation by thyroid hormone. The Journal of endocrinology 179 (3): 367–377.
91. Shih C, Chen S, Yen C, Huang Y, Chen C et al. (2004) Thyroid hormone receptor-dependent transcriptional regulation of fibrinogen and coagulation proteins. Endocrinology 145 (6): 2804–2814.
92. Tseng F, Chen Y, Chi Y, Chen P, Yang W (2016) Serum Levels of Follistatin Are Positively Associated With Serum-Free Thyroxine Levels in Patients With Hyperthyroidism or Euthyroidism. Medicine 95 (5): e2661.
93. Andersen S, Pedersen KM, Bruun NH, Laurberg P (2002) Narrow individual variations in serum T(4) and T(3) in normal subjects: a clue to the understanding of subclinical thyroid disease. The Journal of clinical endocrinology and metabolism 87 (3): 1068–1072.
94. Benhadi N, Fliers E, Visser TJ, Reitsma JB, Wiersinga WM (2010) Pilot study on the assessment of the setpoint of the hypothalamus-pituitary-thyroid axis in healthy volunteers. European journal of endocrinology 162 (2): 323–329.
95. Toft AD, Beckett GJ (2003) Thyroid function tests and hypothyroidism. BMJ (Clinical research ed.) 326 (7384): 295–296.
96. Andersen S, Bruun NH, Pedersen KM, Laurberg P (2003) Biologic variation is important for interpretation of thyroid function tests. Thyroid : official journal of the American Thyroid Association 13 (11): 1069–1078.
97. Thienpont LM, van Uytfanghe K, Beastall G, Faix JD, Ieiri T et al. (2010) Report of the IFCC Working Group for Standardization of Thyroid Function Tests; part 2: free thyroxine and free triiodothyronine. Clinical chemistry 56 (6): 912–920.
98. Thienpont LM, van Uytfanghe K, Beastall G, Faix JD, Ieiri T et al. (2010) Report of the IFCC Working Group for Standardization of Thyroid Function Tests; part 1: thyroid-stimulating hormone. Clinical chemistry 56 (6): 902–911.

99. Flores-Morales A, Gullberg H, Fernandez L, Ståhlberg N, Lee NH et al. (2002) Patterns of liver gene expression governed by TRbeta. Molecular endocrinology (Baltimore, Md.) 16 (6): 1257–1268.
100. Visser WE, Heemstra KA, Swagemakers SMA, Ozgür Z, Corssmit EP et al. (2009) Physiological thyroid hormone levels regulate numerous skeletal muscle transcripts. The Journal of clinical endocrinology and metabolism 94 (9): 3487–3496.
101. Clément K, Viguerie N, Diehn M, Alizadeh A, Barbe P et al. (2002) In vivo regulation of human skeletal muscle gene expression by thyroid hormone. Genome research 12 (2): 281–291.
102. Montoya GA, Strauss V, Fabian E, Kamp H, Mellert W et al. (2014) Mechanistic analysis of metabolomics patterns in rat plasma during administration of direct thyroid hormone synthesis inhibitors or compounds increasing thyroid hormone clearance. Toxicology letters 225 (2): 240–251.
103. Wu S, Gao Y, Dong X, Tan G, Li W et al. (2013) Serum metabonomics coupled with Ingenuity Pathway Analysis characterizes metabolic perturbations in response to hypothyroidism induced by propylthiouracil in rats. Journal of pharmaceutical and biomedical analysis 72: 109–114.
104. Wu S, Tan G, Dong X, Zhu Z, Li W et al. (2013) Metabolic profiling provides a system understanding of hypothyroidism in rats and its application. PloS one 8 (2): e55599.
105. Göttlich M, Heldmann M, Göbel A, Dirk A, Brabant G et al. (2015) Experimentally induced thyrotoxicosis leads to increased connectivity in temporal lobe structures: a resting state fMRI study. Psychoneuroendocrinology 56: 100–109.
106. Westphal U (1986) Steroid-Protein Interactions II. Berlin, Heidelberg: Springer Berlin Heidelberg. 1 online resource p.
107. Anderson DC (1974) Sex-hormone-binding globulin. Clinical endocrinology 3 (1): 69–96.
108. Földes J, Vana S, Bános C, Lakatos P, Tarján G (1990) The measurement of the serum sex-hormone binding globulin in various thyroid diseases. Acta medica Hungarica 47 (1-2): 81–90.
109. Dittrich R, Beckmann MW, Oppelt PG, Hoffmann I, Lotz L et al. (2011) Thyroid hormone receptors and reproduction. Journal of reproductive immunology 90 (1): 58–66.
110. Siemińska L, Foltyn W, Głogowska-Szeląg J, Kajdaniuk D, Marek B et al. (2013) Relationships between adiponectin, sex hormone binding globulin and insulin resistance in hyperthyroid Graves' disease women. Endokrynologia Polska 64 (1): 26–29.
111. Nielsen J, Jensen RB, Juul A (2013) Increased sex hormone-binding globulin levels in children and adolescents with thyrotoxicosis. Hormone research in paediatrics 79: 157–161.
112. Sarne DH, Refetoff S, Rosenfield RL, Farriaux JP (1988) Sex hormone-binding globulin in the diagnosis of peripheral tissue resistance to thyroid hormone: the

value of changes after short term triiodothyronine administration. The Journal of clinical endocrinology and metabolism 66 (4): 740–746.
113. Jänne M, Hammond GL (1998) Hepatocyte nuclear factor-4 controls transcription from a TATA-less human sex hormone-binding globulin gene promoter. The Journal of biological chemistry 273 (51): 34105–34114.
114. Manetti L, Pardini E, Genovesi M, Campomori A, Grasso L et al. (2005) Thyroid function differently affects serum cystatin C and creatinine concentrations. Journal of endocrinological investigation 28 (4): 346–349.
115. Kotajima N, Yanagawa Y, Aoki T, Tsunekawa K, Morimura T et al. (2010) Influence of thyroid hormones and transforming growth factor-β1 on cystatin C concentrations. The Journal of international medical research 38 (4): 1365–1373.
116. Aydın B, Winters SJ (2016) Sex Hormone-Binding Globulin in Children and Adolescents. Journal of clinical research in pediatric endocrinology 8 (1): 1–12.
117. Karakas SE (2017) New biomarkers for diagnosis and management of polycystic ovary syndrome. Clinica chimica acta; international journal of clinical chemistry 471: 248–253.
118. Wan Z, Wang J, You S, Liu H, Zhu B et al. (2013) Cystatin C is a biomarker for predicting acute kidney injury in patients with acute-on-chronic liver failure. World journal of gastroenterology 19 (48): 9432–9438.
119. Soni SS, Ronco C, Katz N, Cruz DN (2009) Early diagnosis of acute kidney injury: the promise of novel biomarkers. Blood purification 28 (3): 165–174.
120. Debeij J, van Zaane B, Dekkers OM, Doggen, C J M, Smit, J W A et al. (2014) High levels of procoagulant factors mediate the association between free thyroxine and the risk of venous thrombosis: the MEGA study. Journal of thrombosis and haemostasis : JTH 12 (6): 839–846.
121. Horacek J, Maly J, Svilias I, Smolej L, Cepkova J et al. (2015) Prothrombotic changes due to an increase in thyroid hormone levels. European journal of endocrinology 172 (5): 537–542.
122. Stuijver, Danka J F, van Zaane B, Romualdi E, Brandjes, Dees P M, Gerdes, Victor E A et al. (2012) The effect of hyperthyroidism on procoagulant, anticoagulant and fibrinolytic factors: a systematic review and meta-analysis. Thrombosis and haemostasis 108 (6): 1077–1088.
123. Miller LD, Park KS, Guo QM, Alkharouf NW, Malek RL et al. (2001) Silencing of Wnt signaling and activation of multiple metabolic pathways in response to thyroid hormone-stimulated cell proliferation. Molecular and cellular biology 21 (19): 6626–6639.
124. Niessen RW, Pfaffendorf BA, Sturk A, Lamping RJ, Schaap MC et al. (1995) The influence of insulin, beta-estradiol, dexamethasone and thyroid hormone on the secretion of coagulant and anticoagulant proteins by HepG2 cells. Thrombosis and haemostasis 74 (2): 686–692.

125. Hertzberg KM, Pindyck J, Mosesson MW, Grieninger G (1981) Thyroid hormone stimulation of plasma protein synthesis in cultured hepatocytes. The Journal of biological chemistry 256 (2): 563–566.
126. Elbers, Laura P B, Moran C, Gerdes VE, van Zaane B, Meijers J et al. (2016) The Hypercoagulable state in Hyperthyroidism is mediated via the Thyroid Hormone β Receptor pathway. European journal of endocrinology.
127. Inoue Y, Peters LL, Yim SH, Inoue J, Gonzalez FJ (2006) Role of hepatocyte nuclear factor 4alpha in control of blood coagulation factor gene expression. Journal of molecular medicine (Berlin, Germany) 84 (4): 334–344.
128. Lu H (2016) Crosstalk of HNF4α with extracellular and intracellular signaling pathways in the regulation of hepatic metabolism of drugs and lipids. Acta pharmaceutica Sinica. B 6 (5): 393–408.
129. O'Brien T, Katz K, Hodge D, Nguyen TT, Kottke BA et al. (1997) The effect of the treatment of hypothyroidism and hyperthyroidism on plasma lipids and apolipoproteins AI, AII and E. Clinical endocrinology 46 (1): 17–20.
130. de Bruin, T W, van Barlingen H, van Linde-Sibenius Trip, M, van Vuurst de Vries, A R, Akveld MJ et al. (1993) Lipoprotein(a) and apolipoprotein B plasma concentrations in hypothyroid, euthyroid, and hyperthyroid subjects. The Journal of clinical endocrinology and metabolism 76 (1): 121–126.
131. Rassart E, Bedirian A, Do Carmo S, Guinard O, Sirois J et al. (2000) Apolipoprotein D. Biochimica et biophysica acta 1482 (1-2): 185–198.
132. Dominiczak MH, Caslake MJ (2011) Apolipoproteins: metabolic role and clinical biochemistry applications. Annals of clinical biochemistry 48 (Pt 6): 498–515.
133. Coppola M, Glinni D, Moreno M, Cioffi F, Silvestri E et al. (2014) Thyroid hormone analogues and derivatives: Actions in fatty liver. World journal of hepatology 6 (3): 114–129.
134. Lopez D, Abisambra Socarrás, Jose F, Bedi M, Ness GC (2007) Activation of the hepatic LDL receptor promoter by thyroid hormone. Biochimica et biophysica acta 1771 (9): 1216–1225.
135. Shin D, Osborne TF (2003) Thyroid hormone regulation and cholesterol metabolism are connected through Sterol Regulatory Element-Binding Protein-2 (SREBP-2). The Journal of biological chemistry 278 (36): 34114–34118.
136. Jokinen EV, Landschulz KT, Wyne KL, Ho YK, Frykman PK et al. (1994) Regulation of the very low density lipoprotein receptor by thyroid hormone in rat skeletal muscle. The Journal of biological chemistry 269 (42): 26411–26418.
137. Nedvidkova J, Haluzik M, Bartak V, Dostalova I, Vlcek P et al. (2004) Changes of noradrenergic activity and lipolysis in the subcutaneous abdominal adipose tissue of hypo- and hyperthyroid patients: an in vivo microdialysis study. Annals of the New York Academy of Sciences 1018: 541–549.
138. Walport MJ (2001) Complement. First of two parts. The New England journal of medicine 344 (14): 1058–1066.

139. Mathern DR, Heeger PS (2015) Molecules Great and Small: The Complement System. Clinical journal of the American Society of Nephrology : CJASN 10 (9): 1636–1650.
140. Skerka C, Chen Q, Fremeaux-Bacchi V, Roumenina LT (2013) Complement factor H related proteins (CFHRs). Molecular immunology 56 (3): 170–180.
141. Dousset B, Straczek J, Maachi F, Nguyen DL, Jacob C et al. (1998) Purification from human plasma of a hexapeptide that potentiates the sulfation and mitogenic activities of insulin-like growth factors. Biochemical and biophysical research communications 247 (3): 587–591.
142. Yu H, Yang Y, Zhang M, Lu H, Zhang J et al. (2006) Thyroid status influence on adiponectin, acylation stimulating protein (ASP) and complement C3 in hyperthyroid and hypothyroid subjects. Nutrition & metabolism 3: 13.
143. Jafarzadeh A, Poorgholami M, Izadi N, Nemati M, Rezayati M (2010) Immunological and hematological changes in patients with hyperthyroidism or hypothyroidism. Clinical and investigative medicine. Medecine clinique et experimentale 33 (5): E271-9.
144. Zhang B, Jiang Y, Yang Y, Peng F, Hu X (2008) Correlation between serum thyroxine and complements in patients with multiple sclerosis and neuromyelitis optica. Neuro endocrinology letters 29 (2): 256–260.
145. Oleesky DA, Ratanachaiyavong S, Ludgate M, Morgan BP, Campbell AK et al. (1986) Complement component C9 in Graves' disease. Clinical endocrinology 25 (6): 623–632.
146. Weetman AP, Cohen SB, Oleesky DA, Morgan BP (1989) Terminal complement complexes and C1/C1 inhibitor complexes in autoimmune thyroid disease. Clinical and experimental immunology 77 (1): 25–30.
147. Riis, Anne Lene Dalkjaer, Hansen TK, Thiel S, Gravholt CH, Gjedde S et al. (2005) Thyroid hormone increases mannan-binding lectin levels. European journal of endocrinology 153 (5): 643–649.
148. Sorensen CM, Hansen TK, Steffensen R, Jensenius JC, Thiel S (2006) Hormonal regulation of mannan-binding lectin synthesis in hepatocytes. Clinical and experimental immunology 145 (1): 173–182.
149. Potlukova E, Jiskra J, Freiberger T, Limanova Z, Zivorova D et al. (2010) The production of mannan-binding lectin is dependent upon thyroid hormones regardless of the genotype: a cohort study of 95 patients with autoimmune thyroid disorders. Clinical immunology (Orlando, Fla.) 136 (1): 123–129.
150. Rakhshandehroo M, Stienstra R, Wit NJ de, Bragt MCE, Haluzik M et al. (2012) Plasma mannose-binding lectin is stimulated by PPARalpha in humans. American journal of physiology. Endocrinology and metabolism 302 (5): E595-602.
151. Tachibana K, Takeuchi K, Inada H, Sugimoto K, Ishimoto K et al. (2013) Human mannose-binding lectin 2 is directly regulated by peroxisome proliferator-activated

receptors via a peroxisome proliferator responsive element. Journal of biochemistry 154 (3): 265–273.

152. Pucci E, Chiovato L, Pinchera A (2000) Thyroid and lipid metabolism. International journal of obesity and related metabolic disorders : journal of the International Association for the Study of Obesity 24 Suppl 2: S109-12.
153. Lee W, Suh J, Rhee E, Park J, Sung K et al. (2004) Plasma CRP, apolipoprotein A-1, apolipoprotein B and Lpa levels according to thyroid function status. Archives of medical research 35 (6): 540–545.
154. Teixeira PdFdS, Reuters VS, Ferreira MM, Almeida CP, Reis FAA et al. (2008) Lipid profile in different degrees of hypothyroidism and effects of levothyroxine replacement in mild thyroid failure. Translational research : the journal of laboratory and clinical medicine 151 (4): 224–231.
155. Pearce EN, Wilson PWF, Yang Q, Vasan RS, Braverman LE (2008) Thyroid function and lipid subparticle sizes in patients with short-term hypothyroidism and a population-based cohort. The Journal of clinical endocrinology and metabolism 93 (3): 888–894.
156. Ye Y, Gai X, Xie H, Jiao L, Zhang S (2013) Impact of thyroid function on serum cystatin C and estimated glomerular filtration rate: a cross-sectional study. Endocrine practice : official journal of the American College of Endocrinology and the American Association of Clinical Endocrinologists 19 (3): 397–403.
157. Goede DL, Wiesli P, Brändle M, Bestmann L, Bernays RL et al. (2009) Effects of thyroxine replacement on serum creatinine and cystatin C in patients with primary and central hypothyroidism. Swiss medical weekly 139 (23-24): 339–344.
158. An JH, Song K, Kim D, Kim SK (2017) Effects of thyroid hormone withdrawal on metabolic and cardiovascular parameters during radioactive iodine therapy in differentiated thyroid cancer. The Journal of international medical research 45 (1): 38–50.
159. Fricker M, Wiesli P, Brändle M, Schwegler B, Schmid C (2003) Impact of thyroid dysfunction on serum cystatin C. Kidney international 63 (5): 1944–1947.
160. Wiesli P, Schwegler B, Spinas GA, Schmid C (2003) Serum cystatin C is sensitive to small changes in thyroid function. Clinica chimica acta; international journal of clinical chemistry 338 (1-2): 87–90.
161. Ozden TA, Tekerek H, Baş F, Darendeliler F (2010) Effect of hypo-and euthyroid status on serum cystatin C levels. Journal of clinical research in pediatric endocrinology 2 (4): 155–158.
162. Cavaliere H, Abelin N, Medeiros-Neto G (1988) Serum levels of total testosterone and sex hormone binding globulin in hypothyroid patients and normal subjects treated with incremental doses of L-T4 or L-T3. Journal of andrology 9 (3): 215–219.
163. Bicíková M, Hampl R, Hill M, Stanická S, Tallová J et al. (2003) Steroids, sex hormone-binding globulin, homocysteine, selected hormones and markers of lipid and carbohydrate metabolism in patients with severe hypothyroidism and their

changes following thyroid hormone supplementation. Clinical chemistry and laboratory medicine 41 (3): 284–292.

164. Kuusi T, Taskinen MR, Nikkilä EA (1988) Lipoproteins, lipolytic enzymes, and hormonal status in hypothyroid women at different levels of substitution. The Journal of clinical endocrinology and metabolism 66 (1): 51–56.
165. Lecomte P, Lecureuil N, Lecureuil M, Osorio Salazar C, Valat C (1995) Age modulates effects of thyroid dysfunction on sex hormone binding globulin (SHBG) levels. Experimental and clinical endocrinology & diabetes : official journal, German Society of Endocrinology [and] German Diabetes Association 103 (5): 339–342.
166. Brenta G, Schnitman M, Gurfinkiel M, Damilano S, Pierini A et al. (1999) Variations of sex hormone-binding globulin in thyroid dysfunction. Thyroid : official journal of the American Thyroid Association 9 (3): 273–277.
167. Brenta G, Bedecarras P, Schnitman M, Gurfinkiel M, Damilano S et al. (2002) Characterization of sex hormone-binding globulin isoforms in hypothyroid women. Thyroid : official journal of the American Thyroid Association 12 (2): 101–105.
168. Squizzato A, Gerdes, V E A, Ageno W, Büller HR (2007) The coagulation system in endocrine disorders: a narrative review. Internal and emergency medicine 2 (2): 76–83.
169. Franchini M, Lippi G, Manzato F, Vescovi PP, Targher G (2010) Hemostatic abnormalities in endocrine and metabolic disorders. European journal of endocrinology 162 (3): 439–451.
170. Erem C, Kavgaci H, Ersöz HO, Hacihasanoglu A, Ukinç K et al. (2003) Blood coagulation and fibrinolytic activity in hypothyroidism. International journal of clinical practice 57 (2): 78–81.
171. Ford HC, Carter JM (1990) Haemostasis in hypothyroidism. Postgraduate medical journal 66 (774): 280–284.
172. Marongiu F, Cauli C, Mariotti S (2004) Thyroid, hemostasis and thrombosis. Journal of endocrinological investigation 27 (11): 1065–1071.
173. Bennett NB, Ogston CM, McAndrew GM (1967) The thyroid and fibrinolysis. British medical journal 4 (5572): 147–148.
174. Biondi B, Cooper DS (2008) The clinical significance of subclinical thyroid dysfunction. Endocrine reviews 29 (1): 76–131.
175. Chadarevian R, Bruckert E, Ankri A, Beucler I, Giral P et al. (1998) Relationship between thyroid hormones and plasma D-dimer levels. Thrombosis and haemostasis 79 (1): 99–103.
176. Gullu S, Sav H, Kamel N (2005) Effects of levothyroxine treatment on biochemical and hemostasis parameters in patients with hypothyroidism. European journal of endocrinology 152 (3): 355–361.
177. Marongiu F, Biondi G, Conti M, Murtas ML, Mameli G et al. (1992) Is a hypercoagulable state present in hypothyroidism. Thrombosis and haemostasis 67 (6): 729.

178. Severino V, Locker J, Ledda-Columbano GM, Columbano A, Parente A et al. (2011) Proteomic characterization of early changes induced by triiodothyronine in rat liver. Journal of proteome research 10 (7): 3212–3224.
179. Williams MT, Carrington H, Herrera A (1986) Stimulation of mouse liver glutathione S-transferase activity in propylthiouracil-treated mice in vivo by tri-iodothyronine. The Biochemical journal 233 (2): 595–598.
180. Davidson NO, Carlos RC, Drewek MJ, Parmer TG (1988) Apolipoprotein gene expression in the rat is regulated in a tissue-specific manner by thyroid hormone. Journal of lipid research 29 (11): 1511–1522.
181. Diffenderfer MR, Schaefer EJ (2014) The composition and metabolism of large and small LDL. Current opinion in lipidology 25 (3): 221–226.
182. Dashty M, Motazacker MM, Levels J, Vries M de, Mahmoudi M et al. (2014) Proteome of human plasma very low-density lipoprotein and low-density lipoprotein exhibits a link with coagulation and lipid metabolism. Thrombosis and haemostasis 111 (3): 518–530.
183. Mestas J, Hughes CCW (2004) Of mice and not men. Differences between mouse and human immunology. Journal of immunology (Baltimore, Md. : 1950) 172 (5): 2731–2738.
184. Jonas AM (1984) The mouse in biomedical research. The Physiologist 27 (5): 330–346.
185. Santarpia L, Grandone I, Contaldo F, Pasanisi F (2013) Butyrylcholinesterase as a prognostic marker. A review of the literature. Journal of cachexia, sarcopenia and muscle 4 (1): 31–39.
186. Das UN (2007) Acetylcholinesterase and butyrylcholinesterase as possible markers of low-grade systemic inflammation. Medical science monitor : international medical journal of experimental and clinical research 13 (12): RA214-21.
187. Cucuianu M, Nistor T, Hâncu N, Orbai P, Muscurel C et al. (2002) Serum cholinesterase activity correlates with serum insulin, C-peptide and free fatty acids levels in patients with type 2 diabetes. Romanian journal of internal medicine = Revue roumaine de medecine interne 40 (1-4): 43–51.
188. Stone NJ (1994) Secondary causes of hyperlipidemia. The Medical clinics of North America 78 (1): 117–141.
189. Das UN (2012) Acetylcholinesterase and butyrylcholinesterase as markers of low-grade systemic inflammation. Annals of hepatology 11 (3): 409–411.
190. Zhou Y, Rui L (2010) Major Urinary Protein Regulation of Chemical Communication and Nutrient Metabolism. In: Litwack G, editor. Pheromones. s.l.: Elsevier textbooks. pp. 151–163.
191. Knopf JL, Gallagher JF, Held WA (1983) Differential, multihormonal regulation of the mouse major urinary protein gene family in the liver. Molecular and cellular biology 3 (12): 2232–2240.

192. Wallace H, Ledent C, Vassart G, Bishop JO, al-Shawi R (1991) Specific ablation of thyroid follicle cells in adult transgenic mice. Endocrinology 129 (6): 3217–3226.
193. Hui X, Zhu W, Wang Y, Lam KSL, Zhang J et al. (2009) Major urinary protein-1 increases energy expenditure and improves glucose intolerance through enhancing mitochondrial function in skeletal muscle of diabetic mice. The Journal of biological chemistry 284 (21): 14050–14057.
194. Salloum-Asfar S, Boelen A, Reitsma PH, van Vlijmen BJM (2015) The immediate and late effects of thyroid hormone (triiodothyronine) on murine coagulation gene transcription. PloS one 10 (5): e0127469.
195. Safdar H, Cheung KL, Vos HL, Gonzalez FJ, Reitsma PH et al. (2012) Modulation of mouse coagulation gene transcription following acute in vivo delivery of synthetic small interfering RNAs targeting HNF4α and C/EBPα. PloS one 7 (6): e38104.
196. Burkhardt AM, Zlotnik A (2013) Translating translational research: mouse models of human disease. Cellular & molecular immunology 10 (5): 373–374.
197. Justice MJ, Dhillon P (2016) Using the mouse to model human disease: increasing validity and reproducibility. Disease models & mechanisms 9 (2): 101–103.

CONTENT OF SUPPLEMENTARY MATERIAL

The following additional material can be found on the attached CD.

S1_Human model of experimentally induced thyrotoxicosis_Median normalized and adjusted data.pdf Log_{10}, median normalized and subsequent adjusted (age, BMI, and age) protein intensities from all subjects and time points are presented here for all proteins considered for relative quantification. Proteins that were not detected are labeled *NA*.

S2_Human model of experimentally induced thyrotoxicosis_Results of the Pearson correlation analysis.pdf Results of the Pearson correlation analysis are displayed. *P*-value and correlation coefficient *r* are given for each protein. Proteins with $r > |0.9|$ are highlighted in bold. Additionally, proteins with $r > 0.9$ and $r < -0.9$ are marked in red and green, respectively.

S3_Human model of experimentally induced thyrotoxicosis_Results of the mixed effect linear regression model.pdf Results of the mixed-effect linear regression model are listed. False discovery rate and estimate of free T4 are given for each protein. Significantly associated proteins are printed in bold.

S4_Human model of experimentally induced thyrotoxicosis_Results of the paired t-test_t2 vs. t1.pdf Results of the paired t-test analysis applied to time point t2 (4 weeks of L-T_4 administration) and the t1 (baseline) are displayed by *p*-value and fold change for each protein. Significantly altered proteins are highlighted in bold.

S5_Mouse model of transient thyrotoxicosis_Median normalized data.pdf Log_{10} and median normalized protein intensities from individual mice are presented here for all proteins considered for relative quantification. Proteins that were not detected are labeled *NA*.

S6_Mouse model of transient thyrotoxicosis_Results of the Welchs t-tests after ANOVA.pdf Included are proteins significantly altered after ANOVA. Results of the Welch's t-test analyses for T4 group *vs.* controls, T4 recovery group *vs.* T4 group and T4 recovery *vs.* controls are listed. *P*-value, *p*(FDR) and fold change of the single group comparisons is given. Fold changes > 1.5 and < -1.5 are marked in red and green, respectively.

S7_Mouse model analyzing T4, T3 and MMI induced alterations_Median normalized data.pdf Log_{10} and median normalized protein intensities from individual mice are presented here for all proteins considered for relative quantification. Proteins that were not detected are labeled *NA*.

S8_Mouse model analyzing T4, T3 and MMI induced alterations_Results of the Welchs t-tests.pdf Results of Welch's t-test analyses for induced hyperthyroid (T4, T3) and hypothyroid (MMI) state *vs.* controls are listed. *P*-value and fold change of the single group comparisons are given. Fold changes > 1.5 and < -1.5 are marked in red and green, respectively. Data that was not available is labeled *NA*.

S9_Proteome analysis of human primary hepatocytes_Median normalized data_intracellular proteome.pdf Log_{10} and median normalized protein intensities from three donors (each control and one/two T4-treated samples) are displayed. Proteins that were not detected are labeled *NA*.

S10_Proteome analysis of human primary hepatocytes_Impact of T4 treatment on intracellular protein levels.pdf Presented is the fold change of T4 treated sample *vs.* the respective control of each donor calculated from the median normalized protein intensity of each given protein. Proteins with a fold change > 1.5 are highlighed in red boxes, proteins with a fold change < -1.5 are highlighed in green boxes.

S11_Proteome analysis of human primary hepatocytes_LFQ values of MaxQuant analysis_secretome.pdf Generated LFQ values representing normalized quantities for all proteins from three donors (each control and one or two T4-treated samples) are displayed. Only proteins considered for relative quantification (proteins with less than two missing values across all samples) are presented. Proteins that were not detected are labeled *NA*.

S12_Proteome analysis of human primary hepatocytes_Impact of T4 treatment on extracellular protein levels.pdf Presented is the fold change of T4 treated sample *vs.* the respective control of each donor calculated from the median normalized protein intensity of each given protein. Proteins with a fold change > 1.5 are highlighed in red boxes, proteins with a fold change < -1.5 are highlighed in green boxes.

EIGENSTÄNDIGKEITSERKLÄRUNG

Hiermit erkläre ich, dass diese Arbeit bisher von mir weder an der Mathematisch-Naturwissenschaftlichen Fakultät der Ernst-Moritz-Arndt-Universität Greifswald noch einer anderen wissenschaftlichen Einrichtung zum Zwecke der Promotion eingereicht wurde.

Ferner erkläre ich, dass ich diese Arbeit selbstständig verfasst und keine anderen als die darin angegebenen Hilfsmittel und Hilfen benutzt und keine Textabschnitte eines Dritten ohne Kennzeichnung übernommen habe.

_____

Beatrice Engelmann

PUBLICATIONS

Journal articles

Pietzner M, Engelmann B, Kacprowski T, Golchert J, Dirk AL, Hammer E, Iwen KA, Nauck M, Wallaschofski H, Führer D, Münte TF, Friedrich N, Völker U, Homuth G, Brabant G.
Plasma proteome and metabolome characterization of an experimental human thyrotoxicosis model.
BMC Med. 2017 Jan 9;15(1):6. doi: 10.1186/s12916-016-0770-8

Engelmann B, Bischof J, Dirk AL, Friedrich N, Hammer E, Thiele T, Führer D, Homuth G, Brabant G, Völker U.
Effect of Experimental Thyrotoxicosis onto Blood Coagulation: A Proteomics Study.
Eur Thyroid J. 2015 Sep;4(Suppl 1):119-24. doi: 10.1159/000381769

Sandetskaya N, Engelmann B, Brandenburg K, Kuhlmeier D.
Application of immobilized synthetic anti-lipopolysaccharide peptides for the isolation and detection of bacteria.
Eur J Clin Microbiol Infect Dis. 2015 Aug;34(8):1639-45. doi: 10.1007/s10096-015-2399-5

Contributions to scientific meetings

Beatrice Engelmann, Julia Bischof, Anne-Luise Dirk, Nele Friedrich, Elke Hammer, Thomas Thiele, Dagmar Führer, Georg Homuth, Georg Brabant, Uwe Völker.
Protein plasma profiling of individuals with induced hyperthyroidism by T4-administration
"Annual Meeting", Essen, Germany, 11.04.-12.04.2014 [Talk]

Beatrice Engelmann, Elke Hammer, Yvonne Reinke, Marcus Dörr, Kerstin Weitmann, Stefan B. Felix, Uwe Völker.
Influence of immunoadsorption therapy on the plasma protein profile of DCM patients
"8th European Summer School in Advanced Proteomics", 03.08.-08.08.2014, Brixen, Italy [Poster]

Beatrice Engelmann, Maik Pietzner, Anne-Luise Dirk, Elke Hammer, Nele Friedrich, Dagmar Führer, Georg Homuth, Georg Brabant, and Uwe Völker.
Effects of experimental thyrotoxicosis on the human plasma proteome
"1st International Thyroid Trans Act Conference", 04.12.-07.12.2014, Bremen, Germany [Poster]

Beatrice Engelmann, Anne-Luise Dirk, Elke Hammer, Nele Friedrich, Dagmar Führer, Georg Homuth, Georg Brabant, and Uwe Völker.
A plasma proteomics study of experimental thyrotoxicosis on humans
"Proteomic Forum - Annual meeting of the German Society for Proteome Research", 22.03.-25.03.2015, Berlin, Germany [Poster]

Maik Pietzner, Beatrice Engelmann, Tim Kacprowski, Anne-Luise Dirk, Janine Golchert, Georg Homuth, Elke Hammer, Matthias Nauck, Henri Wallaschofski, Nele Friedrich, Uwe Völker, Georg Brabant.
Multi-OMICS analyses of a mid-term human thyrotoxicosis model.
"Summer School on Endocrinology", 02.08.-06.08.2015, Bregenz, Austria [Poster]

Beatrice Engelmann, Maik Pietzner, Anne-Luise Dirk, Elke Hammer, Nele Friedrich, Georg Brabant, Georg Homuth, Uwe Völker.
Comprehensive proteomic characterization of a human thyrotoxicosis model – Proteomics part of the story
"6th Workshop on Genetic Epidemiology – On the Tip of Omics", Grainau, Germany, 12.04-16.04.2016 [Talk]

Beatrice Engelmann, Maik Pietzner, Tim Kacprowski, Anne-Luise Dirk, Janine Golchert, Elke Hammer, Matthias Nauck, Henri Wallaschofski, Thomas Münte, Nele Friedrich, Georg Brabant, Uwe Völker, and Georg Homuth.
Multi-OMICS analyses of an experimental human thyrotoxicosis model
"Proteomic Forum - Annual meeting of the German Society for Proteome Research" 02.04.-05.04.2017, Potsdam, Germany [Poster]

Presenting author

DANKSAGUNG

An erster Stelle möchte ich mich bei Prof. Dr. Völker für die Möglichkeit bedanken, meine Doktorarbeit unter so hervorragenden Bedingungen verfassen zu dürfen. Ich bin dankbar für die Überlassung des Themas sowie für hilfreiche Diskussionen.

Ein unendlich großes Dankeschön richte ich an alle Mitglieder der Funktionellen Genomforschung!

Mein besonderer Dank gilt dabei Dr. Elke Hammer, die mich während der letzten Jahre und auch schon zu Zeiten der Diplomarbeit immer unterstützt hat und mich in zahlreichen Diskussionen voranbrachte. Ihre Hilfsbereitschaft und Geduld haben maßgeblich zum Verfassen dieser Arbeit beigetragen.

Für seine Zeit und Unterstützung möchte ich im gleichen Zuge Dr. Georg Homuth danken, dessen Hilfe ich mit fortschreitender Doktorarbeit häufiger in Anspruch genommen habe.

Für unzählige MS Messungen bin ich Dr. Vishnu M. Dhople, Dr. Manuela Gesell Salazar und Annette Murr zu großem Dank verpflichtet.

Bei den Leuten aus meinem Büro möchte ich mich herzlich für jegliche fachlichen Gespräche und solche, die darüber hinausgingen, bedanken. Gleiches gilt für alle lieb gewonnenen Menschen der Kaffeerunde!

Mein Dank gilt weiterhin Ulrike Lissner, Sophie Eisenlöffel, Katrin Schoknecht, Jette Anklam und Kirsten Bartels für ihre alltägliche Unterstützung im Labor.

Lars Brinkmann und Dirk Lewerentz danke ich für das Lösen von immer wieder auftauchenden IT-Problemen. Für das Lösen von allerhand kleinerer wie größerer Probleme möchte ich auch Dr. Leif Steil danken.

Außerhalb des eigenen Labors danke ich an erster Stelle Maik Pietzner aus dem Institut für Klinische Chemie der Universitätsmedizin Greifswald für seine Unterstützung vielfältigster Art, vor allem bei Auswerteproblemen. In diesem Zusammenhang ein großer Dank auch an Dr. Nele Friedrich.

Ich danke weiterhin den Kooperationspartnern der Universität zu Lübeck, namentlich Prof. Dr. Georg Brabant, Prof. Dr. Jens Mittag und Lisbeth Harder sowie Dr. Carolin Höfig (Charité Universitätsmedizin Berlin) für die Bereitstellung aller Proben, die dieser Arbeit zu Grunde liegen.

Zu Dank verpflichtet bin ich auch dem DFG Schwerpunktprogramm SPP1629 „ThyroidTransAct“ für die finanzielle Ermöglichung der Projekte.

Der PRIMACYT Cell Culture Technology GmbH (Dieter Runge und Anett Ullrich) danke ich für die Zusammenarbeit im Projekt der humanen primären Hepatozyten. Hier möchte ich

außerdem auch Janine Golchert nennen, mit der die Zusammenarbeit sehr viel Spaß gemacht hat.

Neben großartigen Arbeitskollegen und Freunden im Labor möchte ich auch jene Freunde nicht vergessen, die außerhalb des Instituts eine Rolle gespielt haben. Durch ihren Rückhalt, ihre Unterstützung und das Teilen von unzähligen wunderbaren Erfahrungen und Erlebnissen bin ich überhaupt nur soweit gekommen.

Die letzten Worte sollen meiner Familie gelten. Ihr Verständnis, ihre Zuneigung und Hilfe der letzten Jahre haben diese Arbeit von Grund auf erst möglich gemacht.